

# REPORT DOCUMENTATION PAGE

Form Approved  
OMB No. 0704-0188

Public reporting burden for this collection of information is estimated to average 1 hour per response, including the time for reviewing instructions, searching existing data sources, gathering and maintaining the data needed, and completing and reviewing the collection of information. Send comments regarding this burden estimate or any other aspect of this collection of information, including suggestions for reducing this burden to Washington Headquarters Services, Directorate for Information Operations and Reports, 1215 Jefferson Davis Highway, Suite 1204, Arlington, VA 22202-4302, and to the Office of Management and Budget, Paperwork Reduction Project (0704-0188), Washington, DC 20503.

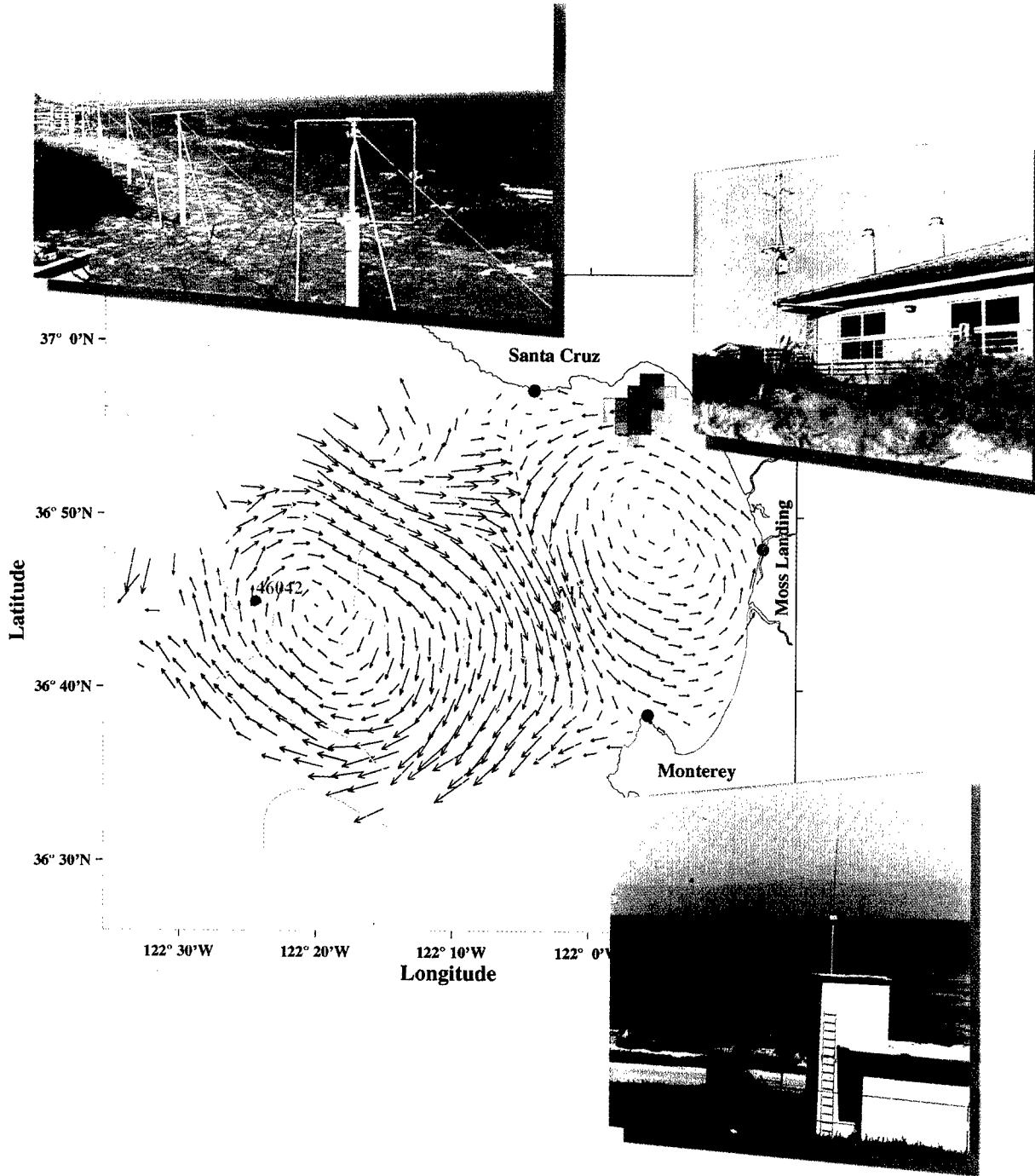
|  |  |   |   |  |
|--|--|---|---|--|
| 1. AGENCY USE ONLY (Leave blank)   |  | 2. REPORT DATE<br>11 MAR 1999                           | 3. REPORT TYPE AND DATES COVERED<br>FINAL 15 JUN 97 - 31 DEC 98 |  |
| 4. TITLE AND SUBTITLE<br>Publication and distribution of two special issues of "Oceanography" - High Frequency Radar and Ocean Thin Layers   |  |   | 5. FUNDING NUMBERS<br>N00014-97-1-0851                          |  |
| 6. AUTHOR(S)<br>Larry P. Atkinson, editor, plus various authors (see Table of Contents attached)   |  |   |   |  |
| 7. PERFORMING ORGANIZATION NAME(S) AND ADDRESS(ES)<br>The Oceanography Society (TOS)<br>4052 Timber Ridge Drive<br>Virginia Beach, VA 23455  |  |   | 8. PERFORMING ORGANIZATION REPORT NUMBER<br>2 - Final           |  |
| 9. SPONSORING / MONITORING AGENCY NAME(S) AND ADDRESS(ES)<br>Office of Naval Research<br>800 North Quincy Street<br>Arlington, VA 22217-5660   |  |   | 10. SPONSORING / MONITORING AGENCY REPORT NUMBER                |  |
| 11. SUPPLEMENTARY NOTES  |  |   |   |  |
| 8. DISTRIBUTION / AVAILABILITY STATEMENT<br>V10:N2 High Frequency Radar - 500 delivered to ONR<br>V11:N2 Thin Layers in the Ocean - 500 delivered to ONR<br>Both issues were also sent to all members of TOS and additional copies are available through the TOS office. |  |   | 12. DISTRIBUTION CODE   |  |
| 13. ABSTRACT (Maximum 200 words)<br>The Table of Contents of both V10:N2 and V11:N1 are attached here. Also attached are the introductory articles to each each which together summarize the importance and significant information contained in the two special issues. |  |   |   |  |
| 14. SUBJECT TERMS<br>high-frequency radar, remote sensing, small-scale patterns, upper ocean processes   |  |   | 15. NUMBER OF PAGES<br>1  |  |
|  |  |   | 16. PRICE CODE  |  |
| 17. SECURITY CLASSIFICATION OF REPORT<br>Unclassified  | 18. SECURITY CLASSIFICATION OF THIS PAGE<br>Unclassified | 19. SECURITY CLASSIFICATION OF ABSTRACT<br>Unclassified | 20. LIMITATION OF ABSTRACT<br>U1                                |  |

19990323 129

Standard Form 298 (Rev. 2-89)  
Prescribed by ANSI Std. Z39-18  
298-102

# OCEANOGRAPHY

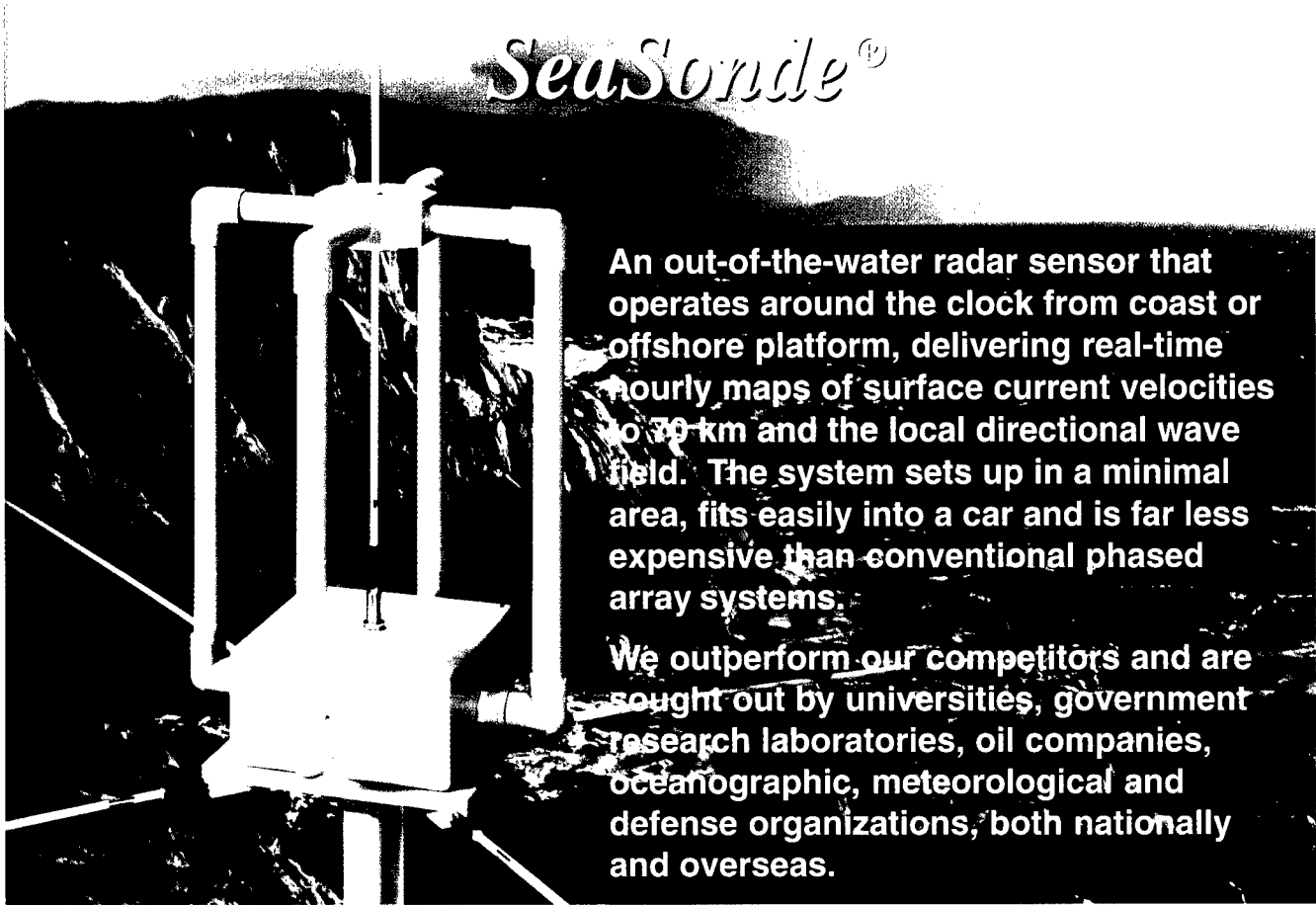
PUBLISHED BY THE OCEANOGRAPHY SOCIETY



*Special Issue on High Frequency Radars for Coastal Oceanography*

Tired of losing your current meter? Interested in area surface current coverage rather than a single vector or trajectory?  
Convert to radar remote sensing!

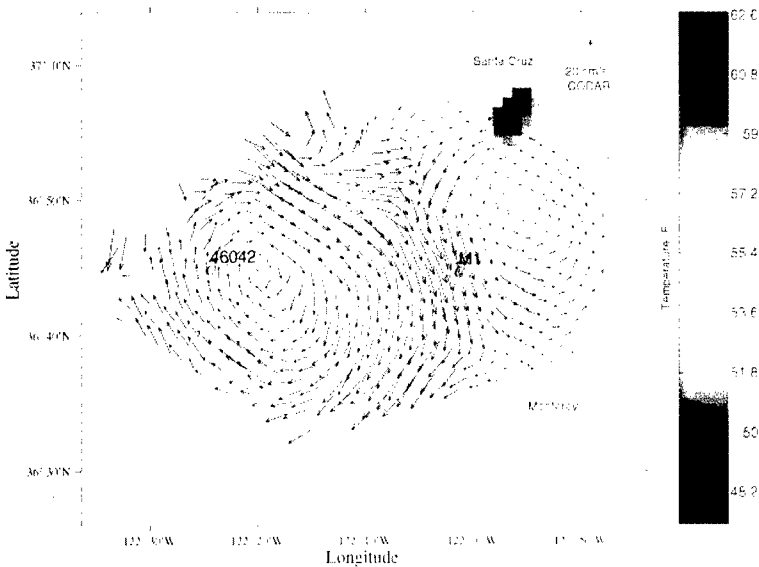
## SeaSonde<sup>®</sup>



An out-of-the-water radar sensor that operates around the clock from coast or offshore platform, delivering real-time hourly maps of surface current velocities to 70 km and the local directional wave field. The system sets up in a minimal area, fits easily into a car and is far less expensive than conventional phased array systems.

We outperform our competitors and are sought out by universities, government research laboratories, oil companies, oceanographic, meteorological and defense organizations, both nationally and overseas.

SeaSonde<sup>®</sup> antenna located on a California coast



*Leaders for 30 years  
in Oceanographic  
Remote Sensing*

Technical data accessible on  
<http://www.CodarOS.com>

*SeaSonde current velocity vectors, AVHRR temperatures in colored background.*

*From: Paduan and Rosenfield, J. Geophys Res, 101, page 20669*

CODAR Ocean Sensors

1000 Fremont Avenue, Suite K,  
Los Altos, CA 94024, USA

Telephone: (408) 773-8240 Fax: (408) 773-0514

VOL. 10, NO. 2

# OCEANOGRAPHY

PUBLISHED BY THE OCEANOGRAPHY SOCIETY

**DISTRIBUTION STATEMENT A**  
Approved for Public Release  
Distribution Unlimited

## Style Guide and Information for Contributors

**Philosophy.** *Oceanography* exists to promote and chronicle all aspects of ocean science and its applications. It publishes brief articles, critical essays and concise reviews that deal with topics of broad interest to the ocean-science community. In addition, *Oceanography* solicits and publishes news and information, meeting reports, book reviews, and other items of current interest.

**Manuscript Requirements:** All manuscripts must be typewritten and double spaced. Manuscripts must include the title, name and affiliation (including city, state and zip code) of each author. Acknowledgements, references and figures should follow the stylistic conventions outlined below. Please submit four hard copies of the manuscript and a copy on disk to: Larry P. Atkinson, Center for Coastal Physical Oceanography, Old Dominion University, Crittenton Hall, Norfolk, VA 23529. Submitted material will be reviewed for style, relevance and quality by the editors and by anonymous external reviewers.

**Language Style:** The desired style of writing is less technical and more compact than that typically used in scientific papers. The readership includes oceanographers from all traditional disciplines, as well as scientifically literate persons with a broad range of interests and responsibilities. Authors should strive for clarity and simplicity and avoid technical and mathematical jargon. Perhaps the best description of the expected style is the following.

Vigorous writing is concise. A sentence should contain no unnecessary words, a paragraph no unnecessary sentences, for the same reason that a drawing should have no unnecessary lines and a machine no unnecessary parts. This requires not that the writer make all his sentences short, or that he avoid all detail and treat his subjects only in outline, but that every word tell.

—William Strunk, Jr. and E. B. White  
*The Elements of Style*, third ed.,  
© 1979 Macmillan Pub. Co., Inc.  
Reprinted with permission.

**Length Limitations** (Maximum length of articles must be strictly followed):

**\* Feature Articles:**

10–12 double-spaced, typed pages; 4–5 figures.

**\* Review and Comment Pieces:**

5–8 pages, 2–3 figures.

**\* Other** (e.g., News and Information, Meeting and Workshop Reports, or Book Reviews) should be as concise as possible. Meeting reports should describe goals, activities and accomplishments; not agendas, programs and attendance.

**References:** *Oceanography* does not use numbered footnotes. Instead, textual references should be given parenthetically as: (author, year). Complete and correct references are the author's responsibility. A complete list of references should be ordered alphabetically by the first author's last name, and placed at the end of the manuscript in following format.

**Article in Journal:**

Author(s), year: Title of article. *Title of Journal (abbreviated)*, volume number, inclusive pages.

\* Example:

Levin, M.E., 1979: Ahab as Socratic philosopher: The Myth of the Cave inverted. *Am. Transcendental Quar.*, 41, 61–73.

**\* Article in Book:**

Author(s), year: Title of article. In: *Title of Book*. Editor's name, ed., Publisher, inclusive pages.

\* Example:

Skirrow, G., 1975: The dissolved gases-carbon dioxide. In: *Chemical Oceanography*, vol. 2, 2nd edition. J.P. Riley and G. Skirrow, eds., Academic Press, New York, 1–192.

**Book:**

Author(s), year: *Title of Book*. Publisher, city, total pages.

\* Example:

Baker, B.B. and E.T. Copson, 1939: *The Mathematical Theory of Huygens' Principle*. Clarendon, Oxford, 155 pp.

**\* Thesis:**

Author, year: Name of thesis. Masters/Ph.D. thesis, name of university, total pages.

\* Example:

Rintoul, S., 1988: Mass, heat and nutrient fluxes in the Atlantic Ocean determined by inverse methods. Ph.D. thesis, Massachusetts Institute of Technology/Woods Hole Oceanographic Institution Joint Program, 287 pp.

**\* Proceedings:**

Author(s), year: Name of report. In: *Name of Proceedings*. Name of conference, publisher, city, inclusive pages.

\* Example:

Knauss, J.A. and M.H. Katsouros, 1986: Recent experiences of the United States in conducting marine scientific research in coastal state Exclusive Economic Zones. In: *The Law of the Sea: What Lies Ahead?*. Proceedings of the Twentieth Annual Conference on the Law of the Sea Institute, 1986, Univ. of Hawaii Press, Honolulu, 297–309.

Abbreviations should conform to the current Chemical Abstracts Service Source Index published by The American Chemical Society, or see the American Meteorological Society's Author's Guide. Works "in progress" or "submitted" may be cited only as "personal communication." Articles that have been accepted for publication may be cited, if the journal name and volume number are provided in the list of references. "In press" citations are acceptable. The correct citation for this publication is *Oceanography*.

**Figures/Tables:** Each figure or table should be accompanied by a complete caption and be cited and explained in the text. All figures and drawings should be of exceptional quality to allow for clear reproduction and reduction. Articles generally are limited to four or five figures. Review and Comment pieces generally are limited to three figures. Line drawings and black-and-white or color photos are acceptable; authors must pay the additional costs of color processing.

# OCEANOGRAPHY

SERVING OCEAN SCIENCE AND ITS APPLICATIONS

## TABLE OF CONTENTS

### QUARTERDECK / 34

#### FEATURES

INTRODUCTION TO HIGH-FREQUENCY RADAR: REALITY AND MYTH  
By Jeffrey D. Paduan and Hans C. Graber / 36

HF RADAR INSTRUMENTS, PAST TO PRESENT  
By Calvin C. Teague, John F. Vesecky and Daniel M. Fernandez / 40

SYNOPTIC MEASUREMENT OF DYNAMIC OCEANIC FEATURES  
By Brian K. Haus, Hans C. Graber and Lynn K. Shay / 45

MAPPING SURFACE CURRENTS IN MONTEREY BAY WITH CODAR-TYPE HF RADAR  
By Jeffrey D. Paduan and Michael S. Cook / 49

THE COASTAL JET: OBSERVATIONS OF SURFACE CURRENTS OVER THE OREGON  
CONTINENTAL SHELF FROM HF RADAR  
By P. Michael Kosro, John A. Barth and P. Ted Strub / 53

TIDAL AND WIND-DRIVEN CURRENTS FROM OSCAR  
By David Prandle / 57

INTERNAL WAVE-DRIVEN SURFACE CURRENTS FROM HF RADAR  
By Lynn K. Shay / 60

LARVAL TRANSPORT AND COASTAL UPWELLING: AN APPLICATION  
OF HF RADAR IN ECOLOGICAL RESEARCH  
By Eric Bjorkstedt and Jonathan Roughgarden / 64

TRANSPORT PATTERNS OF TROPICAL REEF FISH LARVAE BY SPIN-OFF EDDIES  
IN THE STRAITS OF FLORIDA  
By Hans C. Graber and Claire B. Limouzy-Paris / 68

EVOLUTION OF BEARING DETERMINATION IN HF CURRENT MAPPING RADARS  
By Donald E. Barrick and Belinda J. Lipa / 72

VALIDATION OF HF RADAR MEASUREMENTS  
By Rick D. Chapman and Hans C. Graber / 76

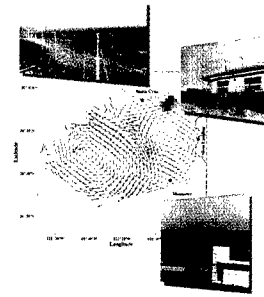
SHIPBOARD DEPLOYMENT OF A VHF OSCAR SYSTEM FOR MEASURING  
OFFSHORE CURRENTS  
By Richard A. Skop and Nicholas J. Peters / 80

EXPERIENCE WITH SHIPBORNE MEASUREMENTS OF SURFACE CURRENT FIELDS  
BY RADAR  
By Klaus-Werner Gurgel / 82

THE OCEAN WAVE DIRECTIONAL SPECTRUM  
By Lucy Wyatt / 85

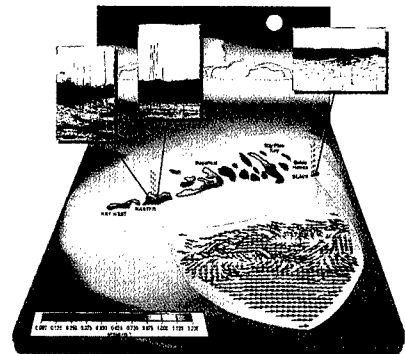
WAVE HEIGHT MEASUREMENTS FROM HF RADAR  
By Hans C. Graber and Malcolm L. Heron / 90

*Contents continued on page 35.*



### FRONT COVER

Daily averaged surface current vectors from the CODAR/SeaSonde HF radar network around Monterey Bay for 6 August 1994, together with satellite-derived sea surface temperatures in the range 9°C (blue) to 17°C (red). Symbols denote off-shore mooring locations (red) and radar sites (black). Photographs show the phased-array antennas recently deployed in Santa Cruz (see Teague *et al.*, 1997, this issue), the older-style CODAR antenna deployed at MBARI in Moss Landing, and the SeaSonde antenna deployed on a Coast Guard building at Pt. Pinos near Monterey. These images were produced by G. Hatcher (MBARI) and P. Braccio (NPS).



### BACK COVER

Surface vector current map from the OSCAR HF radar in the South Florida Keys for 0000 UTC 25 May 1994 showing the presence of a mesoscale eddy inshore of the Florida Current (red) and convergence and divergence zones. The vectors indicate the current direction and the colors represent the speed (see scale). The radar sites "master" and "slave" were located at Boca Chica and Bahia Honda, respectively. Photographs show the receive phased-array antennas (left and right inset) and the transmit antenna array (center inset). These images were produced by E.H. Augustus.

*Oceanography* (ISSN 1042-8275) is published by The Oceanography Society, 4052 Timber Ridge Drive, Virginia Beach, VA 23455 USA. © 1997, The Oceanography Society, Inc. All rights reserved. Permission is granted to copy an article in this publication for use in teaching or research. For more extensive copying, a fee of \$1.00 per article can be paid through the Copyright Clearance Center, 21 Congress Street, Salem, MA 01970. Republication, systemic reproduction, or collective redistribution of any material in this publication is permitted only with the approval of The Oceanography Society. Send change-of-address information to the Society address. Postmaster: Bulk mail postage paid Lancaster, PA 17603; Permit 161.

# HIGH-FREQUENCY RADAR REMOTE SENSING: THE NEW REVOLUTION IN COASTAL OCEANOGRAPHY

**T**HE LITTORAL OCEAN with its complicated coastline and complex bathymetry poses great challenges to oceanographers, coastal managers, and naval forces that have an ever increasing need to understand and predict its behavior. However, the prediction of coastal environmental parameters is particularly difficult because winds, waves, and currents interact with the boundaries on much smaller space and time scales than in the open "deep blue" ocean. As a result, the dynamics of coastal waters and the resulting circulation are dependent on many physical mechanisms and interactions that are not well understood and have not been measured extensively with the necessary spatial and temporal resolution. Conventional measurement techniques are limited to single-point, temporal observations (e.g., current or wave measurements from a mooring) or to poorly resolving spatial snapshots (e.g., ship surveys or drifting buoy arrays). The broad spectrum of societal and environmental issues that arise from our increasing interest in, and dependence on, the coastal ocean (e.g., coastal pollution, fisheries recruitment, search and rescue, beach erosion, and sediment transport) demands that we improve our ability to monitor coastal processes and to fine-tune models to more accurately predict impending changes.

This improved measurement capability is important for the Navy in its tactical decision making. For example, Naval operations in the littoral ocean encounter numerous challenges in mine countermeasures and also during amphibious landings, whereas detailed information on meteorological conditions is critical during takeoff and landing operations on aircraft carriers. Additionally, improved knowledge of the local sea state is crucial for the detection and defense of surface-skimming missiles. The Army's need to observe the coastal ocean stems from its dual function in our society. On the military side, logistics over the shore (LOTS) are critical to disembarkation of equipment and the temporary maintenance of harbors. On the civilian side, the Army Corps of Engineers has responsibilities for the health and maintenance of our shorelines and beaches. Huge sums of money are expended in the dredging of harbors and shipping lanes to maintain the safety and viability of our waterways, whereas it is the near-shore circulation patterns and relentless impact of shoaling waves that force these expensive actions through sediment transport and shoreline erosion.

With the beginning of operation of high-frequency (HF) radars in coastal zones some forty years ago and the application of near-shore current mapping some twenty years ago, it became feasible to simultaneously observe large regions of the coastal ocean and construct maps of surface currents, waves, and wind direction. Depending on the system configuration, horizontal resolutions can be from hundreds of meters to tens of kilometers whereas offshore ranges are from tens to hundreds of kilometers. The shore-based, noninvasive nature of this remote sensing technology means that, in principle, these two-dimensional observations can be collected continuously for relatively low costs compared with at-sea measurements. The potential of HF radars to advance our understanding of coastal oceanography by providing much of the necessary space-time observations is truly incredible. This special issue of *Oceanography* is dedicated to the presentation of a diverse set of examples in which HF radars were used to observe the coastal ocean. The Office of Naval Research and the U.S. Army Engineer Waterways Experiment Station are pleased to sponsor this publication. We would like to thank the authors and the editors, Hans Graber and Jeff Paduan, for the efforts in putting this special issue together. We hope it will both introduce you to this revolutionary tool and also foster your interest in coastal oceanography research, but with a somewhat different perspective than before this encounter.

—Dennis B. Trizna and Robert E. Jensen

Dennis B. Trizna, Office of Naval Research (Code 321SR); and Robert E. Jensen, USAE Waterways Experiment Station (CEWES-CN).



## THE OCEANOGRAPHY SOCIETY

4052 Timber Ridge Drive  
Virginia Beach, VA 23455 USA  
(757) 464-0131; fax: (757) 464-1759

### OFFICERS

Robert A. Duce, President  
Kenneth Brink, President-Elect  
Melbourne G. Briscoe, Secretary  
David Evans, Treasurer  
Margaret Leinen, Past-President

### COUNSELORS

Ann Gargett  
Larry Mayer  
Bess Ward  
Larry Atkinson  
Kenneth Brink  
Anthony Knap  
Robert F. Anderson  
Rick Spinrad

### EXECUTIVE DIRECTOR

Judi Rhodes

### CORPORATE/INSTITUTIONAL SPONSORS

Monterey Bay Aquarium Research Institute,  
Pacific Grove, CA, USA  
National Marine Fisheries Service,  
Silver Spring, MD, USA  
Ober, Kaler, Grimes & Shriver,  
Washington, DC, USA  
RD Instruments, San Diego, CA, USA  
Scripps Institution of Oceanography,  
La Jolla, CA, USA

## OCEANOGRAPHY

### CO-EDITORS

Larry P. Atkinson  
Center for Coastal Physical Oceanography  
Old Dominion University  
Crittenton Hall  
Norfolk, VA 23529  
(757) 683-5558  
Internet: atkinson@ccpo.odu.edu

Connie Sancetta  
National Science Foundation  
Ocean Sciences Division  
Room 725  
4201 Wilson Blvd.  
Arlington, VA 22230  
(703) 306-1586  
Internet: csancett@nsf.gov

### ASSOCIATE EDITORS

James W. Ammerman  
Department of Oceanography  
Texas A&M University  
College Station, TX 77843 USA  
(409) 845-5105

Gregg J. Brunskill  
Australian Institute of Marine Science  
PMB No. 3, Townsville, M.C.  
Queensland 4810, Australia  
(077) 789 211; FAX (077) 725 852;  
Internet: g\_brunskill@aims.gov.au

ASSOCIATE EDITORS (Continued)

Ellen R.M. Druffel  
 Department of Earth System Sciences, PSRF-207  
 University of California, Irvine, CA 92717  
 (714) 725-2116  
 Internet: druffel@bro.ps.uci.edu

Donald B. Olson  
 RSMAS  
 University of Miami  
 Miami, FL 33149 USA  
 (305) 361-4074  
 Internet: don@loquat.rsmas.miami.edu

Makoto Omori  
 Department of Aquatic Biosciences  
 Tokyo University of Fisheries  
 4-5-7, Konan, Minato-ku, Tokyo, Japan  
 (03)471-1251

Louis M. Prieur  
 Laboratoire de Physique et Chimie Marines  
 Observatoire Oceanologique de Villefranche sur Mer  
 BP 08 La Darse  
 06230 Villefranche Sur Mer, France  
 (33)93763739  
 Internet: prieur@ccrv.obs-vlfr.fr

Richard W. Spinrad  
 CORE  
 1755 Massachusetts Ave, NW Suite 800  
 Washington, DC 20036-2102  
 (202) 232-3900 x219

James Syvitski  
 Director, Institute of Arctic and Alpine Research  
 University of Colorado at Boulder  
 1560 30th St., Campus Box 450  
 Boulder, CO 80309-0450  
 (303) 492 7909  
 (303) 492 6388 (FAX)  
 email james.syvitski@colorado.edu

Peter Wadhams  
 Scott Polar Research Institute  
 University of Cambridge  
 Lensfield Road  
 Cambridge CB2 1ER England  
 223-336542  
 Internet: pw11@phx.cam.ac.uk

PRINTER  
 Lancaster Press  
 Lancaster, PA USA

A W A R D

**Thorpe Received 1997 Munk Award**

The 1997 winner of the Walter Munk Award for Distinguished Research in Oceanography Related to Sound and the Sea has been announced by the U.S. Navy and TOS. The Award Selection Committee has unanimously selected Dr. Stephen A. Thorpe of the Department of Oceanography, The University, Southampton, UK.

Dr. Thorpe was selected for his outstanding work and many contributions to the understanding of ocean processes, including his pioneering measurements on the generation of ocean bubbles by breaking waves using high-frequency acoustics, his seminal work on Langmuir circulation, and his investigations of the structure of turbulence in tidal passes based on sidescan measurements of the surface of the ocean. He has also made very significant contributions to our understanding of the role of bubbles in air/sea gas fluxes. The Selection Committee was very impressed with the insights Dr. Thorpe was able to develop on small scale physical oceanographic processes through the use of a relatively simple back-scatter sonar. He is recognized as an outstanding fluid dynamicist and physical oceanographer who has very effectively utilized acoustics to understand fundamental processes in the ocean.

In keeping with Dr. Munk's contributions to ocean science, the award is granted jointly by The Oceanography Society, the Office of Naval Research, and the Oceanographer of the Navy for:

- Significant original contributions to the understanding of physical ocean processes related to sound in the sea;
- Significant original contributions to applications of acoustic methods to that understanding; and/or
- Outstanding service that fosters research in ocean science and instrumentation contributing to the above.

To date this internationally prestigious award has been presented, in accordance with the above criteria, to three other eminent scientists.

- 1993 Dr. Walter Munk, Scripps Institution of Oceanography, USA
- 1994 Dr. David Farmer, Institute of Ocean Sciences, Canada
- 1996 Dr. Leonid Brekhovskikh, P. P. Shirshov Oceanology Institute, Russia

This issue was made possible by the U.S. Army Corps of Engineers and the Department of the Navy:

—Headquarters, U.S. Army Corps of Engineers (HQUSACE), under Civil Works Coastal Navigation Hydrodynamics Program Research Work Unit 32869, "Modeling the Evolution of Wave Spectra in Shallow Water." Funds were provided through the Coastal and Hydraulics Laboratory (CHL), U.S. Army Engineer Waterway Experiment Station.

—Department of Navy grant N00014-97-1-0851 issued by the Office of Naval Research.

**TABLE OF CONTENTS** *Continued*

MAPPING WIND DIRECTION WITH HF RADAR

By Daniel M. Fernandez, Hans C. Graber, Jeffrey D. Paduan  
 and Donald E. Barrick / 93

TOS STANDING COMMITTEES / 96

TOS AND IOC 1998 SCIENTIFIC MEETING / 97

ADDENDUM TO "THE OCEANOGRAPHY TEXT PATTERN: A REVIEW AND COMPARISON OF INTRODUCTORY OCEANOGRAPHY TEXTS"

By Richard W. Spinrad / 99

# INTRODUCTION TO HIGH-FREQUENCY RADAR: REALITY AND MYTH

By Jeffrey D. Paduan and Hans C. Graber

. . . we focus on the measurements of primary interest to coastal oceanographers . . .

THE CONCEPT OF USING high-frequency (HF) radio pulses to remotely probe the ocean surface has been around for decades. In this paper and the companion paper by Teague *et al.* (1997) we strive to introduce this technique to a broad oceanographic audience. Teague *et al.* (1997) provides the historical context plus an outline of different system configurations, whereas we focus on the measurements of primary interest to coastal oceanographers, i.e., maps of near-surface currents, wave heights, and wind direction. Another goal of this paper and, indeed, this entire issue is to present a realistic assessment of the state-of-the-art in HF radar techniques vis-à-vis coastal oceanography. When evaluating any new measurement technique, it is important to separate issues related to system design from fundamental limitations of the technique. The former are engineering shortcomings, which are subject to continuous improvement. The latter are real limitations in the use of the particular geophysical signal in the presence of realistic noise. Most of the “myths” about HF radar measurements, in our view, stem from the confusion of these two issues.

One common misconception about HF radar stems from the word “radar” itself. A more descriptive name would be HF “radio,” as the HF portion of the electromagnetic spectrum is within the radio bands. Figure 1 shows a broad range of the electromagnetic spectrum, including the nomenclature commonly applied to different portions of the spectrum. The HF band, with frequencies of ~3–30 MHz and wavelengths of ~10–100 m, sits between the spectral bands used for television and (AM) radio transmissions. Often, the term radar is applied to instruments operating in the microwave portion of the spectrum, for which wavelengths are measured in millimeters or centimeters.

Throughout oceanography, many different instruments exploit many different portions of the

electromagnetic spectrum. Figure 2 illustrates several of these remote sensing techniques used to extract information about the ocean surface. The figure is adapted from the review by Shearman (1981) and it contrasts space-borne systems, such as altimeters and scatterometers, which use microwave frequencies, with shore-based systems, which use a range of frequencies depending on the application. (Not shown are aircraft-borne systems, which also operate in the microwave band.) The figure also illustrates the different types of transmission paths, including true line-of-sight paths, “sky wave” paths, which reflect off the ionosphere, and “ground wave” paths, which exploit coupling of the radiowaves with the conducting ocean water to achieve extended ranges. For HF radars, instruments that operate using sky wave transmissions are often referred to as over-the-horizon (OTH) radars (e.g., Georges, 1980), although HF ground wave radars, which are the major focus of this issue, also achieve beyond-the-horizon ranges.

Reflection (or backscatter) of electromagnetic energy from the sea surface can be expected to produce an energy “spectrum” at the receiver, even if the energy source was single-frequency, because of the complicated shape and motion of the sea surface. Interpreting these spectral returns for various transmit frequencies is the key to extracting information about the ocean. Many instruments rely on a resonant backscatter phenomenon known as “Bragg scattering,” which results from coherent reflection of the transmitted energy by ocean surface waves whose wavelength is exactly one-half as long as the transmitted radar waves. The inset in Figure 2 attempts to illustrate this process by showing how energy reflected at one wave crest is precisely in phase with other energy that traveled  $\frac{1}{2}$  wavelength down and  $\frac{1}{2}$  wavelength back to reflect from the next wave crest. These coherent reflections result in a strong peak in the backscatter spectrum. Scatterometers exploit Bragg scattering from capillary waves (~1 cm) to obtain information about winds. HF radars, on the other hand, exploit Bragg scattering from surface

Jeffrey D. Paduan, Code OC/Pd, Naval Postgraduate School, Monterey, CA 93943, USA; Hans C. Graber, Rosenstiel School of Marine and Atmospheric Science, University of Miami, Miami, FL 33149-1049, USA.

gravity waves (~10 m) to obtain information about currents (and winds).

### Measuring Currents

The history of HF backscatter measurements is better outlined by Teague *et al.* (1997). We point to the work of Crombie (1955) as the first to identify strong sea echoes in the HF band with resonant Bragg scattering. Bragg waves in the HF band happen to be “short” surface gravity waves, which can be assumed to be traveling as deep-water waves, except in very shallow depths of a few meters or less. This is important because it allows information contained in the Doppler shift of Bragg peaks to be used to estimate ocean currents.

Figure 3 illustrates the Doppler technique for ocean current determination from HF radar backscatter. It shows an actual spectrum from the Ocean Surface Current Radar (OSCR) system. The spectrum contains obvious Bragg peaks due to the presence of Bragg waves traveling toward and away from the receiver. The frequencies of these peaks are offset from that of the transmitted energy for the two following reasons: 1) the Bragg waves are moving with the deep-water phase speed given by  $c = \sqrt{g\lambda/4\pi}$ , where  $\lambda$  is the wavelength of the transmitted energy and  $g$  is the gravitational acceleration and 2) the Bragg waves are moved by the underlying ocean current. Because the expected Doppler shift due to the Bragg waves is known, any additional Doppler shift is attributed to the current as shown in Figure 3.

It is important to keep in mind the following points about HF radar-derived currents: 1) a single radar site is capable of detecting only the component of flow traveling toward or away from the site for a given look angle; 2) the effective depth of the measurement depends on the depth of influence of the Bragg waves and is quite shallow (~1 m); 3) stable estimates require scattering from hundreds of wave crests plus ensemble averaging of the spectral returns, which sets the space-time resolution of the instruments; 4) the precision is limited by the frequency resolution of the Doppler spectrum and is typically 2–5 cm s<sup>-1</sup>; and 5) the accuracy is controlled by numerous factors, such as signal-to-noise ratios, pointing errors, and geometry.

Because a single radar station measures only the component of flow along a radial beam emanating from the site, “radial” currents from two or more sites should be combined to form vector surface current estimates. Figure 4 illustrates this principle using radial data from two radar sites. It also illustrates the “baseline problem” that occurs where both radar sites measure the same (or nearly the same) component of velocity, such as along the baseline between the sites or at great distances from both sites. Generally two radials must have an angle >30° and <150° to resolve the current vector. This geometric sensitivity is similar to the familiar geo-

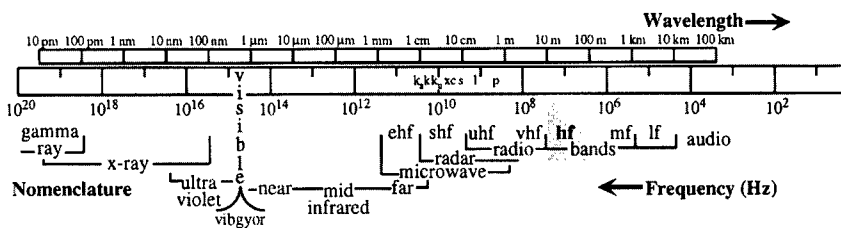


Fig. 1: Electromagnetic spectrum showing the HF band relative to other radio wave bands and the broader spectrum.

metric dilution of precision (GDOP) in the global positioning system (Chapman and Graber, 1997). If currents are assumed to be constant over several radial bins, it is also possible to estimate velocities using a single radar site as was done by Bjorkstedt and Roughgarden (1997), although the GDOP-related errors will be relatively large in this case.

The current measurement by HF radars is close to a “true” surface current measurement. Because radar pulses scatter off ocean waves, the derived currents represent an integral over a depth that is proportional to the radar wavelength. Stewart and Joy (1974) show this depth to be  $\sim d = \lambda/8\pi$ . Because wavelength depends on the radar frequency, it is feasible to use multifrequency HF radars to estimate vertical shear in the top two meters of the ocean.

Present system and coverage capabilities of HF radars are quite impressive. Measurements can be made in range as short as 1 km and as long as 150 km from the shore at a resolution of ~0.3–3 km along a radial beam. Radio interference or high sea states can limit the actual range at times as well as

The current measurement by HF radars is close to a “true” surface current measurement.

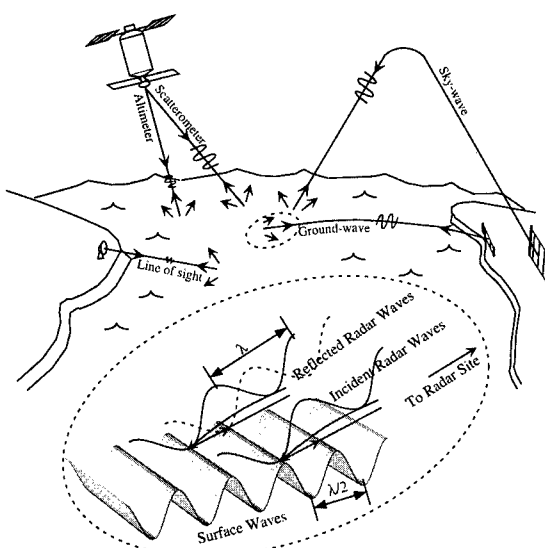


Fig. 2: Schematic representation of various remote sensing methods exploiting signals backscattered from the sea surface (adapted from Shearman, 1981). The inset illustrates the resonant Bragg scattering process that occurs due to reflection from waves whose wavelength is  $\frac{1}{2}$  as long as that of the incident energy.

the ground conditions in the vicinity of the receive antennas. Wet and moist sandy soils enhance the ground wave propagation, whereas dry and rocky grounds reduce signal strengths. Typical azimuthal resolutions are  $\sim 5^\circ$ . Near the coast, this gives a measurement width of  $\sim 0.5$  km; the width is  $\sim 10.0$  km at range cells 100 km offshore (Fig. 4).

### Measuring Winds and Waves

Although the focus of this special issue, and many of the experiments using ground wave HF radar systems, is on surface currents, it is also possible to extract information about surface waves and winds from HF backscatter spectra. Wave techniques are discussed by Wyatt (1997) and by Graber and Heron (1997), whereas the method for extracting wind direction is discussed by Fernandez *et al.* (1997). Very crudely, wave information is obtained by fitting a model of surface wave backscatter to the observed second-order portion of the spectrum (Fig. 3). That portion is due to reflections from waves at all frequencies and not just the resonant Bragg waves. Wind direction, on the other hand, is related to the ratio of the strength of the advancing and receding Bragg peaks.

### System Configurations

Although the basic scattering principle is the same for all existing HF radars, distinct differences are found in the antenna configurations that transmit and receive the electromagnetic signals. The compact antenna system utilized by the Coastal Ocean Dynamics Applications Radar (CODAR) consists of crossed loops and a whip for receiving and a whip for transmitting radio pulses (Barrick *et al.*, 1977). This antenna system is small and lends itself for deployment in highly populated and rocky coastal areas (e.g., cover photos). Radars of this type have been in use in the Monterey Bay area (Paduan and Rosenfeld, 1996; Paduan and Cook, 1997) and, with modifications, in Germany (Essen *et al.*, 1981). The omnidirectional characteristic of the cross-loop whip combination makes it possible to scan wider ocean sectors (e.g., Fig. 4), but this requires direction-finding techniques to determine angle for a given range cell (Lipa and Barrick, 1983; Barrick and Lipa, 1997).

In contrast, linear phased-array antennas consist of numerous (typically 8–16) elements separated by one ocean wavelength and aligned normal to the principal receive direction (e.g., cover photos). These radars, such as the University of Miami's OSCR system, are positioned at the seaward edge of a beach or cliff and require open space up to 100 m in length. The radio pulses are transmitted from a separate antenna array, which in the case of OSCR is a four-element Yagi array. Azimuthal resolution (direction) is obtained from well-established beam forming techniques. Other radars utilizing phased arrays are found in Germany (Gurgel

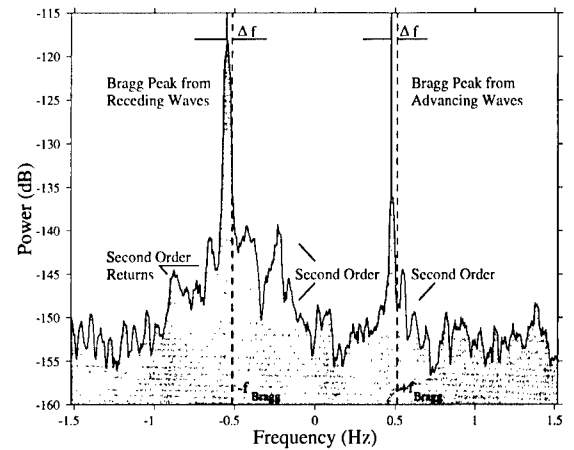


Fig. 3: Sample backscatter spectrum showing prominent Bragg peaks due to waves advancing toward and receding from the receiver. The smaller Doppler shift,  $\Delta f$ , is due to ocean currents that, in this example, are moving away from the receiver.

and Antonischki, 1997), Japan (Hisaki, 1996), Australia (Heron *et al.*, 1985), France (Forget *et al.*, 1981), Canada (Howell and Walsh, 1993), and United Kingdom (Wyatt, 1986; Prandle, 1991).

It is misleading to attempt to describe one HF radar configuration that will be optimum for all situations. Direction-finding (DF) and phased-array systems each have their advantages and disadvantages. For example, DF systems like CODAR were developed to be able to deploy the antennas on a small coastal outcrop, or even on a building, where a long secure stretch of beach or cliff may not be available. In addition, the angular coverage from DF techniques is much greater than the, at most,  $90^\circ$  sector that is available using phased-array pointing techniques.

At the same time, phased-array systems have important advantages over DF systems. Because the "beam" can be steered to a particular look direc-

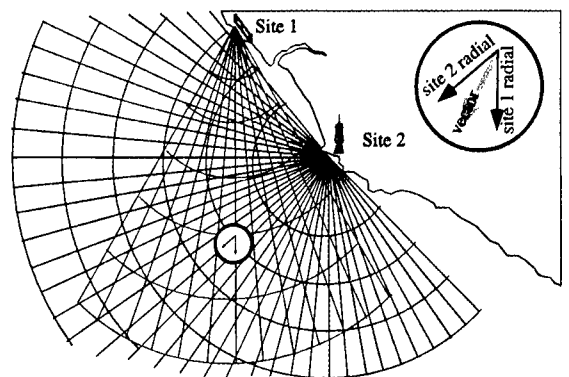


Fig. 4: Sample radial current coverage for a phased-array radar (site 1) covering a  $60^\circ$  swath and a direction-finding radar (site 2), which in principle can cover up to  $360^\circ$ . At overlapping ocean bins (e.g.,  $\odot$ ) a vector current estimate can be made, providing the angular separation between the radial currents is large enough.

... using ground wave HF radar systems. ... it is also possible to extract information about surface waves and winds ...

tion, it is possible to collect backscatter spectra from a single patch of ocean (e.g., Fig. 3) and, thereby, infer surface wave characteristics from the second-order portions of the spectra. (DF systems, by contrast, collect spectra on the basis of ocean backscatter over an entire range cell, which obscures the wave information.) The determination of wind direction is also more straightforward when using individual spectra from phased-array systems.

## Conclusions

The purpose of this special issue on HF radars is to describe in simple terms how the radars work and demonstrate the usefulness and capabilities of such instrument technology for today's problems in ocean research. The following short feature articles present a wide variety of applications that are important in physical and biological oceanography in the coastal zone. Beyond their utility to the scientist, these measurements are also of great interest to both military and civilian coastal engineers, public safety officers, and planners who must maintain navigational seaways, mitigate ocean pollution, conduct search and rescue operations, and attempt to balance the health of coastal habitats, public access, and private property rights.

The advantages of HF radar as a noninvasive measurement tool that can acquire vector surface current, wave, and wind information should be obvious. However, although the concept of this technology is old, its acceptance in science, government, and industry has been slow. Today there is no reason not to develop better hardware and software components while, simultaneously, exploiting what existing systems can tell us about the ocean. By analogy, the acoustic Doppler current meter (ADCP) was, a few years ago, considered experimental and mysterious by many in the oceanographic community, whereas now its use is common. We are confident that the use of HF radars will also become commonplace and, as a result, a new level of understanding of the coastal ocean will be possible.

## Acknowledgments

We thank D. Trizna, F. Herr, T. Kinder, and S. Sandgathe at ONR and C.L. Vincent at USAE/ONR for their long-range visions of HF radar's potential. The editors of this special issue on High-Frequency Radar Remote Sensing gratefully acknowledge the continued support of ONR through grants N00014-91-J-1775 (HIRES), 92-J-1807 (REINAS), 94-1-1016 (DUCK94), 95-3-0022 (MRY BAY), 96-1-1065 (COPE), and 97-1-0348 (SHOALING WAVES).

## References

- Barrick, D.E., M.W. Evans and B.L. Weber, 1977: Ocean surface currents mapped by radar. *Science*, 198, 138-144.
- Barrick, D.E. and B.J. Lipa, 1997: Evolution of bearing determination in HF current mapping radars. *Oceanography*, 10, 72-75.
- Bjorkstedt, E.P. and J. Roughgarden, 1997: Larval transport and coastal upwelling: an application of HF radar in ecological research. *Oceanography*, 10, 64-67.
- Chapman, R.D. and H.C. Graber, 1997: Validation of HF radar measurements. *Oceanography*, 10, 76-79.
- Crombie, D.D., 1955: Doppler spectrum of sea echo at 13.56 Mc/s. *Nature*, 175, 681-682.
- Essen, H.H., E. Mittelstaedt and F. Schirmer, 1981: On nearshore surface current measurements by means of radar. *Dtsch. Hydrogr. Z.*, 34, 1-14.
- Fernandez, D.M., H.C. Graber, J.D. Paduan and D.E. Barrick, 1997: Mapping wind direction with HF radar. *Oceanography*, 10, 93-95.
- Forget, P., P. Broche, J.C. De Maistre and A. Fontanel, 1981: Sea state frequency features observed by ground wave HF Doppler radar. *Radio Sci.* 16, 917-925.
- Georges, T.M., 1980: Progress toward a practical skywave sea-state radar. *IEEE Trans. Antennas Propag.*, AP-28, 751-761.
- Graber, H.C. and M.L. Heron, 1997: Wave height measurements from HF radar. *Oceanography*, 10, 90-92.
- Gurgel, K.-W. and G. Antonischki, 1997: Measurement of surface current fields with high spatial resolution by the HF radar WERA. *Proceedings, IEEE Int. Geoscience and Remote Sens. Symposium*, Singapore, 1820-1822.
- Heron, M.L., P.E. Dexter and B.T. McGann, 1985: Parameters of the air-sea interface by high-frequency ground-wave HF Doppler radar. *Aust. J. Mar. Freshwater Res.*, 36, 655-670.
- Hisaki, Y., 1996: Nonlinear inversion of the integral equation to estimate ocean wave spectra from HF radar. *Radio Sci.*, 31, 25-39.
- Howell, R. and J. Walsh, 1993: Measurement of ocean wave spectra using narrow beam HF radar. *IEEE J. Ocean. Eng.*, 18, 296-305.
- Lipa, B.J. and D.E. Barrick, 1983: Least-squares method for the extraction of surface currents from CODAR Crossed-loop data: Application at ARSLOE. *IEEE J. Ocean. Eng.*, 8, 226-253.
- Paduan, J.D. and M.S. Cook, 1997: Mapping surface currents in Monterey Bay with CODAR-type HR radar. *Oceanography*, 10, 49-52.
- and L.K. Rosenfeld, 1996: Remotely sensed surface currents in Monterey Bay from shore-based HF radar (CODAR). *J. Geophys. Res.*, 101, 20669-20686.
- Prandle, D., 1991: A new view of near-shore dynamics based on observations from HF radar. *Prog. Oceanogr.*, 27, 403-438.
- Shearman, E.D.R., 1981: Remote sensing of ocean waves, currents and surface winds by deka metric radar. In: *Remote Sensing in Meteorology, Oceanography and Hydrology*. A.P. Cracknell, ed. Ellis Horwood, London, 312-335.
- Stewart, R.H. and J.W. Joy, 1974: HF radar measurement of surface current. *Deep-Sea Res.*, 21, 1039-1049.
- Teague, C.C., J.F. Vesecky and D.M. Fernandez, 1997: HF radar instruments, past to present. *Oceanography*, 10, 40-44.
- Wyatt, L.R., 1986: The measurement of the ocean wave directional spectrum from HF radar Doppler spectra. *Radio Sci.*, 12, 473-485.
- , 1997: The ocean wave directional spectrum. *Oceanography*, 10, 85-89. □

The advantages of HF radar as a noninvasive measurement tool that can acquire vector surface current, wave, and wind information should be obvious.

# HF RADAR INSTRUMENTS, PAST TO PRESENT

By Calvin C. Teague, John. F. Vesecky  
and Daniel M. Fernandez

That observation launched the field that is now termed "radar oceanography," the use of radar systems to study oceanographic properties.

RADAR RETURNS FROM the ocean surface have been observed since the earliest days of radar. They were characterized as "clutter" because they often obscured targets, such as ships or aircraft. However, Crombie (1955) observed that some high-frequency (HF, 3–30 MHz) signals recorded near the sea had a distinctive Doppler shift of a fraction of a hertz above and below the transmitted signal. He correctly deduced that they were the result of Bragg scattering by ocean waves that were traveling radially toward or away from the radar and had a wavelength of one-half the radar wavelength. That observation launched the field that is now termed "radar oceanography," the use of radar systems to study oceanographic properties. Radar systems can be characterized by a number of parameters including operating frequency, geometry, platform, propagation mode, means of obtaining distance and angular resolution, etc. In the limited space of this paper only a few of the highlights of HF systems can be covered. For in-depth reviews, the reader is referred to articles by Croft (1972), Barrick (1978), and Shearman (1981, 1983).

## Radar Operation

An oceanographic radar differs somewhat from a radar intended to track ships or aircraft. First is the operating frequency; most aircraft radars operate at microwave frequencies with wavelengths on the order of centimeters, whereas the radars that are the subject of this issue operate in the HF range with wavelengths of tens of meters. This is important because the energetic ocean waves interact directly with an HF radar signal rather than in-

directly as they do in microwave systems. Second, because the wavelengths are so large the directivity that can be obtained by physical antennas is limited. Here we define directivity as a measure of the antenna array's capability to resolve a given direction. Third, direction scanning usually is confined to just azimuth, rather than azimuth and elevation. The main measurements performed by typical HF radars are the range or distance to the target, the direction to the target as a bearing from some reference azimuth, the Doppler frequency of the target, and the power of the signal returned by the target. Here, the target is a patch of ocean.

## Distance Measurement

*Single pulse.* The simplest means of determining distance is to use a short pulse of radar energy. The range resolution is given by  $ct/2$  where  $c$  is the velocity of light,  $3 \times 10^8$  m s<sup>-1</sup>, and  $t$  is the pulse width in seconds. A disadvantage of this technique is that if the pulse is short to obtain good range resolution, the average power transmitted power is low and so is the resulting signal-to-noise ratio of the received signal, thus limiting the radar range.

*Coded waveform.* An alternative to a single pulse is a coded waveform. Figure 1 illustrates an 11-element Barker code used to observe two targets of unequal amplitudes. The radar transmits a sequence of short pulses coded so their autocorrelation function has a single, sharp central peak and low sidelobes. The range resolution is determined by the width of the individual pulses but the average power is raised by the number of pulses in the sequence. There are some limitations to this approach, however. If the sequence is too long, short-range targets cannot be seen because a portion of the echo arrives while the later part of the sequence is still being transmitted. (Most radars cannot receive signals while they are transmitting, because of severe overloading of the receiver.) Figure 1 also illustrates another problem of coded waveforms; there can be spurious responses (range sidelobes) from strong targets. Both of these prob-

---

Calvin C. Teague, Space, Telecommunications and Radio-science Laboratory, Stanford University, Stanford, CA 94305-9515, USA; John F. Vesecky, Department of Atmospheric, Oceanic, and Space Science, 2455 Hayward, University of Michigan, Ann Arbor, MI 48109-2143, USA; Daniel M. Fernandez, Institute of Earth Systems Science and Policy, California State University, Monterey Bay, 100 Campus Center, Seaside, CA 93955-8001, USA.

lems can be reduced or eliminated by using more complicated waveforms, at the expense of additional data processing.

**FMCW.** Instead of transmitting short pulses, a radar can transmit a relatively long frequency-modulated (FM) continuous-wave (CW) signal as sketched in Figure 2. If the transmitted frequency is linearly swept and used as a reference for the received signals, a target at a particular range will produce a constant difference frequency whose value depends on its distance; more distant targets will produce higher frequencies. By analyzing the frequency content of the returned signal, targets at various ranges can be discerned. For most radars, the linear sweep is interrupted periodically to avoid overloading the receiver during reception of the echo.

#### Doppler Measurement

Doppler resolution, used to measure the velocity of the target, is obtained by repeating the range measurements, whether single pulse, coded waveform, or FMCW, at a regular rate and performing a time-series analysis on the samples obtained from each individual range measurement. A coherent integration time of  $T$  s provides a frequency resolution of roughly  $\Delta f = 1/T$  Hz. The target velocity resolution, in turn, is given by  $\Delta v = \lambda \Delta f / 2$   $m\ s^{-1}$ , where  $\lambda$  is the radar wavelength in meters.

#### Azimuth Angle Measurement

Because of the long wavelengths involved, HF radars do not physically move antennas to look in different directions. Rather, they control the direction to which they are sensitive electronically using a variety of techniques.

**Phased array.** Conceptually, the simplest antenna system is a phased array of identical receiving elements spaced no more than  $\lambda/2$  apart (to avoid severe sidelobes) with the line of the array perpendicular to the center of the desired set of beam directions. The beam is steered by adjusting the amplitude and phase of the signals from each of the elements and adding these signals coherently. The phase adjustment can be done using physical devices (coaxial cables, phase-shift networks, etc.) or digitally in the data processing after the signals from each element have been separately recorded. The angular resolution that can be obtained from an array with a total aperture of  $D$  is roughly  $\lambda/D$  radians. To obtain an angular resolution of  $5^\circ$  (0.1 radian), an aperture of  $10\lambda$  is required. In practice, it may not be possible to obtain enough area on a beach for this resolution, particularly at frequencies below 10 MHz.

**Synthetic aperture.** At the low end of the HF spectrum, it is impractical to obtain any appreciable directivity with a physical aperture. However, it is possible to use a technique borrowed from satellite technology, synthetic aperture. A simple antenna, for example, a loop or short whip, is carried along a straight line at a constant velocity that

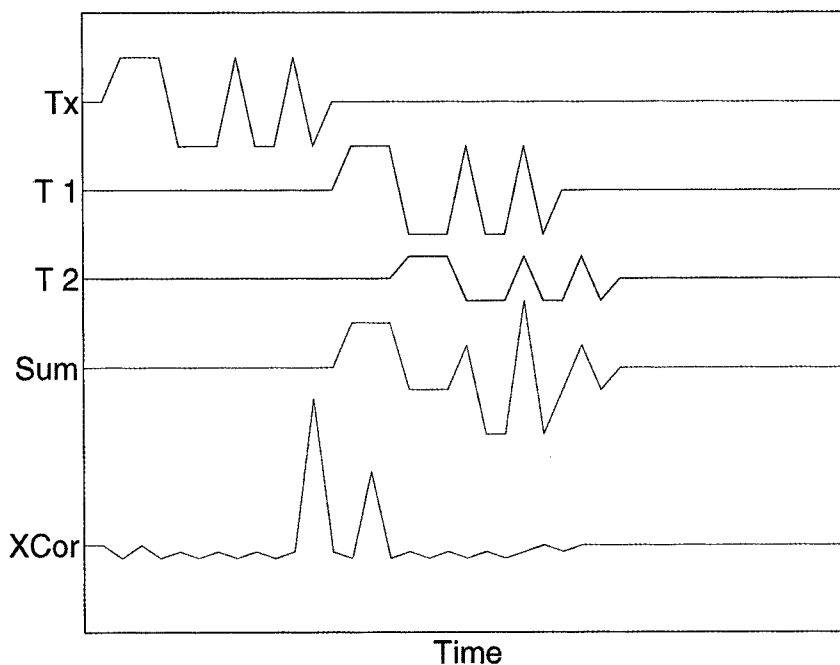


Fig. 1: Sketch of waveforms for a radar using an 11-element Barker code. The transmitted waveform ( $T_x$ ) is at the top, followed by individual returns from two discrete targets ( $T_1$ ,  $T_2$ ) of relative amplitude 1.0 and 0.5, their sum ( $Sum$ ), and the cross-correlation function ( $XCor$ ) between the received composite signal and the transmitted signal at the bottom. The two targets are clearly resolved.

is less than the phase velocity of the Bragg-resonant ocean waves. The motion of the antenna spreads a narrow Bragg line into a band of direction-dependent frequencies, and Fourier analysis of the signals can yield their direction of arrival if it is assumed that currents are insignificant compared with the phase velocity of the Bragg waves. This technique works best at low frequencies (2 MHz,  $\lambda = 150$  m) and apertures of up to 2 km have been synthesized this way (Tyler *et al.* 1974; Shearman 1981).

**Direction finding.** An alternative to the beamforming techniques is direction finding. The signals from two or more relatively closely spaced (Crombie 1972) or even co-located (Barrick *et al.*, 1977) antennas are compared, either in phase or amplitude. This is done at each frequency bin in the analysis bandwidth. With  $N$  antennas, it is possible to resolve at most  $N - 1$  directions at each frequency. A significant advantage of this technique is that the antennas are much smaller than in a phased array.

With all of these techniques, it is important that the amplitude and phase response of the antennas is very well known. Usually it is not sufficient to depend on ideal theoretical patterns or even electromagnetic modeling programs. Antenna-ground planes, cables, buried conductors, fences, and finite ground conductivity all contribute to the antenna patterns and ultimately they must be measured, usually with a portable signal source or a transponder. As the desired directivity

... the simplest antenna system is a phased array of identical receiving elements ...

An alternative to the beamforming techniques is direction finding.

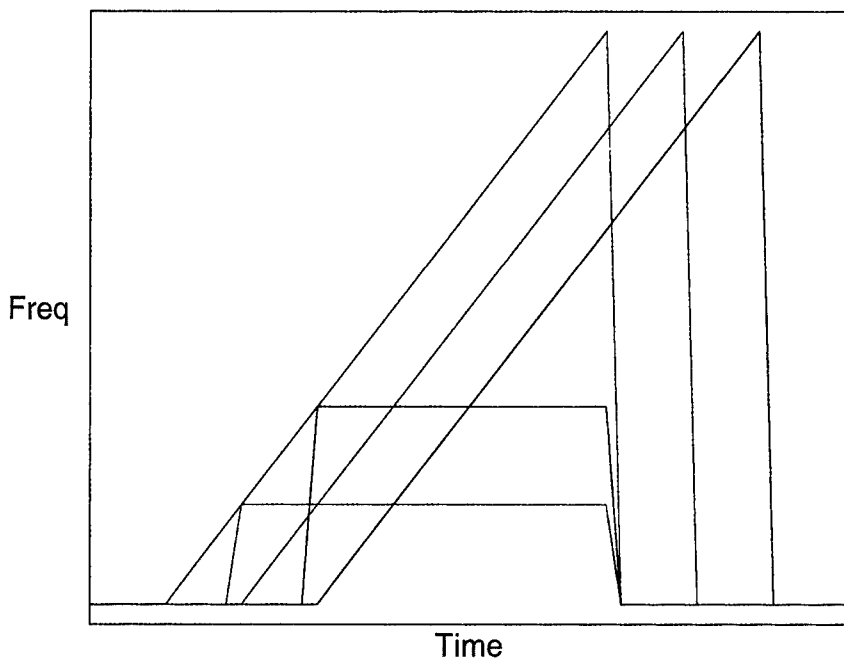


Fig. 2: Sketch of transmitted and received signals for an FMCW system. The transmitted waveform is shown in red, with returns from two different targets shown in green and blue. The frequency difference (---) between the transmitted and received signals is constant with time and has a larger value for more distant targets.

Another significant result from this experiment was a measure of the absolute value of the radar cross section of the ocean . . .

increases, so does the required precision of the required antenna pattern measurement.

#### Wave Measurements

Early wave measurements were made using both *monostatic* (co-located transmitter and receiver) and *bistatic* (separated transmitter and receiver) geometries, radars located on land and on ships, various antenna configurations, and surface wave and sky wave (ionospheric) radio propagation. Estimation of ocean wave parameters using surface-wave radars usually involves receiving first-order scattered signals from a wide range of angles and assumes that the sea is homogeneous over the area surveyed; sky-wave radars generally look in a narrow range of directions and make use of the second-order signals. A few key experiments are mentioned below.

#### Bistatic Geometry

In the late 1960s Allen Peterson of Stanford University collaborated with Walter Munk and Bill Nierenberg of the Scripps Institution of Oceanography to investigate techniques of using HF surface-wave radar to make oceanographic measurements over large areas. Under Office of Naval Research sponsorship, Peterson, C.C. Teague, and G.L. Tyler of the Radioscience Laboratory at Stanford began experiments along the northern California coast using Prof. Peterson's weekend cottage at Sunset Beach (south of Santa Cruz) as a field site. These experiments led to the first HF radar measurements of directional wave spectra for ocean

swell (Peterson *et al.*, 1970). They employed a bistatic geometry, which made use of LORAN-A transmitters operating near 1.9 MHz. These transmitters, now removed from service, had a peak power of many hundreds of kilowatts and used short pulses, so they made an ideal transmitter for a radar system. By receiving the direct signal and echoes a few hundred kilometers from the transmitter, it was possible to map a portion of the ocean-wave directional spectrum to the received Doppler shift by assuming that the sea was homogeneous over the observation region and that currents were small (Teague, 1971). However, because of gaps in coverage of the ocean wave spectrum, other techniques were sought.

#### Synthetic Aperture

*Steady state.* Several experiments were performed using a synthetic aperture receiving antenna in conjunction with LORAN-A transmitters. For these experiments, a small antenna was carried on a vehicle traveling in a straight line at a constant velocity close to the transmitter so that the geometry was essentially monostatic. In an experiment at Wake Island, a small island in the trade winds region, the directional distribution of 77 m ocean waves was measured under fully developed conditions (Tyler *et al.*, 1974). The directional distribution was found to be consistent with a  $\cos^s(\theta/2)$  form, with  $s$  in the range of 2–12, and with a small pedestal to account for ~1% of the wave energy traveling upwind. Another significant result from this experiment was a measure of the absolute value of the radar cross section of the ocean (Teague *et al.*, 1975). This measurement was made by observing the ratio of the echo energy to the direct energy from the transmitter a few kilometers from the receiver. Similar experiments were performed in the United Kingdom by Shearman *et al.* (1979) using a former LORAN-A transmitter in Wales.

*Wave growth and shadowing.* An experiment complementary to Wake Island was performed at Galveston, TX, along a long straight coastline (Stewart and Teague, 1980). Observations were made after the wind had shifted from onshore to offshore and the wave growth with distance and time was measured, again using a nearby LORAN-A transmitter. In Southern California wave shadowing by San Clemente and San Nicholas Islands was reported by Vesecky *et al.* (1980).

#### Phased Array

A dual-frequency phased-array radar was operated on the French Mediterranean coast by the University of Toulon (Broche, 1979) and used to estimate the significant wave height  $H_{1/3}$ , dominant wave frequency, and wind direction. A similar radar was used by the Institut Français du Pétrole in the Shetland Islands (Shearman, 1983). A multifrequency radar constructed at Stanford Univer-

sity was operated on a ship during the 1978 Joint Air-Sea Interaction (JASIN) experiment (Teague, 1986). Although the emphasis in this issue is on surface-wave propagation, several sky-wave phased-array radars employing very narrow beam widths have been used. Maresca and Georges (1980) describe the 2.5 km Wide Aperture Research Facility (WARF) operated by SRI International, and Georges and Harlan (1994) describe the use of military surveillance radars to obtain oceanic winds.

#### Direction Finding

In an early experiment Crombie *et al.* (1970) and Crombie (1972) used a multifrequency coherent radar with a pair of phased-receiving whip antennas to observe the growth of wave energy offshore of Barbados. Using one antenna in a nondirectional mode, Crombie also observed small but significant wave energy traveling in opposition to the wind (Crombie *et al.*, 1978). Direction-finding systems usually are used to measure currents rather than waves, as discussed in the next section.

#### Wind Measurements

Although HF radars do not directly respond to the wind, several researchers have estimated the direction and, in some cases, the speed of winds near the ocean surface by examining the signals scattered by the ocean waves raised in response to the wind. Long and Trizna (1973) used radar at Chesapeake Bay to map winds in the North Atlantic, and Stewart and Barnum (1975) evaluated the accuracy of that technique. Shearman and Wyatt (1982) describe the results of mapping winds during the JASIN experiment. Recent results from an experiment conducted at Duck, NC in 1994 show wind direction maps obtained with OSCAR (Fernandez *et al.*, 1997).

#### Current Measurements

Recently there has been considerable emphasis on mapping ocean currents. By examining the coherence between signals received on two closely spaced whips, Crombie (1972) observed that the phase of the coherence varied with Doppler frequency, implying that signals having different Doppler shifts were coming from different directions, and interpreted this as viewing a uniform current from different aspect angles. This result led to the development of the Coastal Ocean Dynamics Applications Radar (CODAR) (Barrick *et al.*, 1977; Lipa and Barrick 1983), which is the subject of several papers in this issue (Barrick and Lipa, 1997; Bjorkstedt and Roughgarden, 1997; Paduan and Cook, 1997). The CODAR system extends Crombie's direction-finding array to a compact set of co-located antennas and thus requires very little beach space for operation. Phased-array radars have also been used to measure currents. Stewart and Joy (1974) used a multifrequency radar on San Clemente Island to measure the ver-

tical current shear at two bearings. Ha (1979) used the multifrequency Stanford radar with a highly directional transmitting antenna to measure currents along its boresight and compared his measurements with drifting spar buoys. The same radar was used with a phased-array receiving antenna at Granite Canyon, south of Monterey, to study the effects of upwelling along the California coast (Fernandez, 1993; Shkedy *et al.*, 1995; Fernandez *et al.*, 1996). Maresca *et al.* (1980) examined tidal currents in the San Francisco Bay. Building on work by the CODAR, NOAA Wave Propagation Laboratory, and Stanford groups, a new array type HF radar system for the commercial market was developed by Marex Ltd., England. This radar, called Ocean Surface Current Radar (OSCR), uses a 16-element antenna array ~80 m long. OSCAR instruments have been used for mapping tidal and residual surface currents along the coasts of Britain (Prandle, 1987). OSCAR units have been sold in the United States; the Rosenstiel School of Marine and Atmospheric Science of the University of Miami used a pair of OSCAR radars for coastal observations in a number of locations (Shay *et al.*, 1995; Graber *et al.*, 1996). A new multifrequency radar was constructed jointly by the University of Michigan, the Environmental Institute of Michigan, and Stanford and is in operation at Santa Cruz, CA.

#### Conclusions

Over the past 25 years HF radar systems have been used to measure the directional distribution of wave energy in the open ocean, the growth of waves offshore after a sudden change in wind direction because of a frontal passage, ocean current shear from a ship in the open ocean, and current and current shear from land-based locations. With proper calibration and data processing, HF radar is capable of providing wide-area measurements that are difficult or impossible to make any other way, and the radar data can provide useful supplements to conventional oceanographic measurements.

#### References

- Barrick, D.E., 1978: HF radio oceanography—a review. *Boundary-Layer Meteorol.*, 13, 23–44.
- , M.W. Evans and B.L. Weber, 1977: Ocean currents mapped by radar. *Science*, 198, 138–144.
- and B.J. Lipa, 1997: Evolution of bearing determination in HF current-mapping radars. *Oceanography*, 10, 72–75.
- Bjorkstedt, E. and J. Roughgarden, 1997: Larval transport and coastal upwelling: an application of HF radar in ecological research. *Oceanography*, 10, 64–67.
- Broche, P., 1979: Estimation du spectre directionnel des vagues par radar decametrique coherent. In: *AGARD Conference Proceedings on Special Topics in HF Propagation*, 263, AGARD, Clearinghouse for Federal Scientific and Technical Information, Springfield, VA, 31-1–31-12.
- Croft, T.A., 1972: A means for observing our environment at great distances. *Rev. Geophys. Space Phys.*, 10, 73–155.

HF radar is capable of providing wide-area measurements that are difficult or impossible to make any other way . . .

- Crombie, D.D., 1955: Doppler spectrum of sea echo at 13.56 Mc/s. *Nature*, 175, 681-682.
- , 1972: Resonant backscatter from the sea and its application to physical oceanography. *IEEE International Conference Proceedings on Engineering in the Ocean Environment*, IEEE, New York, 174-179.
- , K. Hasselmann and W. Sell, 1978: High-frequency radar observations of sea waves travelling in opposition to the wind. *Boundary-Layer Meteorol.*, 13, 45-54.
- , J.M. Watts and W.M. Beery, 1970: Spectral characteristics of HF ground wave signals backscattered from the sea. *AGARD Conference Proceedings*, 77, AGARD, Clearinghouse for Federal Scientific and Technical Information, Springfield, VA, 16-1-16-6.
- Fernandez, D.M., 1993: High-frequency radar measurements of coastal ocean surface currents. Ph.D. dissertation, Stanford University, 191 pp.
- , J.F. Vesecky and C.C. Teague, 1996: Measurements of upper ocean surface current shear with high-frequency radar. *J. Geophys. Res.*, 101, 28,615-28,625.
- , H.C. Graber, J.D. Paduan and D.E. Barrick, 1997: Mapping wind direction from HF radar. *Oceanography*, 10, 93-95.
- Georges, T.M. and J.A. Harlan, 1994: New horizons for over-the-horizon radar? *IEEE Antennas Propag. Magazine*, 36, 14-24.
- Graber, H.C., D.R. Thompson and R.E. Carande, 1996: Ocean surface features and currents measured with SAR interferometry and HF radar. *J. Geophys. Res.*, 101, 25813-25832.
- Ha, E.C., 1979: Remote sensing of ocean surface current and current shear by HF backscatter radar. Ph.D. dissertation Tech. Rep. D415-1, Stanford Electronics Labs, Stanford University, 134 pp.
- Lipa, B.J. and D.E. Barrick, 1983: Least-squares method for the extraction of surface currents from CODAR crossed-loop data: application at ARSLOE. *IEEE J. Ocean Eng.*, 8, 226-253.
- Long, A.E. and Trizna, D.B., 1973: Mapping of North Atlantic winds by HF radar sea backscatter interpretation, *IEEE Trans. Antennas Propag.*, AP-21, 680-685.
- Maresca, J.W., Jr. and T.M. Georges, 1980: Measuring rms waveheight and the scalar ocean wave spectrum with HF sky wave radar. *J. Geophys. Res.*, 85, 2759-2771.
- , Jr., R.R. Pladden, R.T. Cheng and E. Seibel, 1980: HF radar measurements of tidal currents flowing through the San Pablo Strait, San Francisco Bay. *Limnol. Oceanogr.*, 25, 929-935.
- Paduan, J.D. and M.S. Cook, 1997: Mapping currents in Monterey Bay with CODAR-type HF radar. *Oceanography*, 10, 49-52.
- Peterson, A.M., C.C. Teague and G.L. Tyler, 1970: Bistatic radar observations of long-period directional ocean-wave spectra with LORAN-A. *Science*, 170, 158-161.
- Prandle, D., 1987: The fine-structure of nearshore tidal and residual circulations revealed by H.F. radar surface current measurements. *J. Phys. Oceanogr.*, 17, 231-245.
- Shay, L.K., H.C. Graber, D.B. Ross and R.D. Chapman, 1995: Mesoscale ocean surface current structure detected by high-frequency radar. *J. Atmos. Ocean. Tech.*, 12, 881-900.
- Shearman, E.D.R., 1981: Remote sensing of ocean waves, currents and surface winds by dekameter radar. In: *Remote Sensing in Meteorology, Oceanography and Hydrology*. A.P. Cracknell, ed., Ellis Horwood, London, 312-334.
- , 1983: Radio science and oceanography. *Radio Sci.*, 18, 299-320.
- and L.R. Wyatt, 1982: Dekametric radar for surveillance of sea-state and oceanic winds. *J. Navig.*, 35, 397-409.
- , W.A. Sandham, E.N. Bramley and P.A. Bradley, 1979: Ground-wave and sky-wave sea-state sensing experiments in the UK. *AGARD Conference Proceedings on Special Topics in HF Propagation*, 263, AGARD, Clearinghouse for Federal Scientific and Technical Information, Springfield, VA, 30-1-30-11.
- Shkedy, Y., D. Fernandez, C. Teague, J. Vesecky and J. Roughgarden, 1995: Detecting upwelling along the central coast of California during an El Niño year using HF-radar. *Cont. Shelf Res.*, 15, 803-814.
- Stewart, R.H. and J.W. Joy, 1974: HF radio measurement of surface currents. *Deep-Sea Res.*, 21, 1039-1049.
- , J.R. Barnum, 1975: Radio measurements of oceanic winds at long ranges: an evaluation. *Radio Sci.*, 10, 853-857.
- and C.C. Teague, 1980: Dekameter radar observations of ocean wave growth and decay. *J. Phys. Oceanography*, 10, 128-143.
- Teague, C.C., 1971: Bistatic radar techniques for observing long wavelength directional ocean-wave spectra. *IEEE Trans. Geosci. Electr.*, GE-9, 211-215.
- , 1986: Multifrequency HF radar observations of currents and current shears. *IEEE J. Ocean. Eng.*, OE-11, 258-269.
- , G.L. Tyler and R.H. Stewart, 1975: The radar cross section of the sea at 1.95 MHz: comparison of in-situ and radar determinations. *Radio Sci.*, 10, 847-852.
- Tyler, G.L., C.C. Teague, R.H. Stewart, A.M. Peterson, W.H. Munk and J.W. Joy, 1974: Wave directional spectra from synthetic aperture observations of radio scatter. *Deep-Sea Res.*, 21, 989-1016.
- Vesecky, J.F., S.V. Hsiao, C.C. Teague, O.H. Shemdin and S.S. Pawka, 1980: Radar observations of waves in the vicinity of islands. *J. Geophys. Res.*, 85, 4977-4986. □

# SYNOPTIC MEASUREMENT OF DYNAMIC OCEANIC FEATURES

By Brian K. Haus, Hans C. Graber  
and Lynn K. Shay

**S**HORE-BASED RADAR systems operating at the high-frequency (HF) mode are becoming a widely used and accepted tool for measuring surface currents for coastal oceanographic research. Their history, theory of operation, and accuracy relative to other sensors are discussed elsewhere in this issue. We will focus on the advantages of the HF radar sampling strategy.

The Ocean Surface Current Radar (OSCR) HF (25.4 MHz) radar provides a time series of surface currents at each of its 700 measurement cells. Current velocities have been reported to agree with moorings and shipboard current observations to within 10–15% over a wide range of conditions by Matthews *et al.* (1987), Shay *et al.* (1995), Chapman *et al.* (1997) and Graber *et al.* (1997). This order of agreement between sensors is obtained even though there are considerable differences in measurement depth and spatial and temporal sampling resolution. The advantage of HF radars is their capability to sample a large region synoptically at a resolution on the order of 1 km, which provides maps of dynamic flow features that can greatly enhance understanding of important oceanic processes.

Four different OSCR experiments conducted between 1993 and 1996 will be discussed in the context of the different types of oceanic processes that can be effectively sampled. In each of these experiments the OSCR system was used in conjunction with *in situ* observations, which greatly enhance the utility of the measurements.

## Gulf Stream Frontal Features and Mesoscale Eddies

Strong reversals in current meter records were first associated with cyclonic eddies that form along the inshore edge of the Florida Current by Lee (1975). A synoptic picture of these spin-off eddies was obtained using OSCR in a joint study

on pollution transport and fish larvae recruitment off the Florida Keys during May 1994 (Fig. 1). Numerous small scale eddies entered the OSCR domain from the west and exited to the east. These eddies traversed the domain on a timescale of every 2–5 d. The surface expression of these features was easily detected in the OSCR current maps. Vortex-like circulation features were identified with a diameter of 10–30 km and swirl speeds of 10–50 cm s<sup>-1</sup> (Graber *et al.* 1995). The path of the spin-off eddies was generally along the 150-m isobath, which is marked by the presence of the

The advantage of HF radars is their capability to sample a large region synoptically . . .

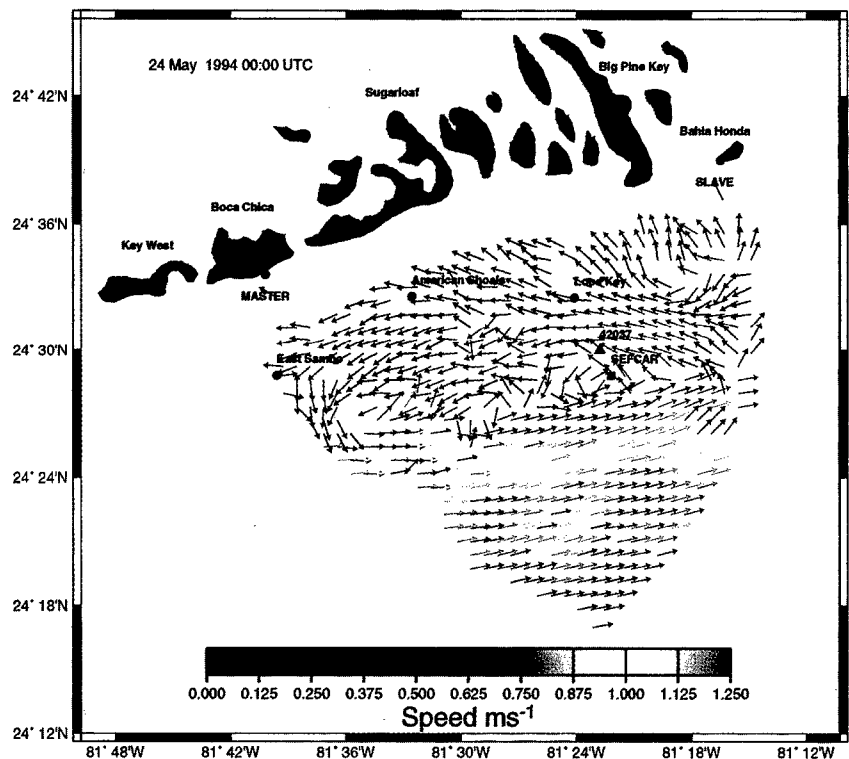


Fig. 1: Surface currents measured using OSCR off the Florida Keys on 24 May 1994 at 0000 GMT. "Master" and "Slave" denote the locations of the two radar stations required to measure vector currents. Looe Key, American Shoals, and East Sambo are shallow coral reefs where bottom-mounted current meters were located. The bathymetry drops off sharply outside these reefs.

Brian K. Haus, Hans C. Graber, and Lynn K. Shay, Rosenstiel School of Marine and Atmospheric Science, University of Miami, 4600 Rickenbacker Causeway, Miami, FL 33149-1049, USA.

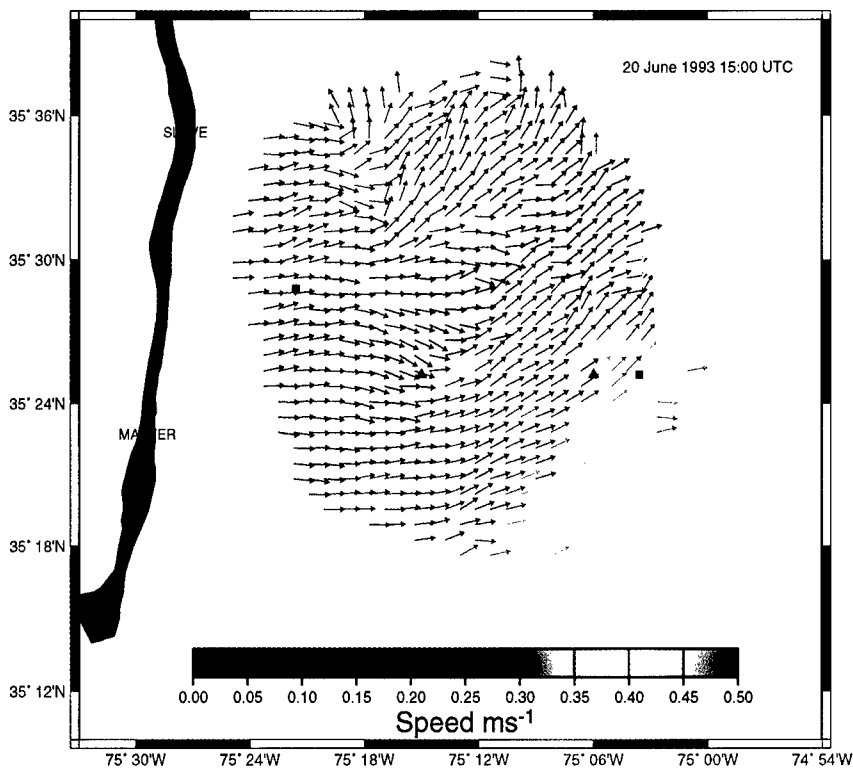


Fig. 2: Surface currents measured using OSCAR during the HighRes-II experiment on 1500 UTC 20 June 1993. ■, positions of current meter moorings; ▲, National Data Buoy Center wave buoys. Note the strong frontal feature in the center of the domain that resulted from the collision of two water masses.

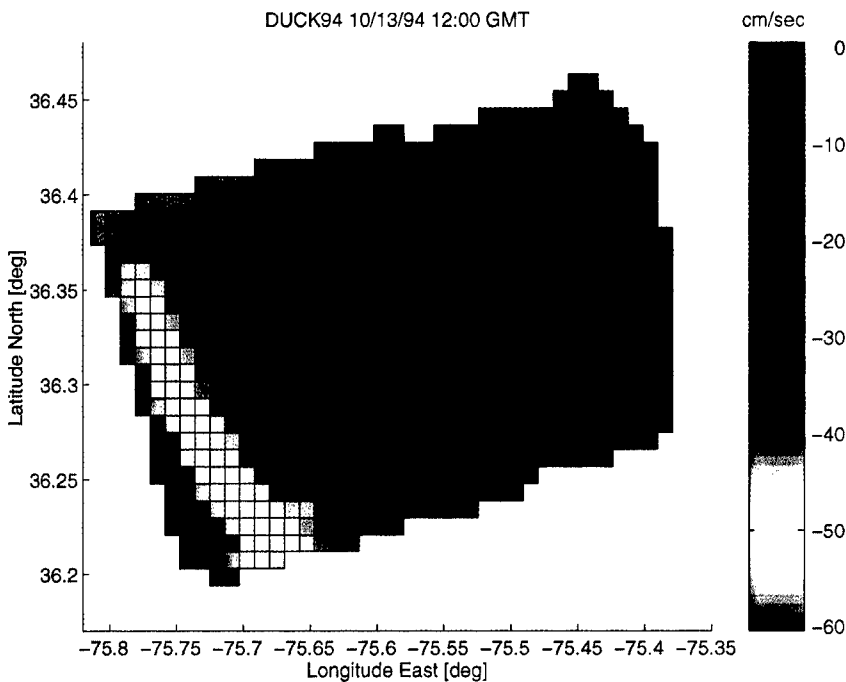


Fig. 3: Detided along-shelf velocities measured by OSCAR during the DUCK94 experiment in October 1994. Negative velocities denote flow toward the southeast in the direction of Kelvin wave propagation.

SouthEast Florida And Caribbean Recruitment program (SEFCAR) buoy in Figure 1, and their propagation speed was  $\sim 1$  km/h.

Limouzy-Paris *et al.* (1997) used these measurements to study the translocation of coral reef fish larvae. The OSCAR surface current maps provided the time, length, and velocity scales of the small scale eddies. Combining these maps with biological measurements of abundance was useful for assessing the recruitment and translocation patterns of coral reef fish larvae in ways that were not possible by conventional measurement techniques (see Graber and Limouzy-Paris, 1997, this issue).

During the high resolution remote sensing experiment (HighRes-II) experiment off the Outer Banks of North Carolina, the OSCAR system was operated for 1 mo. The measurement region was strongly impacted by the position of the "North Wall" of the Gulf Stream. In Figure 2 the surface currents when the Gulf Stream meandered closer to shore are shown. The OSCAR can clearly show the shear in this region as well as frontal features. Convergence and divergence of surface currents can be identified, precisely located, and quantified using the OSCAR data. This is very useful for interpreting interferometric synthetic aperture radar (INSAR) images, because they are strongly influenced by surface currents that may concentrate or diffuse wave energy (Graber *et al.* 1996). The increased concentration of surfactant material in a convergence zone can also have a strong influence on short ocean surface waves.

Although other remote sensing techniques such as advanced very high resolution radiometer (AVHRR) could also show the position of the Gulf Stream North Wall, the presence of flow features is not always marked by temperature changes. This is the case with the buoyant coastal current emanating from the Chesapeake Bay (discussed in the next section), which did not have a significant temperature difference from the ambient shelf water during October 1994. Multispectral sensors would be required to identify this type of frontal boundary.

### Coastal Buoyancy Current

A series of OSCAR observations were obtained during the DUCK94 experiment at the U.S. Army Corps of Engineers Field Research Facility at Duck, NC, in October 1994 (Haus *et al.*, 1995). Three periods of downwelling favorable winds ( $>10$  m s<sup>-1</sup>) were observed during the month of measurements.

During downwelling favorable winds, buoyant water that is propagating at increased speeds relative to the ambient shelf water is forced against the coast and becomes organized into a coastal current (Fig. 3). The coastal current reacts rapidly to shifts in the wind direction. The offshore edge of the buoyant flow moved 5 km closer to shore over a period of 6 h on 10 October 1994 when the

wind turned more onshore. This corresponds to a frontal propagation speed relative to the ground of  $23 \text{ cm s}^{-1}$ . The coastal current has a large degree of variability in the along-shelf direction; bulges and gaps are observed even during periods of consistent downwelling winds. When the buoyant jet was forced close to the coast during the three strong downwelling events, salinity measurements at moorings show that the buoyant flow may contact the bottom (Haus *et al.*, 1996).

It is clear from the surface current maps that under varying wind regimes, buoyancy and wind forcing interact to drive nearshore circulation patterns. Hickey and Hamilton (1980) used a spin-up model of the Washington-Oregon shelf to determine that the buoyancy flow could become detached from the shelf during upwelling winds. Khourafalou *et al.* (1996) used a 3-D Blumberg-Mellor model for the circulation of the south Atlantic bight to simulate the effects of wind and discharge rates on a coastal buoyancy current. They found that it is possible to have a southward flowing buoyancy current in nearshore waters opposing the predominant wind direction, particularly during periods of strong runoff and light upwelling winds. The OSCR surface current maps collected during DUCK94 show the advection of low salinity water up to 35-km offshore during upwelling winds. Nearshore water was also observed moving southward against the wind direction consistent with the model of Khourafalou *et al.* (1996).

Münchow and Garvine (1993) showed that the Delaware Bay coastal current contacts the bottom in the absence of upwelling favorable winds. They contrasted this with previous work on the Chesapeake Bay outflow that had showed a thin layer of buoyant flow. The ratio of the horizontal shear to the Coriolis parameter was of order one in the source region near the estuary mouth. Further downstream in the coastal current region, they found that this ratio was much smaller. Our results for the spatial distribution of this ratio show a much more complex picture of the coastal current shear. Under both wind regimes there are regions of high lateral shear where the ratio is  $O(1)$ . The water mass boundaries are much sharper and lead to higher shear than Münchow and Garvine (1993) suggest. The high resolution of the OSCR fields and the ability to accurately define the vorticity from gridded surface current fields allows the observation of these localized regions of high lateral shear.

The value of synoptic surface current measurements when used in combination with moorings or shipboard profilers is obvious in the spatial variation of the position and speed of the buoyant coastal current. There is no way to select a single location or even a transect that would adequately describe the behavior of the coastal current in this region, even though the coastline is relatively straight and there are no large bathymetric features. A shipboard survey can cover the region, but it would take a least a day to traverse the nearshore (within 20 km of the coast) enough times to define

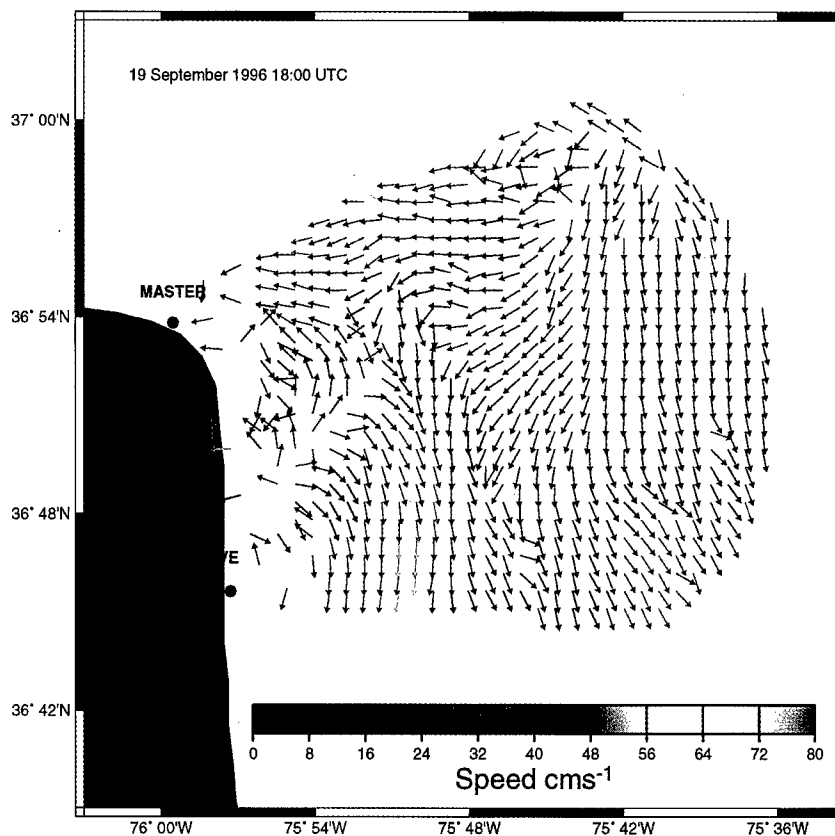


Fig. 4: Surface currents measured by OSCR during the COPE experiment on 1800 UTC 19 September 1996. The currents shown were measured during a tidal inflow into Chesapeake Bay.

the jet shape as it moves along the coast. With a large degree of changes occurring to the jet position and shape in only 6 h, an inaccurate picture of the coastal current behavior would result. During accelerating or decelerating flow a ship survey running two transects at the northern and southern reaches of the OSCR domain would reach different conclusions on the change in the width of the coastal current depending on the order in which the transects were conducted. Matthews (1997) simulated processes such as mesoscale eddies and frontal meanders and showed that a shipboard survey using towed instruments led to a 40–50% increase in the root mean square (rms) error because of temporal changes in the features.

#### Estuarine-Shelf Interactions

The Chesapeake outfall plume experiment (COPE) was conducted using the OSCR HF radar just south of the Chesapeake Bay mouth in October 1996. The surface currents without tidal constituents removed are shown in Figure 4 for a tidal flow moving into Chesapeake Bay. There is a very complex flow pattern during the incoming tide that is strongly influenced by the local bathymetry and wind direction. The overall flow is toward the south, with westerly inflow occurring offshore of the mouth. There are indications that there is flow

Our results for the spatial distribution of this ratio show a much more complex picture of the coastal current shear.

exiting the mouth very close to the master site at Cape Henry, VA. There is also a divergence region between flow moving into the bay and the ambient southward flow at 36°51'N and 75°54'W. Faster moving nearshore flow is most likely because of the buoyancy forcing on fresher water that has exited the estuary. The complexity of these flow patterns emphasizes the difficulty in making *in situ* observations that are representative of the entire flow field.

### Conclusion

HF radars are a valuable tools for measuring ocean processes in a variety of dynamic regimes. The synoptic coverage and well-defined sampling location and interval of the radar measurements are very useful for quantifying tidal flow patterns, submesoscale eddies, coastal buoyancy currents, and estuarine-shelf exchange processes. This is by no means an exhaustive list of the applications of HF radar technology to coastal oceanographic research. The OSCAR system can provide valuable regional surface current vectors and wave height information. However, combining remote sensing with *in situ* observations of important parameters of interest, such as the vertical current structure, salinity, or larval concentrations, can lead to new insights in coastal and biological oceanography.

### Acknowledgments

The authors thank Jorge Martinez, Louis Chemi, John Hargrove, and Nick Peters, whose dedicated field work with OSCAR in all of these experiments was invaluable, and Slavica Nikolic who produced the graphics. The results discussed here were funded by the Office of Naval Research through grants N00014-91-J-4133 and N00014-91-J-1775 (HighRes), N00014-94-1-1016 (DUCK94), and N00014-96-1-1065 (COPE-I) and by the U.S. Coast Guard through SFOSRC/OPRC.

### References

Chapman, R.D., L.K. Shay, H.C. Graber, J.B. Edson, A. Karachintsev, C.L. Trump and D.B. Ross, 1997: On the accuracy of HF radar surface current measurements: in-

tercomparisons with ship-based sensors. *J. Geophys. Res.*, 102, 18,737-18,748.

Graber, H.C., B.K. Haus, L.K. Shay and R.D. Chapman, 1997: HF radar comparisons with moored estimates of current speed and direction: Expected differences and implications. *J. Geophys. Res.*, 102, 18,749-18,766.

———, T.N. Lee, B.K. Haus, C.G.H. Rooth, E.J. Williams and L.K. Shay, 1995: Observations of ocean surface currents off the south Florida Keys using an HF Doppler radar. South Florida Oil Spill Research Center Report, University of Miami, Miami, FL, 177 pp.

——— and C.B. Limouzy-Paris, 1997: Transport patterns of tropical reef fish larvae by spin-off eddies in the Straits of Florida. *Oceanography*, 10, 68-71.

———, D.R. Thompson and R.E. Carande, 1996: Ocean surface features and currents measured with SAR interferometry and HF radar. *J. Geophys. Res.*, 101, 25813-25832.

Haus, B.K., H.C. Graber and L.K. Shay, 1996: Observations of a coastal buoyant jet with HF Doppler radar. Proc. OCEANS 96 MTS/IEEE, Marine Technology Society, Ft. Lauderdale, FL, 1032-1037.

———, H.C. Graber, L.K. Shay and J. Martinez, 1995: Ocean surface current observations with HF Doppler radar during DUCK94 experiment. Technical Report RSMAS 95-010, University of Miami, Miami, FL, 104 pp.

Hickey, B.M. and P. Hamilton, 1980: A spin-up model as a diagnostic tool for interpretation of current and density measurements on the continental shelf of the Pacific northwest. *J. Phys. Oceanogr.*, 10, 12-24.

Khourafalou, V.H., T.N. Lee, L.-Y. Oey and J.D. Wang, 1996: The fate of river discharge on the continental shelf. I. Modeling the river plume and the inner shelf coastal current. *J. Geophys. Res.* 101, 3415-3434.

Lee, T.N., 1975: Florida Current spin-off eddies. *Deep-Sea Res.*, 22, 753-765.

Limouzy-Paris, C.B., H.C. Graber, D.L. Jones, A. Röpke and W.J. Richards, 1997: Translocation of larval coral reef fishes via sub-mesoscale spin-off eddies from the Florida Current. *Bull. Mar. Sci.*, 60, 966-983.

Matthews, J.P., J.H. Simpson and J. Brown, 1987: Remote sensing of the shelf sea currents using an HF radar system. *J. Geophys. Res.*, 93, 2302-2310.

Matthews, P.A., 1997: The impact of nonsynoptic sampling on mesoscale oceanographic surveys with towed instruments. *J. Atmos. Ocean. Tech.*, 14, 162-174.

Münchow, A. and R.W. Garvine, 1993: Dynamical properties of a buoyancy-driven coastal current. *J. Geophys. Res.*, 98, 293-322.

Shay, L.K., H.C. Graber, D.B. Ross and R.D. Chapman, 1995: Mesoscale ocean surface current structure detected by high-frequency radar. *J. Atmos. Ocean. Tech.*, 12, 881-900. □

. . . combining remote sensing with *in situ* observations . . . can lead to new insights in coastal and biological oceanography.

# MAPPING SURFACE CURRENTS IN MONTEREY BAY WITH CODAR-TYPE HF RADAR

By Jeffrey D. Paduan and Michael S. Cook

**H**IGH-FREQUENCY (HF) radar measurements have been employed around Monterey Bay, CA, to measure ocean surface currents since February 1992. The first array consisted of two older-generation CODAR instruments located at sites near Monterey in the south and Moss Landing, halfway around the bay to the north (Front Cover; Fig. 1). In 1994, the southern site was replaced with a newer-generation SeaSonde system at Pt. Pinos and a similar unit was installed near Santa Cruz on the northern shore of Monterey Bay. Finally, in 1996, the CODAR system in Moss Landing was replaced by a modern SeaSonde unit.

Several months time series of two-dimensional surface currents have been collected for Monterey Bay since the first CODAR units were installed. These data represent the most extensive measurements collected to date from compact, direction-finding HF radar systems (Barrick and Lipa, 1997; Paduan and Graber, 1997). Indeed, Monterey Bay is the only location where continuous HF radar measurements are underway. The geometry of the bay (a curving coastline with a radius of ~20 km) is ideal for a multisite HF radar network. The overwater distance is close to the typical radar range and, when three or more shore locations are utilized, the entire region can be observed without lost coverage along the baseline between radar sites.

This geometry also makes Monterey Bay well suited for validation and development of the algorithms for currents, waves, and wind direction because a large ocean region is oversampled. Not only can *in situ* measurements within this region be compared with the remotely sensed estimates, but self-consistency (or lack thereof) in the HF radar measurements can be used to characterize errors in the radar data (Melton, 1995).

---

Jeffrey D. Paduan and Michael S. Cook, Oceanography Department, Code OC/Pd, Naval Postgraduate School, Monterey, CA 93943, USA.

## Dominant Current Patterns

Surface currents around Monterey Bay have strong modes of variability that are well separated in terms of the process timescales. At the longer timescales (weeks to months), the HF radar-derived currents show mesoscale patterns that evolve with major wind reversals and the proximity of mesoscale eddies (Paduan and Rosenfeld, 1996). At the shorter timescales, current fluctuations are dominated by semidiurnal tidal forcing and diurnal wind (seabreeze) forcing (Foster, 1993; Petrucio, 1993).

## Subtidal Current Patterns

Paduan and Rosenfeld (1996) compared five month-long time series of radar-derived current with moored current observations at the Monterey Bay Aquarium Research Institute (MBARI) mooring site M1 (Fig. 1). Both time series were low-pass filtered to remove diurnal and shorter-period fluctuations revealing significant correlation dominated by reversals in the alongshore flow on timescales of a few weeks. These surface current reversals are related to the wind and to cross-shore movement of a warm-core eddy feature often observed near Monterey Bay.

A major advantage of HF radar measurements is their ability to describe these processes in two dimensions. Complicating this description, however, is the rapid response of the ~1 m currents to changes in the wind. The agreement between radar-derived current and deeper flow, or between radar-derived current patterns and temperature patterns, can depend on the elapsed time since the last major wind shift.

An example of the subtidal-period surface current pattern during upwelling conditions is shown on the cover of this issue, together with satellite-derived sea surface temperatures. Several recurring features of the summertime circulation are evident in that figure, including cyclonic flow within Monterey Bay, strong equatorward flow across the mouth of the Bay coincident with a plume of upwelled water originating from further north, and

... the HF radar-derived currents show mesoscale patterns that evolve with major wind reversals and the proximity of mesoscale eddies.

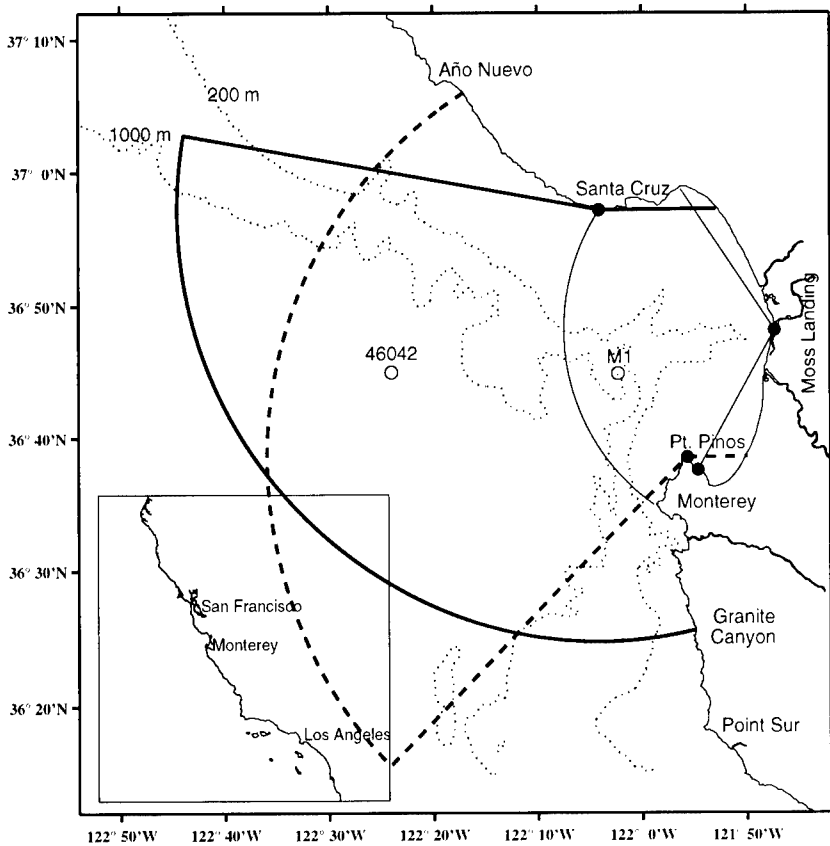


Fig. 1: Monterey Bay HF radar network showing nominal coverage areas for the 12.5 MHz antennae at Santa Cruz (—) and Pt. Pinos (---) and the 25.4 MHz antenna at Moss Landing. MBARI (M1) and NOAA (46042) mooring locations are also shown (O).

anticyclonic flow offshore associated with a warm-core mesoscale feature (Rosenfeld *et al.*, 1994).

An example of the time variable nature of the subtidal current patterns can be seen later in the five month-long record from 1994. Winds measured at the offshore National Oceanic and Atmospheric Administration (NOAA) buoy 46042 and at the M1 mooring are shown in Figure 2 for a 3-wk period in the Fall. The records show upwelling-favorable, equatorward winds interrupted by periods of poleward wind lasting 1–2 d. The M1 site also shows significant diurnal variability as discussed in the next section. The only clear satellite images available between 1–10 November 1994 are from 3 and 8 November at the times indicated on Figure 2. Daily averaged HF radar currents are shown together with these images on Figure 3.

Interpretation of the temperature-current comparisons in Figure 3 benefits from our knowledge of the wind history. The image from 3 November follows a long period of upwelling-favorable winds. A broad band of cold water is seen along the coast and across the mouth of Monterey Bay. Radar-derived surface currents from this day show strong, smoothly varying equatorward flow that follows an anticyclonic arc around the warm feature at the offshore side of the region.

After rapid wind reversal on 4 November, radar-derived current patterns (not shown) quickly develop regions of poleward flow and a lot of sub-mesoscale (~10 km) structure. The poleward flow develops first along the coast. The response timescale of the temperature field after a wind reversal is longer than that of the ~1 m velocity field. For this example, daily averaged currents at the end of the poleward wind event on 6 November (Fig. 2) show better correlation with the features in the temperature field of 8 November than do contemporaneous currents. The comparison on Figure 3 shows how cold water flooding into Monterey Bay from the south changed the surface temperatures in the Bay between 3 November and 8 November.

### Semidiurnal Tidal Currents

In addition to the subtidal-period motions, surface currents around Monterey Bay exhibit strong fluctuations with periods in the tidal bands. The ability to map these fluctuations using HF radar has led to a clearer understanding of the source of these motions. For example, the spatial patterns differ markedly for motions with semidiurnal and diurnal periods. The semidiurnal-period motions are largely due to forcing by the dominant M2 (12.4 h) tidal constituent. Diurnal motions, on the other hand, are largely explained by fluctuations of the wind at, approximately, diurnal (~24 h) periods.

Evidence for tidal forcing of semidiurnal currents can be seen in Figure 4, which presents tidal ellipses resulting from harmonic analyses (e.g., Godin, 1972) of the currents at each radar grid point for the month of August 1994. For the semidiurnal (M2) currents, there is a clear relationship between the ellipse size and orientation and the bathymetry of the Monterey Submarine Canyon. Ellipses are largest over the head of the canyon near Moss Landing and the orientations of their major axes tend to align with topography on either side of the canyon axis. This structure was first seen in two-site CODAR data from 1992 (Petrunccio, 1993). In addition to the correlation with topography, the phases of the M2 currents are such that water flows out of Monterey Bay at the surface during times of rising sea level. This relationship is counter to that expected for barotropic currents successively filling and emptying the bay each tidal cycle. Clearly, the observed M2 currents are surface manifestations of internal (baroclinic) tidal motions driven by the interaction of sea level oscillations and depth changes along the continental margin. Petrunccio *et al.* (1997) describe field measurements that confirm that large amplitude internal waves of semidiurnal period fill the lower few hundred meters of the Monterey Submarine Canyon. This also explains why, at the surface, the semidiurnal current oscillations associated with these waves are strong where the energy intersects the surface (near the coast and far offshore) and

Radar-derived surface currents from this day show strong, smoothly varying equatorward flow . . .

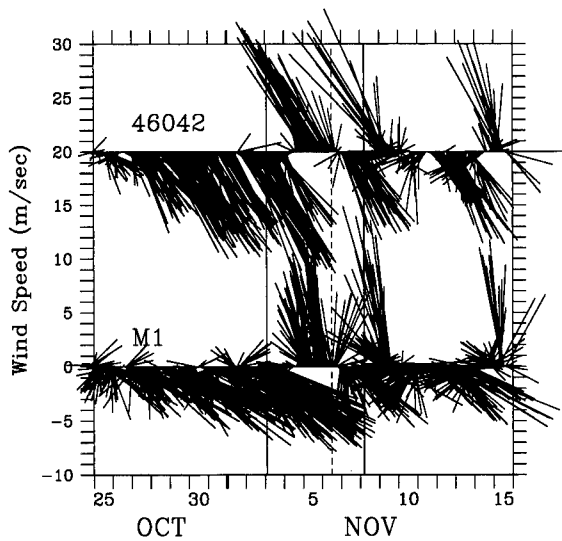


Fig. 2: Wind velocity from NOAA buoy 46042 and MBARI mooring M1 in 1994. Vertical lines denote times of satellite temperature images and HF radar currents in Figure 3. Current measurements in the later image are centered 41 h before the image (---).

weak directly over the deep generation region (near the mouth of Monterey Bay).

#### Diurnal Wind Driven Currents

In stark contrast to the pattern of current oscillations with semidiurnal periods, the diurnal-period surface currents exhibit fairly uniform motions. The K1 (23.9 h) "tidal" ellipses in Figure 4 show large ( $\sim 20 \text{ cm s}^{-1}$ ) oscillations with major axes aligned, primarily, in the northwest-southeast direction. This direction mimics that of the Salinas Valley, which is open to the sea near Moss Landing. Relatively strong heating inland drives a seabreeze flow most afternoons that is strongest at the coast, but still substantial over the ocean at the M1 mooring site and, to a lesser degree, at NOAA buoy 46042. The K1 wind oscillations at these offshore sites during August 1994 are also shown on Figure 4.

The seabreeze cycle in the winds is a broadband process centered near the diurnal period. Harmonic analyses of coastal surface currents at periods close to the diurnal period are dominated by this wind forcing. Other important observations from the K1 ellipses in Figure 4 that deserve further study include the following: 1) the apparent clockwise rotation of the surface K1 currents relative to the wind (this  $\sim 45^\circ$  rotation is in keeping with the Ekman theory, but steady-state Ekman balance is not required for these rapidly changing currents); 2) the rapid decay with depth of the diurnal motions at the M1 mooring site (this is in keeping with the downward transfer of momentum from wind to currents; the amplitude at 10 m on the mooring is 5 times less than the amplitude at  $\sim 1 \text{ m}$ ); and 3) the reduction of K1 oscillations

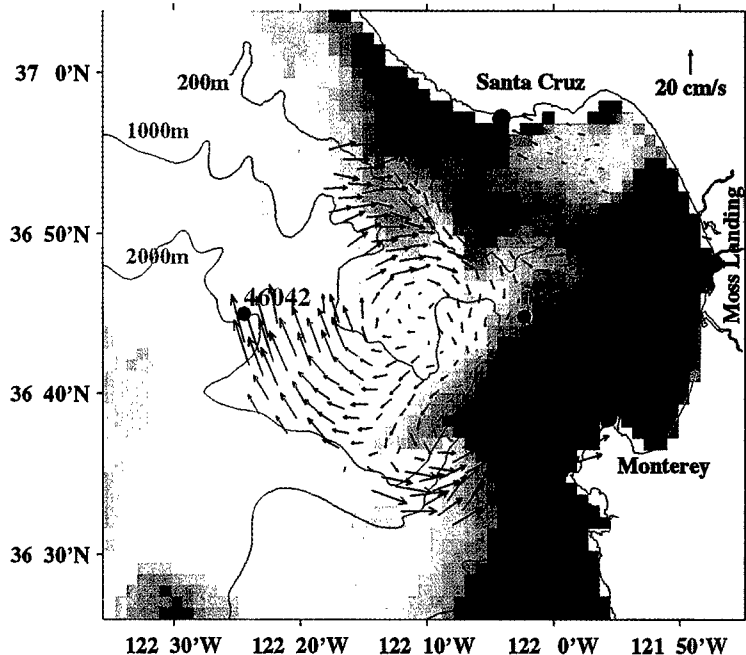
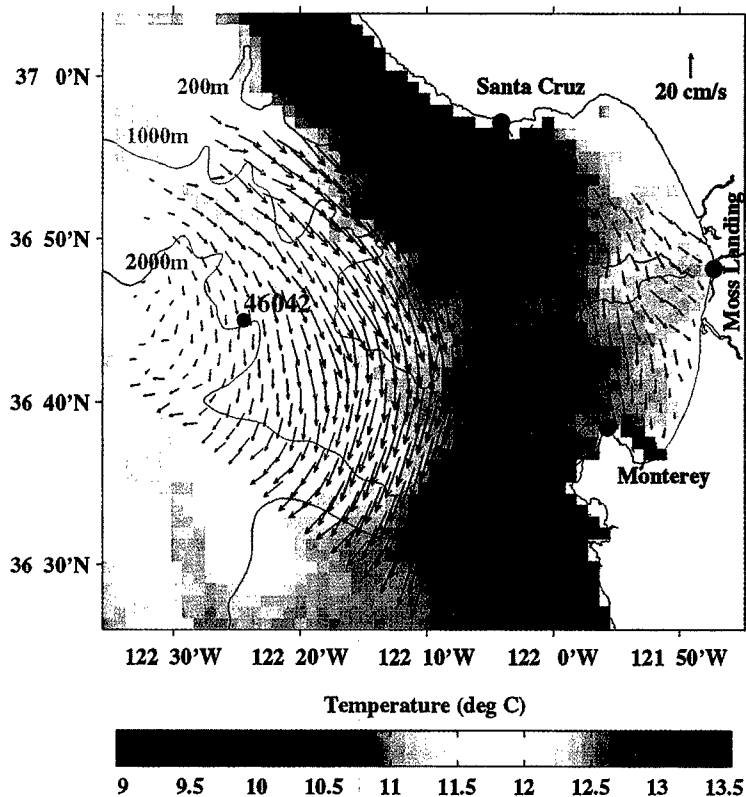


Fig. 3: Uncorrected sea surface temperatures from AVHRR for 0200 GMT, 3 November 1994 (top) and 0500 GMT, 8 November 1994 (bottom) with daily averaged, radar-derived surface currents centered on the image time (top) and 41 h before the image (bottom). Locations of the coastal radar sites and the offshore MBARI mooring M1 and NOAA buoy 46042 are also shown (●).

near the coast (this is in keeping with the expectation that currents will be inhibited by the boundary at some point as the coast is approached).

Looking again at the M2 tidal ellipses, we note that the M2 currents at 10-m depth at the mooring site are of comparable magnitude to those mea-

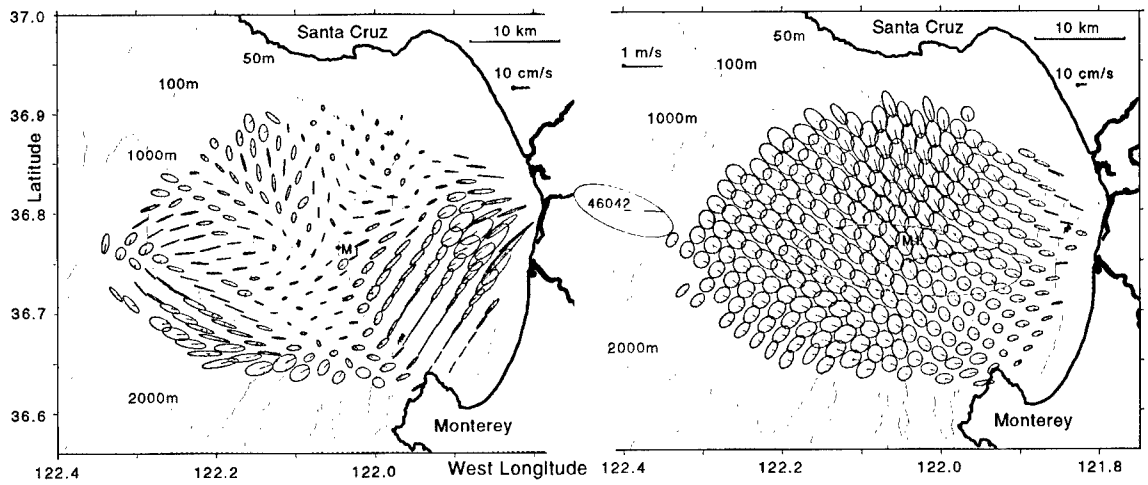


Fig. 4: Tidal ellipses at M2 (12.4 h; **left**) and K1 (23.9 h; **right**) periods from HF radar currents at ~1 m (green), ADCP currents at 10 m at the M1 mooring (red), and wind at the M1 mooring and NOAA buoy 46042 (magenta) for the month of August 1994. Lines emanating from the center of the ellipses denote the flow direction at the time of high coastal sea level for each constituent.

sured at ~1 m using HF radars. This is further evidence that diurnal oscillations observed by the radar network are accurate representations of a near-surface process related to wind forcing, whereas the semidiurnal oscillations have longer vertical scales and are related to the shape of the local bathymetry.

### Conclusions

In summary, we have looked at several applications of direction-finding HF radar measurements to the study of coastal surface currents around Monterey Bay. Evidence pointing to the utility of these remotely sensed data is overwhelming. In no other (practical) way is it possible to obtain two-dimensional current maps on hourly timescales for periods of months on end.

In our area, low-pass-filtered current maps help to describe the evolution of coastal upwelling filaments after reversals of the along-coast wind. This circulation is critical to the distribution of nutrients in the coastal zone, and to the transport of surface dwelling larvae (Bjorkstedt and Roughgarden, 1997). Surface currents respond more quickly to wind changes than do temperatures, a fact which points out the need to use HF radar data in a manner consistent with the very near-surface nature of the measurement (Chapman and Graber, 1997). At higher frequencies, the HF radar data clearly distinguish the effects of tidal and wind-driven forcing for semidiurnal- and diurnal-period motions, respectively.

Finally, we note that the Monterey Bay HF radar network provides an ideal natural laboratory for the study of these coastal processes. It is also ideally suited to investigation of the accuracy of algorithms applied to HF backscatter spectra, such as the new direction-finding technique described by Barrick and Lipa (1997).

### Acknowledgments

We received helpful feedback from Leslie Rosenfeld, and we thank Michael Foreman for providing the harmonic analysis software and Emil Petruncio for helping us to apply it. Gerry Hatcher helped to produce the figures of radar currents and satellite temperatures. This work was supported by the ONR REINAS project and by ONR contract N0001495WR30022.

### References

- Barrick, D.E. and B.J. Lipa. 1997: Evolution of bearing determination in HF current mapping radars. *Oceanography*, 10, 72–75.
- Bjorkstedt, E.P. and J. Roughgarden. 1997: Larval transport and coastal upwelling: an application of HF radar in ecological research. *Oceanography*, 10, 64–67.
- Chapman, R.D. and H.C. Graber. 1997: Validation of HF radar measurement. *Oceanography*, 10, 76–79.
- Foster, M.D., 1993: Evolution of diurnal surface winds and surface currents for Monterey Bay. M.S. thesis, Naval Postgraduate School, 100 pp.
- Godin, G., 1972: *The Analysis of Tides*. Univ. of Toronto Press, Toronto.
- Melton, D.C., 1995: Remote sensing and validation of surface currents from HF radar. M.S. thesis, Naval Postgraduate School, 66 pp.
- Paduan, J.D. and H.C. Graber. 1997: Introduction to high-frequency radar: reality and myth. *Oceanography*, 10, 36–39.
- and L.K. Rosenfeld. 1996: Remotely sensed surface currents in Monterey Bay from shore-based HF radar (CODAR). *J. Geophys. Res.*, 101, 20669–20686.
- Petruncio, E.T., 1993: Characterization of tidal currents in Monterey Bay from remote and in-situ measurements. M.S. thesis, Naval Postgraduate School, 113 pp.
- , L.K. Rosenfeld and J.D. Paduan. 1997: Observations of the internal tide in Monterey Submarine Canyon. *J. Phys. Oceanography*. In press.
- Rosenfeld, L.K., F.B. Schwing, N. Garfield and D.E. Tracy. 1994: Bifurcated flow from an upwelling center: a cold water source for Monterey Bay. *Cont. Shelf Res.*, 14, 931–964. □

. . . low-pass-filtered current maps help to describe the evolution of coastal upwelling filaments after reversals of the along-coast wind.

# THE COASTAL JET: OBSERVATIONS OF SURFACE CURRENTS OVER THE OREGON CONTINENTAL SHELF FROM HF RADAR

By P. Michael Kosro, John A. Barth  
and P. Ted Strub

THE OCEAN CIRCULATION over the Oregon shelf during spring and summer is dominated by the effects of coastal upwelling. Equatorward winds drive an offshore Ekman transport in the surface layer, which produces divergent flow at the coast and the upwelling of deeper, colder, nutrient-enhanced waters (Huyer, 1990). At the surface, the boundary between the upwelled and oceanic waters is often a front, and the upwelling-induced horizontal density gradients support an equatorward coastal jet (Mooers *et al.*, 1976). The annual onset of persistent upwelling conditions often occurs abruptly in an event called the spring transition (Huyer, *et al.*, 1979; Strub, *et al.*, 1987), which is characterized by a persistent drop in coastal sea level and a tendency to persistence of equatorward wind forcing (punctuated by occasional wind reversals). Although fluctuations in the alongshore current have been shown to be coherent over large alongshore scales (Huyer *et al.*, 1975), the local spatial variations in the currents are not well known, mainly due to our past inability to map the current field at high resolution in both space and time.

## Radar and Conventional Measurements

The Ocean Surface Current Radar (OSCR), manufactured by GEC Marconi, is a phased-array HF radar system designed for mapping of surface currents in the coastal ocean. During 11–17 May 1995 an OSCR, broadcasting at 25.4 MHz, was operated from sites near Bandon, Oregon (43.22°N, 124.39°W and 43.12°N, 124.43°W; see Fig. 1). Site selection (balancing the needs for security, access, ocean coverage, proximity to the water, land-owner permissions, and sufficient free space to set up the ~100-m-long OSCR receive antennas) resulted in sites separated by only 12

km. This separation limited the resulting range to 25–35 km (depending on screening criteria), and the geometrical accuracy at longer range. Nevertheless, the radar typically measured radial data to the edge of the continental shelf. The percentage of data return was nearly uniform with azimuth angle, although some very near coast cells showed low rates of valid returns. In support of the radar verification, a 307-kHz narrow-band Acoustic Doppler Current Profiler (ADCP) was moored looking upward from a near-bottom float in ~90 m of water (43.16°N, 124.56°W, Fig. 1) on 15 May from the fishing vessel *Gemini*. During 17–19 May, an *in situ* high-resolution survey was conducted in the region from *R/V Wecoma*, using CTDs mounted in SeaSoar, a towed, undulating vehicle (Barth and Smith, 1997). Both activities were originally scheduled to fully overlap with

. . . the radar typically measured radial data to the edge of the continental shelf.

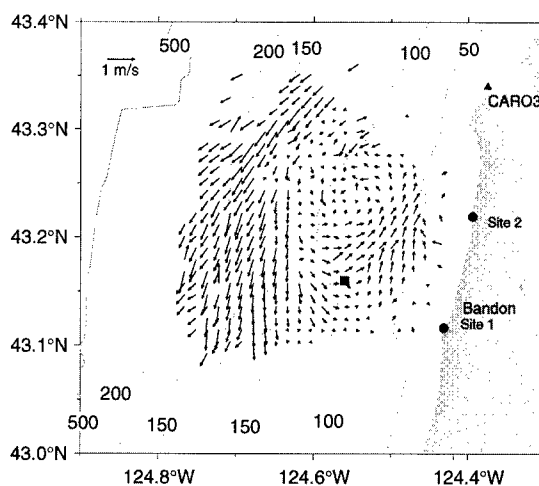


Fig. 1: Example of OSCR map of surface currents at experimental site near Bandon, Oregon, from 12 May 1995, at 10:20 UT. Locations of the two radar sites (circles), of the upward-looking ADCP (square) and of the CMAN wind station (CARO3, triangle) are marked. Depth contours are in meters.

P. Michael Kosro, John A. Barth and P. Ted Strub, College of Oceanic & Atmospheric Sciences, Oregon State University, 104 Ocean Admin. Bldg., Corvallis, OR 97331-5503, USA.

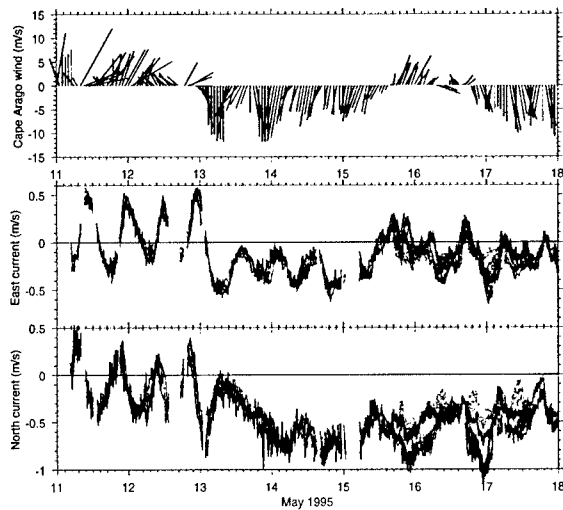


Fig. 2: (A) Hourly winds at Cape Arago C-MAN station (CARO3, Fig. 1) during 11–18 May 1995. (B) Eastward current measured by the ADCP at 7-m subsurface depth (darkest black line), 11 m, 14 m, and 18 m (lighter black lines), and by radar at the surface in cells nearest to the ADCP (red line) and at four adjacent cells (blue lines). (C) Same for northward current.

. . . radar surface currents near the mooring position were dominated by oscillations of the semidiurnal tide . . .

the radar deployment, but last-minute delays in the ship's schedule shortened overlap considerably.

#### Observations Near the Mooring

Winds were variable but generally downwelling favorable at the start of the radar deployment, during 11 and 12 May (Fig. 2). During this period, the time series of radar surface currents near the mooring position (Fig. 2) were dominated by oscillations of the semidiurnal tide, with amplitude

of  $O(0.4 \text{ m/s})$  in each component and with the velocity vector rotating clockwise with time.

On 13 May, the winds turned upwelling favorable. The ocean response was like a spring transition—within half a day, the alongshore radar currents at the mooring site, initially weak in the mean, began to accelerate linearly with time to the south, eventually achieving speeds of  $O(0.7 \text{ m s}^{-1})$ , consistent with the spin-up of the equatorward coastal jet.

During their brief overlap (Fig. 2), the highest correlations between the OSCR and the ADCP were found for ADCP velocities at 7 m (the shallowest uncontaminated measurements) and radar velocities at cells close to, but not exactly at, the one expected to lie over the mooring, probably due to uncertainties in the radar geometry caused by variations in the antennas and in propagation characteristics. Radial ADCP and radar currents showed correlations of 0.84 and 0.78, and root-mean-square (rms) differences of 12.6 and 16.2  $\text{cm s}^{-1}$ , respectively, for radial currents directed toward sites 1 and 2. Some of the differences can be explained by extending the vertical shear in the shallowest ADCP measurements to the surface (e.g., period around 0000 UT on 17 May); however, at other times, the ADCP does not observe a shear below 7-m depth, which is sufficient to explain the difference in the two measurements (e.g., 0600 UT on 16 May).

#### Near-Surface Maps

Does the southward acceleration observed on the 13–14 May correspond to the spin-up of the coastal jet and the onset of upwelling? The record from satellite Advanced High Resolution Radiome-

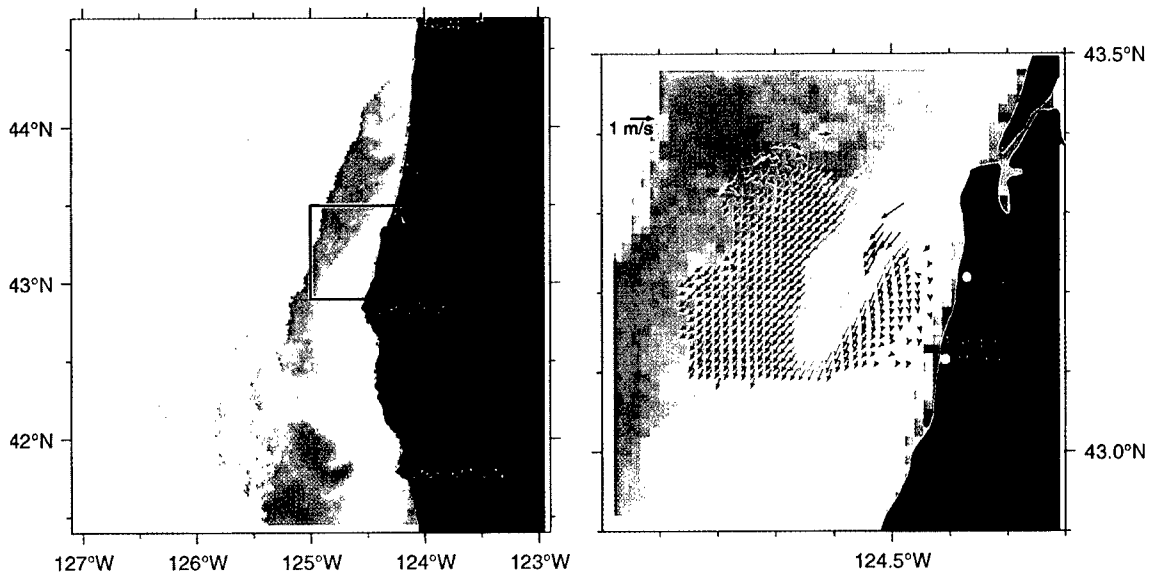


Fig. 3. Left: NOAA AVHRR image of sea surface temperature for 0200 UT on 18 May 1995. Light shades correspond to cold temperatures. Right: enlargement of boxed region from left panel, with tidal average of currents from the end of the deployment (0240 to 1500 UT on 17 May 1995). Current speeds are color coded from blue (lowest) to red (highest).

ter (AVHRR) images of sea surface temperature is very intermittent due to clouds, but the first clear image following the southward acceleration (Fig. 3) is also the first image of spring 1995 to clearly show a band of cold water along the coast. Moreover, when the surface current field from the radar is overlaid on the satellite AVHRR image of sea surface temperature (Fig. 3), the identification of the strong radar currents with the coastal jet is clear. At this time, the core of the jet is directed along 210°T, paralleling the front of cold, coastally upwelled water seen in the satellite image and the local isobaths north of 43.2°N. The core speed of the jet decreases markedly over the sampling region, entering at 0.9 m s<sup>-1</sup> in the northeast, centered just inshore of the 100-m isobath, and slowing to 0.6 m s<sup>-1</sup> as it exits the region 20 km to the southwest and offshore of the 100-m isobath. The cross-shore width of the jet, if defined by the region moving at least 0.5 m s<sup>-1</sup>, is ~12 km, narrowing slightly along the course of the jet.

The near-surface geostrophic flow, shown by the dynamic topography measured from *R/V Wecoma* during 17–19 May 1995 (Barth and Smith, 1997), confirms the presence of the coastal jet near midshelf, at the location indicated by the radar (Fig. 4). The spreading of the dynamic height contours below 43.2°N indicates a slowing

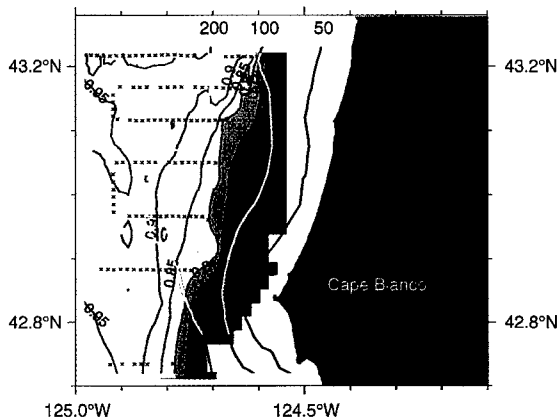


Fig. 4. Dynamic height  $\Delta D_{23/55}$  ( $m^2s^{-2}$ ) from SeaSoar survey conducted 17–19 May 1995. Dots show location of measurements.

of the current to the south, a feature also seen in the radar (Fig. 3). The dynamic height contours at the core of the jet are seen to cross the 100-m isobath, also as seen in the radar.

A more detailed look at the development of the coastal jet can be obtained from a time series of averaged radar maps (Fig. 5; here tidal averages have been made over maps covering 12 h and 20 min, starting at 0000 UT or 1200 UT). During 11

... confirms the presence of the coastal jet near midshelf, at the location indicated by the radar.

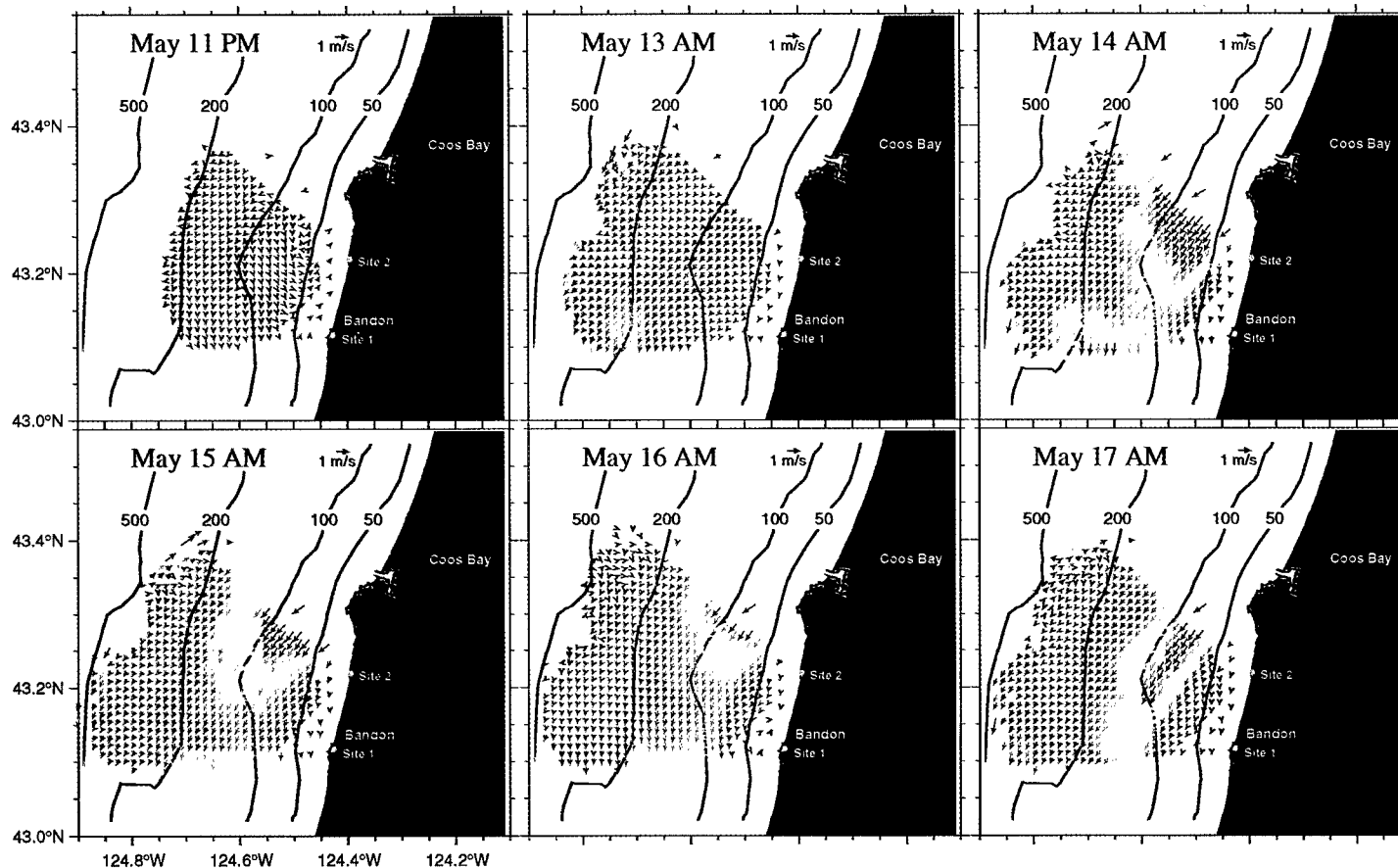


Fig. 5. Maps of surface currents from OSCR. Each map is an average over 12 h and 20 min, to minimize tidal effects. Current speeds are color coded from blue (lowest) to red (highest).

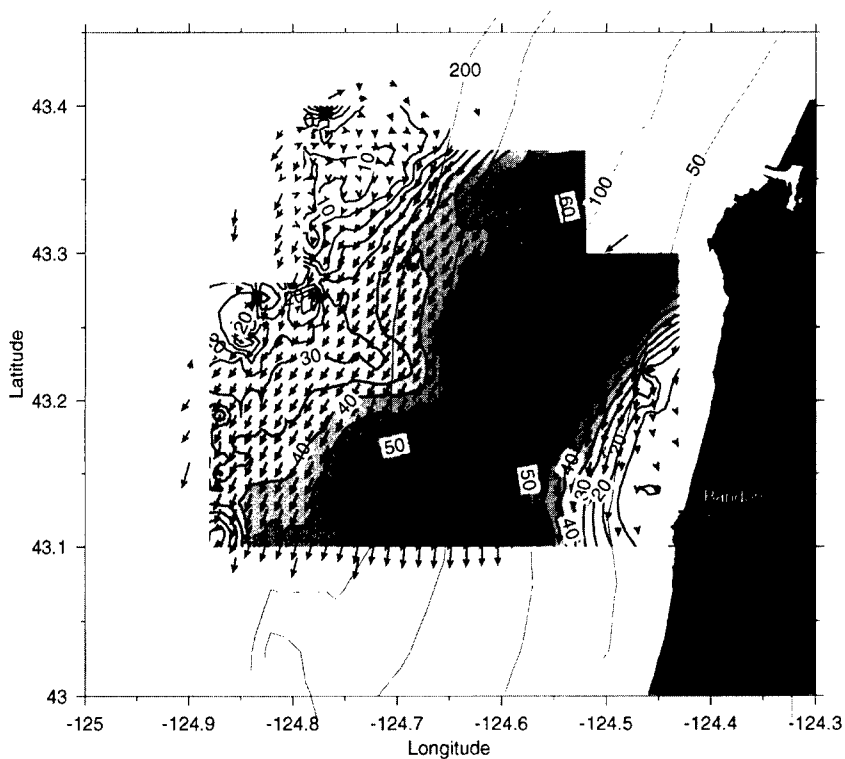


Fig. 6. Average current, 11–17 May 1995. Contours show speed of average current, in  $\text{cm s}^{-1}$ .

The strength and persistence of the spatial variability measured over short distances along the current core is a surprising result . . .

and 12 May, currents were quite weak (except for some outliers at long range that were not detected by automatic screening criteria). During 13–14 May, as the winds became strong and upwelling favorable (Fig. 2), the current field accelerated equatorward (Fig. 5), while during 15 and 16 May, in concert with weakening and even reversing winds, alongshore currents weakened, then reaccelerated on 17 May, again in response to the winds.

The mean radar currents (Fig. 6), as well as most of the twice-daily maps (Fig. 5) show a deceleration of the currents south of  $43.2^\circ\text{N}$ , with a reacceleration of the currents at the very southern end of the radar coverage. The spatial variability along the current core is strong [O(20%)] and persistent, and is seen on scales similar to those of the topographic variability, although there is not a direct correspondence between water depth and current speed in this strongly baroclinic flow. Finally, there is a distinct tendency for the currents to be directed nearly southwestward at the inflow to the mapping region, but to be directed southward at the exit of the mapping region, following the tendency in the bathymetry; the rotation is  $\sim 45^\circ$  in

the overall mean current field along the 100-m isobath.

### Summary

The HF coastal radar provides a new look at the spatial and temporal variability in the coastal ocean off Oregon. Features observed in earlier studies, such as the formation of an alongshore coastal jet at midshelf in response to upwelling-favorable winds, and the steering of currents by topography, are observed clearly in these radar maps, now with very high resolution in time and in space. The strength and persistence of the spatial variability measured over short distances along the current core is a surprising result, as is the apparent tendency for the current jet to accelerate and decelerate in place. A longer time series of radar measurements, in conjunction with measurements in the water column from drifters, moored current meters, and rapid surveys, is needed to understand the detailed dynamics of this wind-driven variability.

### Acknowledgments

We thank Duncan Ross, Ivy Iverson, and the GEC Marconi Corporation for providing and operating the OSCAR during this demonstration; Lynda Shapiro and the staff of Oregon Institute of Marine Biology; Walt Waldorf and Joyce Federiuk; and the Oregon State Parks and Recreation Department. This research was funded by the Office of Naval Research (grant N00014-9511104), National Science Foundation (OCE 9512695 and 9314370), and Oregon State University.

### References

- Barth, J.A. and R.L. Smith, 1997: Separation of a coastal upwelling jet at Cape Blanco, Oregon, USA. *S. Afr. J. Mar. Sci.* In press.
- Huyer, A., 1990: Shelf circulation. In: *The Sea, Ocean Engineering Science*, vol 9, B. Le Mehaute and D.M. Hanes, eds. Wiley, New York. 423–466.
- \_\_\_\_\_, B.M. Hickey, J.D. Smith, R.L. Smith and R.D. Pillsbury, 1975: Alongshore coherence at low frequencies in currents observed over the continental shelf off Oregon and Washington. *J. Geophys. Res.*, 80(24), 3495–3505.
- \_\_\_\_\_, E.J.C. Sobey and R.L. Smith, 1979: The spring transition in currents over the Oregon continental shelf. *J. Geophys. Res.*, 84(C11), 6995–7011.
- Moors, C.N.K., C.A. Collins and R.L. Smith, 1976: The dynamic structure of the frontal zone in the coastal upwelling region off Oregon. *J. Phys. Oceanogr.*, 6, 3–21.
- Strub, P.T., J.S. Allen, A. Huyer and R.L. Smith, 1987: Large-scale structure of the spring transition in the coastal ocean off western North America. *J. Geophys. Res.*, 92 (C2), 1527–1544. □

# TIDAL AND WIND-DRIVEN CURRENTS FROM OSCR

By David Prandle

**T**WO IMPORTANT ASPECTS of tidal currents are (1) their temporal coherence and (2) their constancy (over centuries). The first rigorous evaluation of an Ocean Surface Current Radar (OSCR) system exploited these characteristics using sequential deployments of the one available unit with subsequent combination of radial components to construct tidal ellipses (Prandle and Ryder 1985).

## Specifications for Tidal Mapping

The Rayleigh criterion for separation of closely spaced constituents in tidal analysis suggests observational periods exceeding the related beat frequency, this dictates 15 d of observations to separate the two largest constituents  $M_2$  and  $S_2$ . For tidal elevations this criterion is often relaxed; however, while elevations show a noise:tidal signal ratio of 0(0.1–0.2), the same ratio for currents is 0(0.5). Moreover, wind and wave current components are generally largest at the surface, and hence for OSCAR observations the ratio may be even higher. Consequently 30-d observational periods are recommended. Prandle *et al.* (1993) show that, from analyses of a sequence of data sets of this length, 7 constituents could be determined with standard deviations of  $\sim 0.1$  of amplitude for  $M_2$ ,  $S_2$ , and  $N_2$  and 0.2 for  $O_1$ ,  $K_1$ ,  $M_4$ , and  $MS_4$ . An associated problem arises with selecting specified relationships for closely spaced constituents not explicitly determined; using adjacent elevation data may be suspect. A further difficulty arises in shallow water in comparing OSCAR results with values from either moored instruments or models based on different vertical reference frames. Lane *et al.*, (in press) indicate some possible solutions to this problem.

Figure 1 (Prandle 1991) shows typically close agreement between tidal ellipse distributions derived by combining OSCAR measurements from a total of 10 sites with values from a fine grid numerical model. The extent of this agreement can

be seen by comparing calculations of  $M_2$  tidal vorticity distributions  $\langle \partial V / \partial X - \partial U / \partial Y \rangle$  from OSCAR measurements with corresponding model calculations (Prandle 1987).

## Tidal Residuals

The propagation of tidal energy from the ocean into shelf seas produces an attendant net residual current  $U_o$  of  $0.5(\hat{U}\xi/D)\cos\theta$  ( $\hat{U}$ , oscillating current amplitude;  $\xi$ , elevation amplitude;  $D$ , water depth;  $\theta$ , phase difference between  $\hat{U}$  and  $\xi$ ). In U.K. waters  $U_o$  is typically 0–3  $\text{cm s}^{-1}$  compared with  $\hat{U}$  of 40–100  $\text{cm s}^{-1}$ , thus conventional current meters often fail to resolve  $U_o$ . Moreover, numerical models that accurately simulate  $M_2$  may not resolve  $U_o$  with the same accuracy. Year-long deployments of OSCAR, in the Dover Straits (Prandle *et al.*, 1993) and the North Channel of the Irish Sea (Howarth *et al.*, 1995), enabled, for the first time, these net tidal residual currents to be accurately resolved by direct measurement. But, as so often occurs in science, enhanced resolution of the instrumentation reveals finer scale dynamical processes. Figure 2 shows a residual surface current gyre differentiated from these long-term measurements in the Dover Strait. Such gyres are not exceptional but rather a characteristic of most coastlines, although rarely identified with conventional instrument or airborne sensors.

## Wind-Driven Currents

### Nontidal Currents

Removal of the tidal component from High Frequency (HF) Radar current observations leaves residuals that may include contributions from: direct (localized) wind forcing, indirect (larger scale) wind forcing, surface waves, and horizontal and vertical density gradients. Interaction of any of these components with the tidal component can generate significant modulation of the latter contributing an additional nontidal residual. Selective filtering of the nontidal currents into frequency bands can be used to separate many of these components.

. . . enhanced resolution of the instrumentation reveals finer scale dynamical processes.

David Prandle, Proudman Oceanographic Laboratory, Bidston Observatory, Birkenhead L43 7RA, UK.

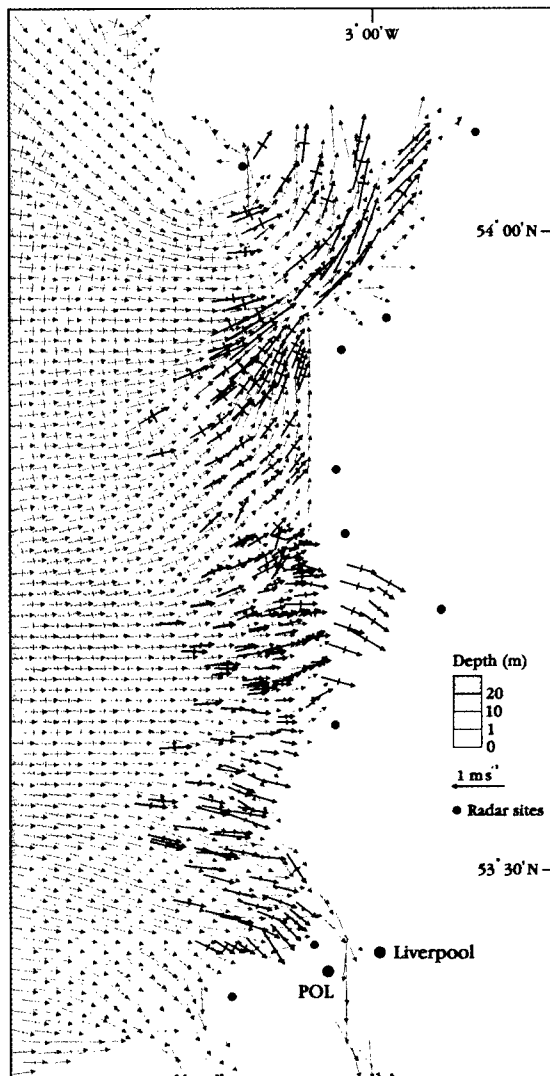


Fig. 1:  $M_2$  tidal ellipses, OSCAR (black) versus model.

Persistent residual surface currents of typically 10–20  $\text{cm s}^{-1}$  are regularly observed with deployments of the OSCAR system around the U.K. coast. These can often be dynamically related to horizontal density gradients (Prandle and Matthews 1990). Likewise jet-like currents of up to 14  $\text{cm s}^{-1}$  have been observed linked with frontal dynamics (Matthews *et al.*, 1993). Souza and Simpson (1996) show how vertical density gradients modulate surface tidal currents.

Persistent residual surface currents of typically 10–20  $\text{cm s}^{-1}$  are regularly observed with deployments of the OSCAR system around the U.K. coast. These can often be dynamically related to horizontal density gradients (Prandle and Matthews 1990). Likewise jet-like currents of up to 14  $\text{cm s}^{-1}$  have been observed linked with frontal dynamics (Matthews *et al.*, 1993). Souza and Simpson (1996) show how vertical density gradients modulate surface tidal currents.

In deep water the oscillatory orbital velocities of surface waves do not show any obvious aliasing on the Bragg peaks, but in shallow water any associated net drift component may influence “current” measurements.

#### Wind-Forced Currents

Relating observed wind-driven currents to wind forcing is notoriously difficult. Both the wind itself and the associated currents exhibit appreciable fine-scale (temporal and spatial)

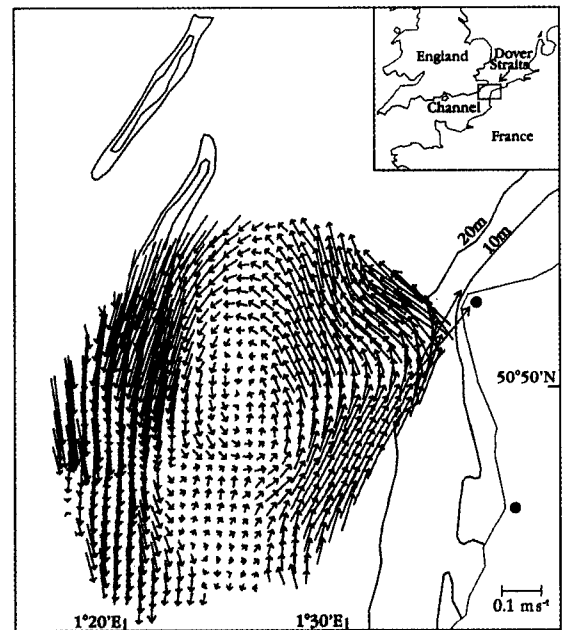


Fig. 2: Residual (30 d mean) gyre from OSCAR Mk II.

variability. In shallower water, wind forcing may be partially balanced by surface slopes. In straits these slopes can subsequently generate currents orders of magnitude greater than indicated by localized forcing (Prandle 1993). However, statistically significant relationships between wind and residual surface currents have been derived from all OSCAR deployments. Both the steady-state Ekman spiral response and rotating inertial currents have been identified (Fig. 3). The steady-state response is typically 1 or 2% of wind speed, increasing in magnitude in deep water and veering increasingly toward the theoretical deep water values of  $45^\circ$  to the right of the wind.

#### Determining Current Profiles From Surface Currents

Construction of tidal current profiles from surface values can be completed, qualitatively, using simple theory that requires the specification of a vertical eddy viscosity coefficient,  $E$ , and a bottom friction coefficient  $k$  (Prandle 1982). Estimates of both  $E$  and  $k$  may be made from the variation in wind-forced response in water of varying depths. Vertical profiles of the wind-forced component in open seas can similarly be calculated from Ekman spiral theory.

By substitution of observed surface currents into the horizontal momentum equation, localized surface gradients can be constructed. By integrating these gradients over the region of radar coverage, both an  $M_2$  co-tidal chart (using a reference value) and a mean sea level distribution were calculated for the Dover Strait (Prandle *et al.*, 1993).

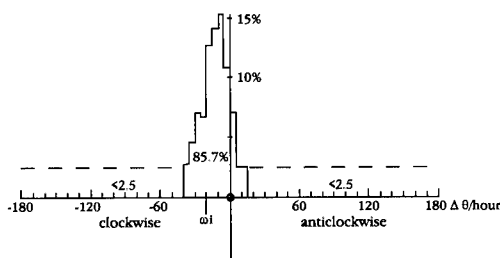
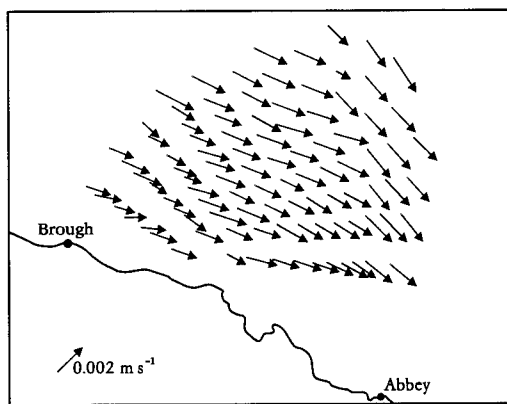


Fig. 3: Wind-forced currents (shown for  $1 \text{ m s}^{-1}$   $W$ ; top panel). Histogram of rotation rate of residual currents (bottom panel).

### Future Applications

The OSCAR results described here have been restricted to the 26-MHz system, the potential of the finer scale resolution afforded by operation at 50 MHz is demonstrated elsewhere. The potential for longer range HF Radar current measurements has yet to be fully exploited. Use of HF Radar for permanent monitoring of strategic straits, such as for the North Channel and Dover Strait described here, could form part of the Global Ocean Observing System to detect net trends in oceanic circulation. With the performance of HF Radar now widely established, the greatest obstacle to wider use is capital cost; however, HF Radar systems are not vulnerable to loss and damage inherent with oceanographic instrumentation.

The range of synergistic modes of linking HF Radar surface current measurements with *in situ* and shipborne Acoustic Doppler Current Profiler (ADCP) (Matthews *et al.*, 1993), remote sensing, numerical modeling, etc., has yet to be fully developed. Perhaps the greatest potential of such synergy is in real-time operational deployments. Examples include use of HF Radar for navigation

into major ports, management of coastal discharges/withdrawal, tracking of accidental spillages, assimilation (updating) of storm surge prediction models, etc.

In principle, horizontal dispersion coefficients can be determined from the spatial variability in velocities observed by HF Radar. In practice, such estimates depend on the spatial resolution, sampling period, and instrumental errors of the system. Experiments to explore such sensitivities involving concurrent dye dispersion and drogue tracking would be useful.

An exciting prospect is to link such extended applications to related development in the radar technology. Thus, for example, a "Grand Challenge" for coastal researchers is to predict coastal bathymetric evolution, involving long-term continuous measurement of currents, waves, winds, and bathymetry. An HF Radar system operating at variable frequency (simultaneous or consecutively) might be optimally tuned for determining each of these parameters.

### References

- Howarth, M.J., A.J. Harrison, P.J. Knight and R.J. Player, 1995: Measurement of net flow through a Channel. In: *Proceedings of the IEEE Fifth Working Conference on Current Measurement*. IEEE, St. Petersburg, Florida, February 7-9, 121-126.
- Lane, A., D. Prandle, A.J. Harrison, P.D. Jones and C.J. Jarvis. Measuring fluxes in tidal estuaries: sensitivity to instrumentation and associated data analyses. *Estuarine, Coastal Shelf Sci.* In press.
- Matthews, J.P., A.D. Fox and D. Prandle, 1993: Radar observation of an along-front jet and transverse flow convergence associated with a North Sea front. *Cont. Shelf Res.*, 13, 109-130.
- Prandle, D., 1982: The vertical structure of tidal currents and other oscillatory flows. *Cont. Shelf Res.*, 1, 191-207.
- \_\_\_\_\_, 1987: The fine-structure of nearshore tidal and residual circulations revealed by HF radar surface current measurements. *J. Phys. Oceanogr.*, 17, 231-245.
- \_\_\_\_\_, 1991: A new view of near-shore dynamics based on observations from HF radar. *Progr. Oceanogr.*, 27, 403-438.
- \_\_\_\_\_, 1993: Year long measurements of flow through the Dover Strait by H.F. Radar and Acoustic Doppler Current Profilers (ADCP). *Oceanologica Acta*, 16, No. 5-6, 457-468.
- \_\_\_\_\_ and K.D. Ryder, 1985: Measurement of surface currents in Liverpool Bay by high-frequency radar. *Nature*, 315, 128-131.
- \_\_\_\_\_ and J. Matthews, 1990: The dynamics of nearshore surface currents generated by tides, wind and horizontal density gradients. *Cont. Shelf Res.*, 10, 665-681.
- \_\_\_\_\_, S.G. Loch and R. Player, 1993: Tidal flow through the Straits of Dover. *J. Phys. Oceanogr.*, 23, 23-27.
- Souza, A.J. and J.H. Simpson, 1996: The modification of tidal ellipses by stratification in the Rhine ROFI. *Cont. Shelf Res.*, 16, 997-1008. □

Perhaps the greatest potential of such synergy is in real-time operational deployments.

# INTERNAL WAVE-DRIVEN SURFACE CURRENTS FROM HF RADAR

By Lynn K. Shay

**S**URFACE CURRENT observations from high-frequency (HF) radar have revealed that not only are the low-frequency and tidal currents resolved by the measurement, higher-frequency motions are also contained within the signals. These higher-frequency current oscillations are within the internal wave continuum from the buoyancy to the inertial frequencies, including the excitation of semidiurnal internal tides forced by a barotropic tide propagating over the shelf-break (Baines, 1986; Paduan and Cook, 1997). Another complicating feature in the coastal regime is oceanic frontal structure that significantly influences internal wave variability because of the background vorticity fields (Mooers, 1975; Kunze, 1985). However, little is known about the internal wave interactions with coastal ocean fronts where these vorticities may be considerably larger than in the deep ocean because of the larger density contrast between the water masses. Synoptic observations of the horizontal flow structure from HF radar provides the spatial context for moored and ship-based measurements to assess the impact of coastal fronts on the internal wave climate.

Observations from recent experiments using the University of Miami's Ocean Surface Current Radar (OSCR) (Shay *et al.*, 1995, 1997), and the U.S. Coast Guard (USCG)-sponsored Ocean Pollution Research Center (OPRC) experiments in the Florida Keys (L.K. Shay, T.N. Lee, E.J. Williams, H.C. Graber and C.G.H. Rooth, unpublished data) have revealed internal wave signatures. These data will be used to show the linkage between HF-derived surface currents and current profiles acquired from an acoustic Doppler current profiler (ADCP) with respect to the internal wave signals.

## Observations

The HF radar system mapped the coastal ocean currents over a  $30 \times 45$  km domain at 20-min intervals with a horizontal resolution of 1.2 km along the Florida Keys during OPRC-2. Over a 25-d period from 18 May to 13 June 1994, five

percent of the surface current images were missing yielding a high data return as found in previous experiments. An upward-looking, narrow-beam ADCP was moored in 150 m off Looe Key in the radar domain and provided current observations at 5-m intervals from 15- to 130-m depths. Surface current data were averaged at one-half hourly intervals to coincide with the ADCP sampling interval and rotated into bottom topographic coordinates.

Data acquired over a 10-d period during the OPRC-2 experiment indicated submesoscale vortices located along the inshore side of the Florida Current that were aligned with the 150-m isobath. Between 22 May (Yearday 142) to 27 May (Yearday 147), the along-shelf flow reversed direction as the Florida current moved further offshore. The maximum cross-shelf component exceeded  $25 \text{ cm s}^{-1}$  toward the north whereas the along-shelf current exceeded  $150 \text{ cm s}^{-1}$  when the Florida Current was located over the mooring (Fig. 1). Root mean square (rms) differences were  $18 \text{ cm s}^{-1}$  between the surface and 15-m records. Previous estimates of rms differences between surface and subsurface currents from HIRES-2 were  $10\text{--}14 \text{ cm s}^{-1}$  because of mesoscale variability associated with low-frequency baroclinic currents of the Gulf Stream and internal waves (Shay *et al.*, 1995; Chapman *et al.*, 1997). In a time-averaged sense, Graber *et al.* (1997) found that  $\geq 50\%$  of these differences may have been due to a combination of surface wave and wind-induced currents and these baroclinic currents. Recent comparisons between surface and subsurface (4 m) currents from vector measuring current meters (VMCM) acquired during the National Science Foundation Coastal Ocean Processes (NSF CoOP) and ONR Duck94 experiments indicated rms differences of  $7 \text{ cm s}^{-1}$  (Shay *et al.*, 1997). These observations were at the uncertainty limits of resolvable processes from the OSCR and VMCM instruments (Weller and Davis, 1980).

## Surface Current Images

Observed current time series were decomposed into the subinertial ( $>48$  h), tidal, inertial (29 h), high-frequency (5 h), and residual currents. Based

Observations from recent experiments . . . have revealed internal wave signatures.

Lynn K. Shay, University of Miami, Miami, FL, 33149, USA.

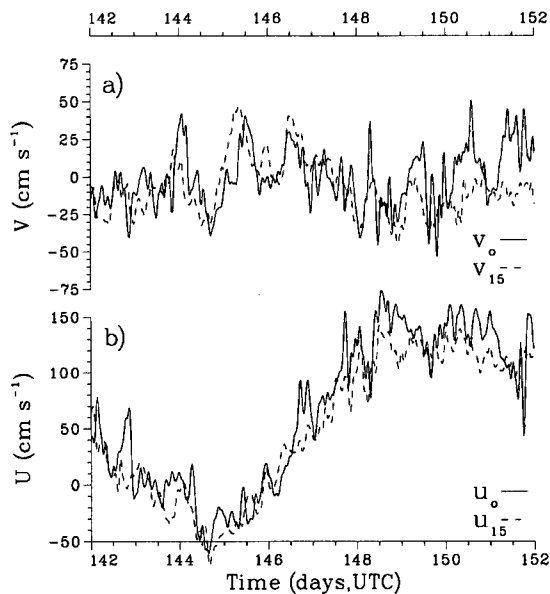


Fig. 1: (a) Cross-shelf and (b) along-shelf surface (—) and 15 m (---) current time series ( $\text{cm s}^{-1}$ ) from 22 May (YD 142) to 1 June (YD 152) 1994 during OPRC-2.

on the peaks in the rotary spectra (Shay *et al.*, 1995, 1997), a harmonic analysis of the tides was performed to determine the diurnal and semidiurnal tidal constituents and removed to form detided records. Using a Lanczos-square window, the detided currents were low-pass filtered at 48 h, band-pass filtered between 25 and 38 h, and high-pass filtered at 8 h to form subinertial, near-inertial and high-frequency current time series, respectively.

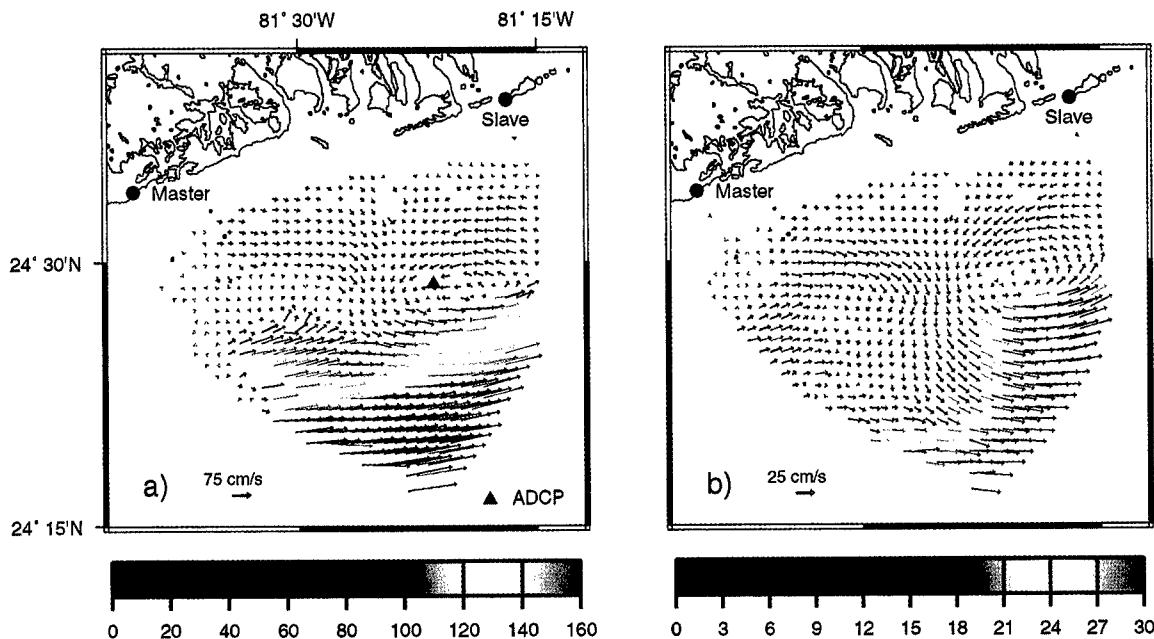


Fig. 2: (a) Observed and (b) near-inertial surface flows from the OPRC-2 experiment in the Florida Keys at 1800 UTC 25 May 1994. The color of the arrows represents the strength of the current as per the color bars in  $\text{cm s}^{-1}$ .

The width of the near-inertial band reflects the subinertial vorticities described below. In addition, the 25-d time series adequately resolved the near-inertial and diurnal tide contributions.

Observed surface velocities indicated structure in the surface velocity field including submesoscale eddylike vortices (Fig. 2). Based on the observed surface current images, these submesoscale vortices translated from the western part of the domain toward the eastern part at a rate of 25–30  $\text{km d}^{-1}$ . This translation rate was not only above the expected envelope of low-frequency baroclinic features such as eddies and rings, but the direction of movement was opposite to coastally-trapped waves propagating along the eastern coast of basins. Although subinertial flows indicated little evidence of this submesoscale feature, the observed signal was embedded in the near-inertial flows. Based on a series of least-square fits, the horizontal wavelength of this feature was  $\sim 35 \text{ km}$  with velocities of up to 30  $\text{cm s}^{-1}$  (Fig. 2b). Thus this submesoscale variability was embedded in the near-inertial current signals.

### Vertical Structure

As shown in Figure 3, high-frequency surface and subsurface signals had 4–5-h periods and vertical wavelengths of 20–25 m (Shay, 1996). During the period of subinertial flow change from YD 144 to 146, the velocities of these high-frequency motions were about 15  $\text{cm s}^{-1}$  and were highly intermittent. The subinertial current velocities were shifted from  $-40 \text{ cm s}^{-1}$  in the surface layer to 150  $\text{cm s}^{-1}$  at 40-m depth as the Florida Current moved back over the mooring. A near-inertial current

Observed surface velocities indicated structure in the surface velocity field including submesoscale eddylike vortices.

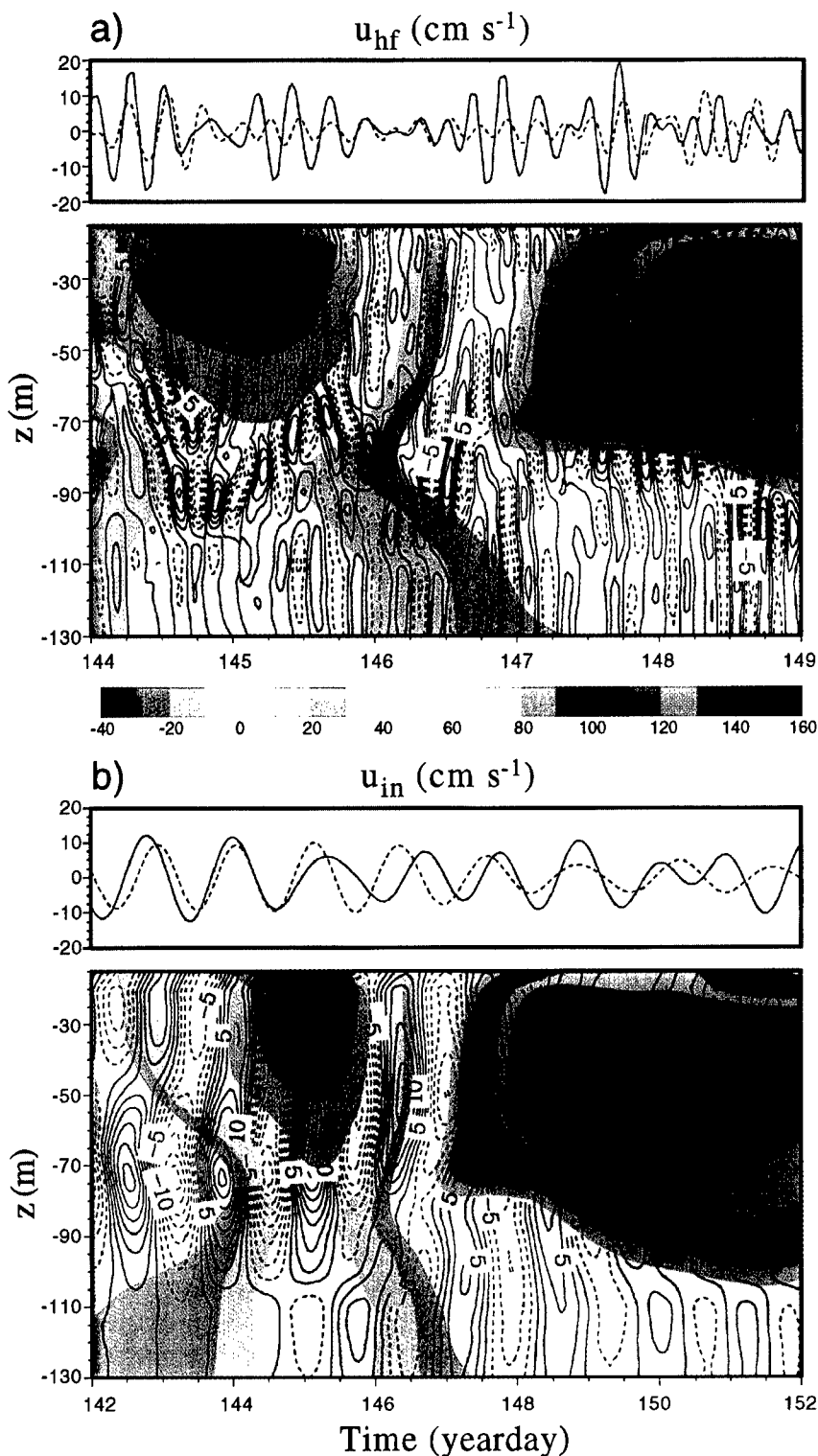


Fig. 3: Comparison (top panels) between surface (solid) and 15 m (dashed) currents and contoured along-shelf current profiles (bottom panels) for (a) high-frequency and (b) near-inertial components (cm s<sup>-1</sup>) from an ADCP deployed in the OPRC-2 experiment from 22 May to 1 June 1994 superimposed on the subinertial flow (color). Panel (a) represents a 5-d timeseries compared with the 10-d series in (b). Contour interval is 2.5 cm s<sup>-1</sup> in the bottom panels.

episode also occurred from YD 142 to 152 when the wave burst had an amplitude of ~20 cm s<sup>-1</sup> and vertical wavelengths of ~50 m (Fig. 3b). Along-

shelf surface current signals were initially in phase with the subsurface currents through YD 147 when the signals indicated phase separation. The opposite situation occurred in the cross-shelf velocity components (not shown) with respect to the phases. The vertical structure of these oscillations indicated a first or second baroclinic mode vertical dependence compared with a second or third baroclinic mode structure for the high-frequency current signals.

### Subinertial Flow Vorticity

Kunze (1985) showed that the vorticity associated with geostrophically balanced currents alters the passband of allowable near-inertial frequencies. An effective Coriolis parameter was defined

$$f_{\text{eff}} = f + 1/2\{\partial V_g/\partial x - \partial U_g/\partial y\}, \quad (1)$$

where  $f$  represents the local Coriolis parameter and  $U_g$  and  $V_g$  are the geostrophic current components. Here the subinertial current records are used as a proxy for these geostrophic components. In an anticyclonically rotating vorticity regime, the frequency of the near-inertial motions will be  $< f_{\text{eff}}$  as near-inertial motions are trapped and advected by the subinertial flow where amplification of the near-inertial wave signal may occur. By contrast, the effective Coriolis parameter is shifted above  $f$  in cyclonically rotating vorticity regimes as near-inertial motions propagate away from the area.

As shown in Figure 4, the horizontal structure of the near-inertial flows on 25 May was affected by the subinertial flow vorticity, which ranged between  $\pm 2f$ . The center of the submesoscale feature, as depicted by the near-inertial flow, was located along the inshore edge of the Florida Current where normalized vorticity changed sign from cyclonic ( $>0$ ) to anticyclonic ( $<0$ ) rotation. There was a strong convergence zone of near-inertial motions centered in the domain. A large fraction of the near-inertial surface current motions were apparently trapped and advected by the anticyclonically rotating subinertial flow vorticity. In this regime, the near-inertial waves cannot propagate into the positive vorticity regime because of the larger  $f_{\text{eff}}$  as per equation (1). This is one explanation of why the near-inertial energy is amplified in the negative vorticity trough inshore of the Florida Current. In addition, the vertical structure of the near-inertial motions suggests a possible amplification of the signal in the areas of strong subinertial current shear consistent with previous theories (Moore, 1975; Kunze, 1985). Previous observations have also found spin-off eddies because of frontal instabilities as the Florida current moves across the shelf break in this complex regime (Lee, 1975).

### Summary

Emerging technological capabilities of *in situ* and remote sensing observational techniques are

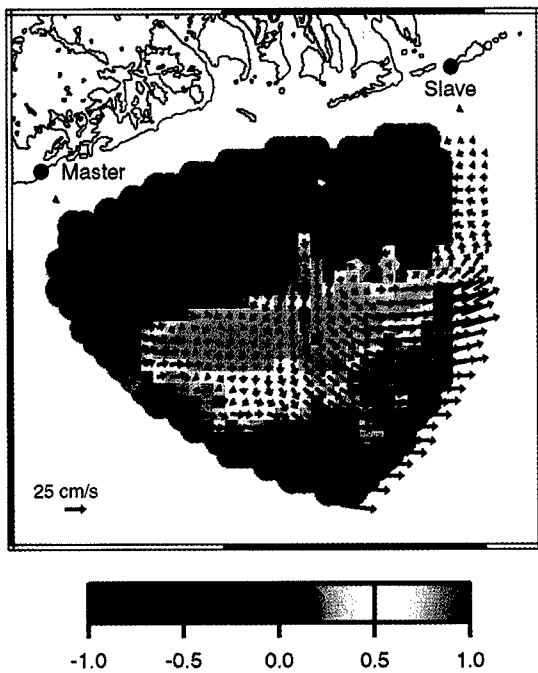


Fig. 4: Near-inertial currents ( $\rightarrow$ ) superposed on the subinertial flow vorticity (color) normalized by  $2f$  ( $f$  is the local Coriolis parameter) from the OPRC-2 experiment at 1800 UTC on 25 May.

providing reliable, spatially evolving snapshots of submesoscale to mesoscale oceanic flows (Shay, 1997). Surface current observations from several experiments in the United Kingdom (Prandle, 1987) as well as the HIREs, OPRC, and Duck94 experiments have suggested that the HF radar-derived surface currents agree well with subsurface current measurements and detect not only the low-frequency and tidal currents, but also internal waves. The surface convergence and divergence patterns of internal wave motions are intrinsically linked to the pycnocline (Gasparovic *et al.*, 1988) and the vertical structure oscillations in the currents. The combination of high-resolution ADCPs embedded within the HF radar grid provides an effective approach to observe evolving, 3-dimensional processes of the internal waves. Thus the 2-dimensional representation of these surface motions and their interactions with the subinertial flows associated with coastal frontal structure observed from HF radar measurements provides a new view to improve our understanding of wave dispersion in the coastal regime.

#### Acknowledgments

The dedicated efforts of Duncan Ross and Jorge Martinez are sincerely appreciated. Hans

Graber, Chris Boyce, Nick Peters, John Hargrove, Brian Haus, and Louis Chemi were involved in the experimental setup and data acquisition efforts. Tom Lee and Liz Williams provided the ADCP data, Jean Carpenter drafted figures, and Terry Faber assisted in the programming effort. The author acknowledges funding support from the USCG-sponsored OPRC (RD9401) directed by Chris Mooers and the continuing support of the ONR Remote Sensing Program through grants N00014-91-J-4133 and N00014-96-1-1101. The Florida Space Grant Consortium under the auspices of the National Aeronautics and Space Administration provided funding for a summer undergraduate internship for Gretzali Perez from the University of Puerto Rico who assisted in processing the observations.

#### References

- Baines, P.G., 1986: Internal tides, internal waves and near-inertial motions. In: *Baroclinic Processes On Continental Shelves*. C.N.K. Mooers, ed. American Geophysical Union, Washington DC, 19-31.
- Chapman, R.D., L.K. Shay, H.C. Graber, J.B. Edson, A. Karachintsev, C.L. Trump and D.B. Ross, 1997: Intercomparison of HF radar and ship-based current measurements. *J. Geophys. Res.*, 102, 18,737-18,748.
- Gasparovic, R.F., J.R. Apel and E.S. Kasische, 1988: An overview of the SAR Internal Wave Experiment. *J. Geophys. Res.*, 93, 12304-12316.
- Graber, H.C., B.K. Haus, R.D. Chapman and L.K. Shay, 1997: HF radar comparisons with moored estimates of current speed and direction: expected differences and implications. *J. Geophys. Res.*, 102, 18,749-18,766.
- Kunze, E., 1985. Near-inertial wave propagation in geostrophic shear. *J. Phys. Oceanogr.*, 15, 544-565.
- Lee, T.N., 1975: Florida current spin-off eddies. *Deep-Sea Res.*, 22, 753-765.
- Mooers, C.N.K., 1975: Several effects of a baroclinic current on the cross-stream propagation of inertial-internal waves. *Geophys. Fluid Dyn.*, 6, 245-275.
- Paduan, J. and M.S. Cook, 1997: Mapping surface currents in Monterey Bay with CODAR-type HF radar. *Oceanography*, 10, 49-52.
- Prandle, D. 1987: The fine-structure of nearshore tidal and residual circulations revealed by HF radar surface current measurements. *J. Phys. Oceanogr.*, 17, 231-245.
- Shay, L.K., 1996: Observed internal wave driven surface currents from HF radar. In: *Coastal Oceanic Conference and Atmospheric Prediction*. American Meteorological Society, Boston, 296-303.
- , in press: Mesoscale Oceanic Flows. In: *Handbook of Fluid Dynamics*. Richard Johnson, ed. CRC Press, Boca Raton, FL.
- , H.C. Graber, D.B. Ross and R.D. Chapman, 1995: Mesoscale ocean surface current structure detected by HF radar. *J. Atmos. Ocean. Tech.*, 12, 881-900.
- , S.J. Lentz, H.C. Graber and B.K. Haus, 1997: Current structure variations detected by HF radar and vector measuring current meters. *J. Atmos. Ocean. Tech.*, (in press).
- Weller, R.A. and R.E. Davis, 1980: A vector measuring current meter. *Deep-Sea Res.*, 27, 575-582. □

. . . HF radar-derived surface currents agree well with subsurface current measurements . . .

# LARVAL TRANSPORT AND COASTAL UPWELLING: AN APPLICATION OF HF RADAR IN ECOLOGICAL RESEARCH

By Eric Bjorkstedt and Jonathan Roughgarden

High-frequency (HF) radar is a recent addition to ecologists' remote sensing toolbox . . .

FOR MANY MARINE FISH and invertebrate species, near-surface currents strongly affect the likelihood of surviving as a planktonic larva and arriving at a suitable location, say, a rocky coastline, a kelp forest, or an estuary, to begin life as a juvenile or adult (i.e., to "recruit" to a population). High-frequency (HF) radar is a recent addition to ecologists' remote sensing toolbox that offers the ability to observe oceanographic processes directly affecting larval ecology at scales appropriate for understanding recruitment dynamics in marine populations.

In this article, we report on our application of HF radar in research focusing on larval ecology at coastal upwelling fronts off central California. Coastal upwelling regions, such as that off the western United States, pose an interesting set of ecological questions that can be addressed with data from HF radar. During active coastal upwelling, the same currents supplying nutrients that support high productivity put planktonic larvae at risk of being swept offshore and away from coastal habitats. Indeed, some fish and invertebrate populations exhibit reduced recruitment success during periods of increased offshore advection (Bailey, 1981; Roughgarden *et al.*, 1988). Coastal upwelling fronts, which form between cold upwelled water near the coast and warmer, fresher surface waters offshore, may reduce offshore transport of planktonic larvae, thereby facilitating nearshore retention and return of larvae to coastal recruitment sites. To test this hypothesis and to assess the utility of HF radar as an ecological tool, we sampled zooplankton along transects spanning coastal upwelling fronts, monitored recruitment to intertidal barnacle populations during the upwelling seasons of 1993 and 1994, and compared our data to coincident HF radar observations.

We used radial data obtained from a single SeaSonde HF radar deployed at Granite Canyon, CA

(36°25.9'N, 121°55.0'W). Before calculating currents, we 1) discarded radial vectors with a standard error to mean ratio >0.1 to ensure data quality, 2) used simple linear interpolation first to fill spatial gaps of <90° within a range bin and then to fill temporal gaps of <24 h in observations in each observation cell, and 3) applied a low-pass filter (PL64) to remove tidal and other high-frequency signals. Under the assumption that the current is uniform across two observation cells, we calculated currents from pairs of radial observations; each result represented the uniform current that would yield both radial currents used in its calculation.

Using a single radar presents a tradeoff between greater spatial resolution (and the increasing likelihood that the current is indeed similar at 2 points closely arranged in space) and the difficulties associated with the "baseline problem" of determining currents from nearly parallel observations. The baseline problem is exacerbated by violations of the assumption that flow is uniform across neighboring observation cells. We screened our results for clear cases where this occurred; currents were discarded and replaced by interpolation if either 1) they were >150 cm s<sup>-1</sup> and within 5° of perpendicular to the radial vectors used in the calculation or 2) they differed from neighboring vectors by a Euclidean distance >30 cm s<sup>-1</sup>.

Figure 1 illustrates an example of the resulting low-frequency current field and a coincident satellite Advanced Very High Resolution Radiometer (AVHRR) image of sea-surface temperature. Patterns in the current field generally coincide with thermal structures. For example, the strong current jet flowing offshore west of Point Sur corresponds directly to the tongue of cool water visible in the AVHRR image. The frontal zone between the cool tongue and warmer water to the north is clearly resolved in the current field as a sharp transition between equatorward flow and the current jet. The southwestern front apparent in the satellite image appears as a transition to weaker currents in the warmer water mass. Temporal series of images demonstrate consistent spatial correlation between HF radar and satellite observations.

Eric P. Bjorkstedt, Department of Biological Sciences, Stanford University, Stanford, CA 94305; Jonathan Roughgarden, Department of Biological Sciences and Department of Geophysics, Stanford University, Stanford, CA 94305, USA.

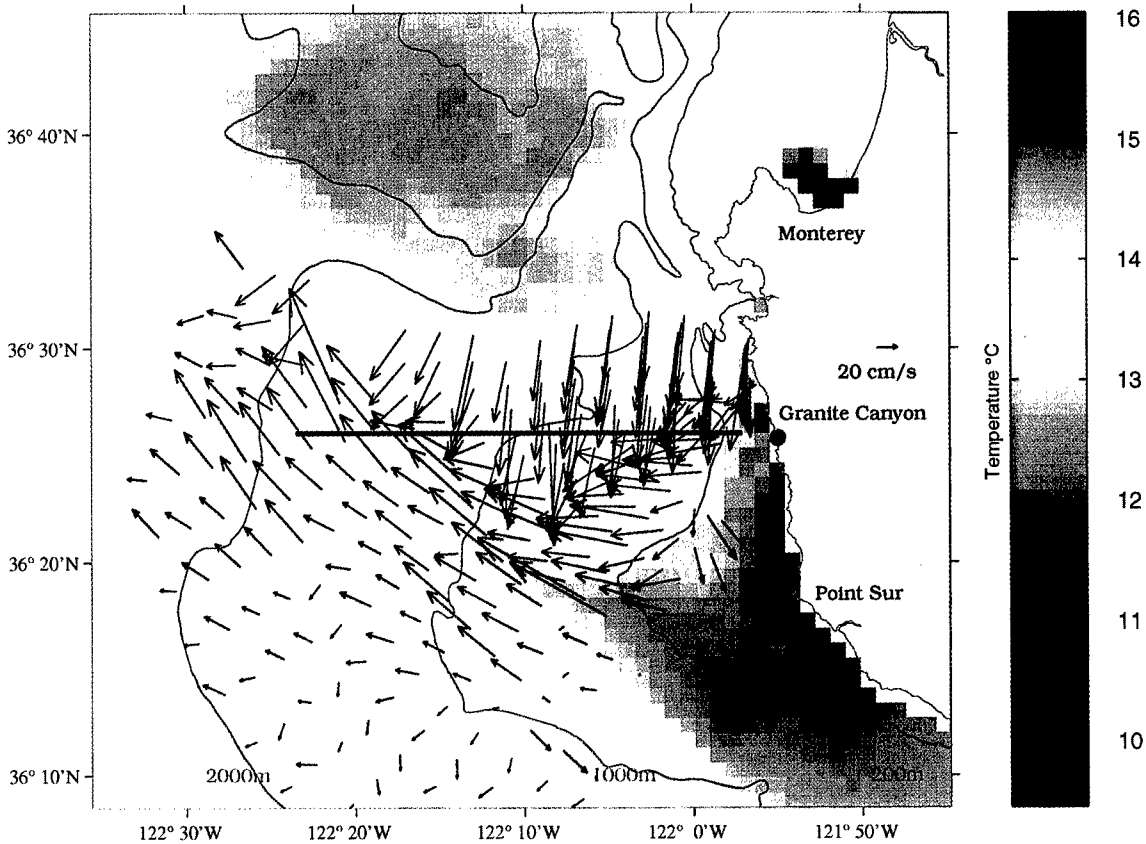


Fig. 1: Surface currents from detided radial data obtained with a single SeaSonde located at Granite Canyon, CA, and satellite AVHRR image of SST for 1700 PST 15 July 1993. Horizontal line shows location of transect data in Figures 2 and 3.

To compare HF radar observations to zooplankton distributions, we calculated divergence from low-frequency surface currents obtained from the SeaSonde data. Convergence zones, marked by negative divergence values, may accumulate buoyant or surface-oriented plankton. Figures 2 and 3 show typical distributions of barnacle and fish larvae, respectively, in relation to divergence and SST. Barnacle larvae are generally bounded inshore of divergences, or accumulate at convergent fronts. Larval fish (mostly rockfish *Sebastes* spp., a coastal group) are most abundant in convergence zones associated with temperature fronts. Fish larvae were sampled from a broader depth range than barnacles (upper 27–37 m and 1 m of the water column, respectively), and distributions of fish larvae across upwelling fronts were observed to follow the slope of the pycnocline. Slight seaward offsets of peak abundances of fish larvae relative to convergent fronts in the ocean surface may therefore occur, but remain consistent with nearshore retention of larvae by the front.

Observations like those described above represent “snapshots” integrating spawning location, timing and intensity, larval survival, and transport processes. Measuring actual larval transport requires time series of such observations. Figure 4 shows a time series of settlement by competent

barnacle larvae to rocks in the upper intertidal zone at a site 15 km north of the radar site in Granite Canyon in relation to surface currents for a period spanning the sole large recruitment pulse of the 1994 upwelling season. In a sense, rather than tracking a patch of larvae with a ship, we use the rocks along the coast to sample temporal vari-

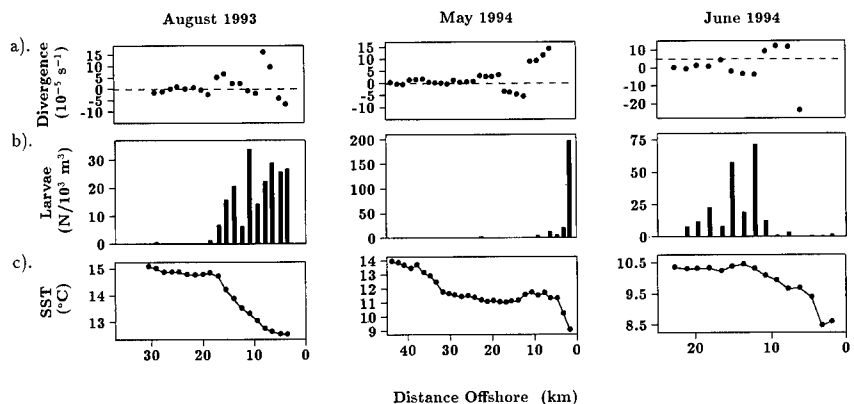


Fig. 2: Distribution of intertidal barnacle larvae in relation to divergence and SST for 11 August 1993, 4 May 1994, and 26 June 1994. Barnacle larvae were sampled in the upper meter of the water column. For each cruise (a) divergence calculated at each sampling station, (b) abundance of barnacle larvae, and (c) SST.

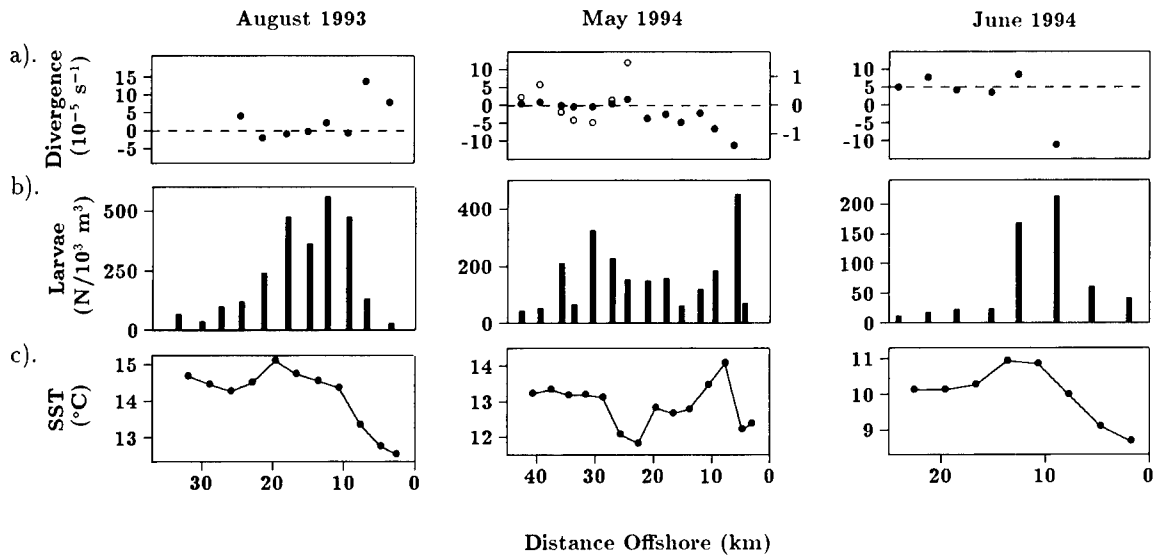


Fig. 3: Distribution of fish larvae in relation to divergence and SST for 11–12 August 1993, 4–5 May 1994, and 26–27 June 1994. Fish larvae were sampled in the upper 27 meters of the water column (upper 37 meters in May 1994). For each cruise: (a) divergence calculated at each sampling station, (b) abundance of fish larvae, and (c) SST. Note: In the divergence plot for May 1994, divergence ( $\times 8$ ) is replotted with (O) at offshore stations to highlight convergence zone associated with an old upwelling front.

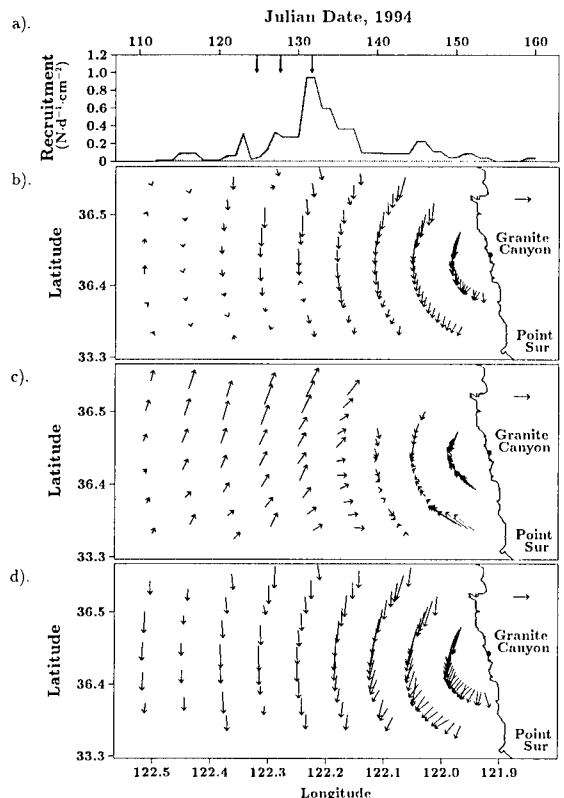
HF radar measures currents affecting ecological processes at important spatial and temporal scales . . .

ation in larval abundance at a given location. During typical upwelling conditions (i.e., surface currents flowing to the south and offshore), recruitment is low (Fig. 4, a and b). The onset of the recruitment pulse, presumably because of the return of larvae to the coastal habitat (Farrell *et al.*, 1991), coincided with a rapid transition to onshore currents in response to a strong relaxation in the winds that drive coastal upwelling (Fig. 4, a and c). After northwesterly winds intensified, typical upwelling currents resumed and recruitment rates fell to low levels (Fig. 4, a and d).

The plankton surveys and recruitment time series provide support for hypotheses that 1) convergence at fronts contributes to accumulation of plankton, 2) coastal upwelling fronts facilitate nearshore retention of coastal larvae, and 3) cessation of upwelling and subsequent shoreward transport of larvae during wind relaxation events is an important mechanism causing recruitment in coastal invertebrate populations (Roughgarden *et al.*, 1988; Farrell *et al.*, 1991).

Fig. 4: Recruitment of barnacle larvae to adult populations in the rocky intertidal zone in relation to changes in surface currents during upwelling relaxation. (a) Recruitment of intertidal barnacles to settlement plates affixed in the rocky intertidal zone at Asilomar (“AB” in Farrell *et al.*, 1991) from 22 April to 29 June 1994. Arrows indicate times of HF radar current maps described below. (b–d) Surface current maps for 1600 PST 4 May, 1600 PST 7 May, and 1600 PST 11 May 1994. The vector on land has a length representing a 50  $\text{cm s}^{-1}$  flow.

Just as importantly, the examples above demonstrate the potential of HF radar as a remote sensing technology enabling researchers to monitor and predict the location and transport of planktonic larvae. HF radar measures currents affecting ecological processes at important spatial (1–100 km) and temporal (hourly-weekly) scales and captures front-scale variability that is absent in larger scale metrics of upwelling intensity (i.e., the



Bakun index). Thus HF radar can support detailed field research and modeling (e.g., Alexander and Roughgarden, 1996) linking upwelling intensity and front structure to marine population dynamics. Such efforts have clear applications in research efforts toward predicting the population dynamics of commercially exploited species and designing effective marine reserves.

#### Acknowledgments

We thank Jeff Paduan and Hans Graber for the opportunity to contribute to this issue and Jeff Paduan for preparing Figure 1. Brian Grantham and Yehoshua Shkedy assisted with shipboard plankton sampling. Leslie Rosenfeld provided physical oceanographic data for the cruises and the PL64 filter. Yehoshua Shkedy collected the barnacle recruitment data. We thank the captains and crew of the R/V *Point Sur*

for their valuable assistance during the sampling cruises. This research has been funded by grants NAGW-2159 from NASA and OCE- 9115876 from the NSF. E.B. was supported by an N.S.F. Graduate Research Fellowship.

#### References

- Alexander, S.E. and J. Roughgarden, 1996: Larval transport and population dynamics of intertidal barnacles: a coupled benthic/oceanic model. *Ecol. Monogr.*, 66, 259–275.
- Bailey, M., 1981: Larval transport and recruitment of Pacific Hake *Merluccius productus*. *Mar. Ecol. Prog. Ser.* 6, 1–9.
- Farrell, T.M., D. Bracher and J. Roughgarden, 1991: Cross-shelf transport causes recruitment to intertidal populations in central California. *Limnol. Oceanogr.*, 36, 279–288.
- Roughgarden, J., S. Gaines and H. Possingham, 1988: Recruitment dynamics in complex life cycles. *Science*, 241, 1460–1466. □

### Oceanographic Consortium Selected as Program Office for National Oceanographic Partnership Program

The Consortium for Oceanographic Research and Education (CORE) has been selected for a \$711,094 contract to become the Program Office for the National Oceanographic Partnership Program (NOPP). The selection was made by a team representing ten Federal agencies (Office of Naval Research, Oceanographer of the Navy, National Science Foundation, National Oceanic and Atmospheric Administration, National Aeronautics and Space Administration, Minerals Management Service, US Geological Survey, Defense Advanced Research Projects Agency, Department of Energy, and the Environmental Protection Agency).

The primary objectives of NOPP are to promote the national goals of assuring national security, advancing economic development, protecting quality of life, and strengthening science education and communication through improved knowledge of the oceans. NOPP includes \$20.5M of appropriations for research and educational activities in oceanography awarded recently on a competitive basis, and it establishes the National Oceanographic Research Leadership Council (NORLC), a high-level group, chaired by the Secretary of the Navy and the Administrator of NOAA (vice-chair). NOPP was introduced in the US Congress as part of the National Oceanographic Partnership Act by Representative Curt Weldon (R-PA), Chair of the Military Research and Development Subcommittee of the House National Security Committee. With the signature of the Fiscal Year 1997 Defense Authorization by President Clinton last fall, NOPP was initiated.

CORE will begin serving as the Program Office for the National Oceanographic Partnership Program on 14 July. As Program Office, CORE will be responsible for providing technical and administrative support to the NORLC, including assistance in preparation of the legislatively mandated annual report to Congress on the status and plans of the NOPP.

CORE is the Washington, DC based association of U.S. oceanographic research and educational institutions, universities, laboratories and aquaria. The 48 CORE members represent the nucleus of U.S. research and education in the ocean. CORE's President, ADM James D. Watkins, USN (Ret), previously served as Chief of Naval Operations and as Secretary of Energy.

Media contact: Dr. Richard W. Spinrad, Director, CORE  
Phone: (202) 232-3900 x219  
E-mail: rspinrad@brook.edu

# TRANSPORT PATTERNS OF TROPICAL REEF FISH LARVAE BY SPIN-OFF EDDIES IN THE STRAITS OF FLORIDA

By Hans C. Graber and Claire B. Limouzy-Paris

Better description of transport patterns . . . is essential for understanding the relationship between replenishment of larvae and their subsequent settlement at sites . . .

**T**ROPICAL REEF FISHES belong to a broad phylogenetic group and, as a result, exhibit considerable diversity. Their only shared characteristic as an ecological entity is their fate as reef-associated adults. Their complex life cycles, in which pelagic larval phases alternate with demersal juvenile and adult phases, varies considerably within the early life history (ELH) stages (i.e., egg, larval, and juvenile stages) (Cowen and Sponaugle, 1997). This variability implies coral reef fishes have adapted differentially to the surrounding dynamic environment and may utilize different pathways while in the pelagic zone, to be transported nearshore at the time they metamorphose. Better description of transport patterns (e.g., dispersal and retention mechanisms) is essential for understanding the relationship between replenishment of larvae and their subsequent settlement at sites where transition into juveniles and adults can be achieved.

Recent large-scale ichthyoplankton and hydrographic surveys in the southern Straits of Florida have suggested that mesoscale circulation processes (i.e., cold core gyres) induce significant recruitment variability of reef fish and lobster larvae along the Florida Keys (Yeung, 1991; Lee *et al.*, 1992, 1994). These gyres of relatively long duration (1–3 mo) often cause shoreward transport and tend to concentrate and retain locally spawned larvae (Porch, 1993; Lee *et al.*, 1994; Criales and Lee, 1995). However, in a nongyre situation, less is known about the dynamics of coastal interactions between the strong frontal boundary of the meandering Florida Current (FC) and the inshore reef system. Numerous researchers have speculated that hydrographic features serve to retain larvae near their spawning sites on the reefs (Leis, 1993; Milicich, 1994; Richards *et al.*, 1995). Cowen *et al.*, (1993) further suggested that dynamic oceanic processes in

conjunction with specific behavior patterns may be involved in translocation of diverse reef fish assemblages and specific-level biota. Thus small-scale flow measurements are needed to characterize these mechanisms acting upon the ELH stages.

Here we report on observations of reef fish larval transport mediated by remotely sensed spin-off eddies. Such eddies were first observed by Lee (1975) in current meter data. However, remote sensing of currents using HF radar provides a unique tool to probe repeatedly and noninvasively the ocean surface at high spatial and temporal resolution over a large domain.

## Biological Sampling and Current Observations

An ichthyoplankton survey was carried out with the R/V *Oregon II* during the 13-h period from 1300 UTC 25 May to 0330 UTC 26 May 1994. The survey consisted of nine stations (7 day and 2 night) along three transects (Figure 1) with 23 hauls sampled via oblique tows using Bongo nets with a 333- $\mu$ m mesh. Expendable bathythermographs were deployed before each haul to determine the depth of the thermocline. The results discussed here are limited to surface samples (0–40 m) that were always within the mixed layer. Details of the biological analysis can be found in Limouzy-Paris *et al.* (1997).

The OSCAR system measured the surface vector current fields associated with coastal eddies over the coral reefs and the adjacent FC. From two sites located at Boca Chica and Bahia Honda in the South Florida Keys, currents were recorded in near real time (20-min sampling) and at 1-km resolution over a 30  $\times$  40-km domain.

Average surface current maps were computed for each biological transect to represent mean reef and oceanic flow conditions. Horizontal trajectories were computed at 20-min intervals for 12 h before (backward) and after (forward) each station was sampled. In these calculations we assume no mixing or external forces (winds and waves) influenced the trajectories. These trajectories were used to estimate the origination and destination of reef fish larvae.

Hans C. Graber, Rosenstiel School of Marine and Atmospheric Science, University of Miami, Miami, FL 33149–1098, USA; Claire B. Limouzy-Paris, Marine Sciences Research Center, State University of New York at Stony Brook, NY 11794–5000, USA.

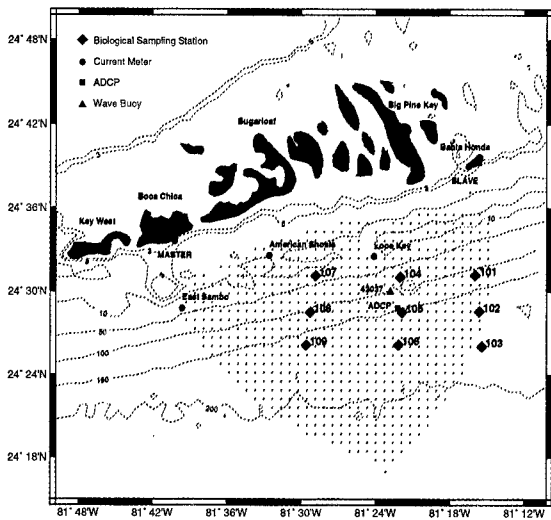


Fig. 1: Experimental setting in the lower South Florida Keys. The small dots show the OSCR cell positions.

### Eddy Dynamics

During the 13-h synoptic sampling period a cyclonic spin-off eddy, 10 km in diameter, with a swirl speed of  $\approx 50 \text{ cm s}^{-1}$ , migrated along the inshore edge of the meandering FC. It had an eastward translation speed of about 25 km/d (see Fig. 1 in Haus *et al.*, 1997). This feature produced a strong cyclonic current reversal and westward flow of 20–30  $\text{cm s}^{-1}$  in the upper 50 m (above the thermocline) at a mooring equipped with an acoustic Doppler current profiler (ADCP) offshore of Looe Reef. Shay *et al.*, (1997) compared OSCR surface current vectors with the upper most bin (15 m below surface) of the ADCP and found very high correlation ( $>0.8$ ) during this sampling period. The vertical distribution of the horizontal

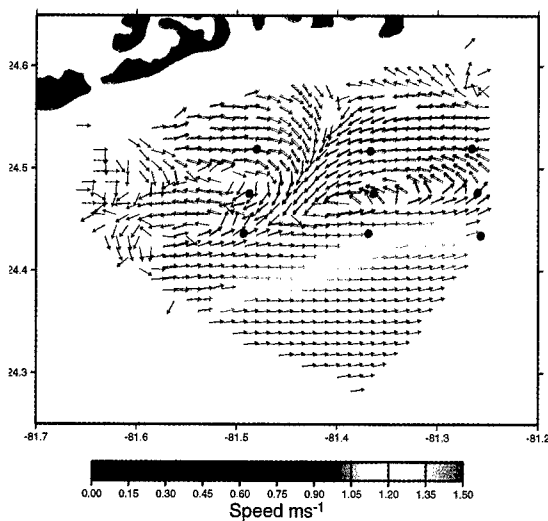


Fig. 2: Average surface vector currents observed by OSCR during the sampling period of the easternmost transect (Stations 101–103). The dots (●) indicate biological sampling stations as defined in Figure 1.

flow was uniform during this period, suggesting little shear in the upper ocean layer above the thermocline. The presence of the eddies was also observed in the subsurface temperature field that showed distinct doming of the 27°C isotherm surface (Graber *et al.*, 1995) that extended to a depth of 50–75 m.

The following flow patterns were observed during the survey of the eastern transect (101–103); these stations sat on the eastern edge of a well-defined eddy causing strong onshore flow (Fig. 2). At the western end of this feature (between the middle and western transects) a strong alongshore flow convergence and offshore jet was observed. In the wake of this eddy, a weak, less-defined eddy formed in the western part of the OSCR array. The dominant FC initially intruded far reefward.

The temporal coverage of the OSCR data showed how these features evolved during the survey. During the middle transect (104–106) the main eddy advected eastward and moved partially out of the domain, producing a weak convergence near the reefward stations. The offshore station was then located on the boundary of the stronger ( $>1 \text{ m s}^{-1}$ ), eastward flowing FC. A weak trailing disturbance was observed near the western transect. By the time stations 107–109 were sampled, the main eddy feature had totally vanished from the OSCR domain and the FC had moved further offshore. For the biological analysis these flow scenarios were related to the micro-distribution and abundance of larval fishes.

### Ichthyoplankton

Results from the 13-h sampling period were representative of the very high biodiversity previously observed in the Florida Straits (Limouzy-Paris, 1994). More than 5,000 fish larvae, representing 246 taxa, were collected. The dominant taxa (61%) were reef fishes. Abundance and distributions were determined for reef, coastal, and oceanic groups. Limouzy-Paris *et al.*, (1997) compared larval fish assemblages over the entire water column to the upper strata; their results indicated the importance of eddies as a mechanism for alongshore dispersal of posthatch larvae and for translocation of late stage reef fish larvae to inshore settlement sites.

### Trajectories

The hypothesis of translocation and longshore dispersal was evaluated by simulating horizontal transport with particle trajectories through each station, using the ocean surface current vectors recorded during the experiment. Figure 3 shows three examples of trajectories passing through positions near selected stations. The trajectories reveal that station 102, at the inshore edge of the FC, was strongly influenced by the passage of the eddy. Water, originating in the FC, was entrained by the eddy and transported onshore and westward (Fig.

. . . a cyclonic spin-off eddy . . .  
migrated along the inshore edge of the meandering FC.

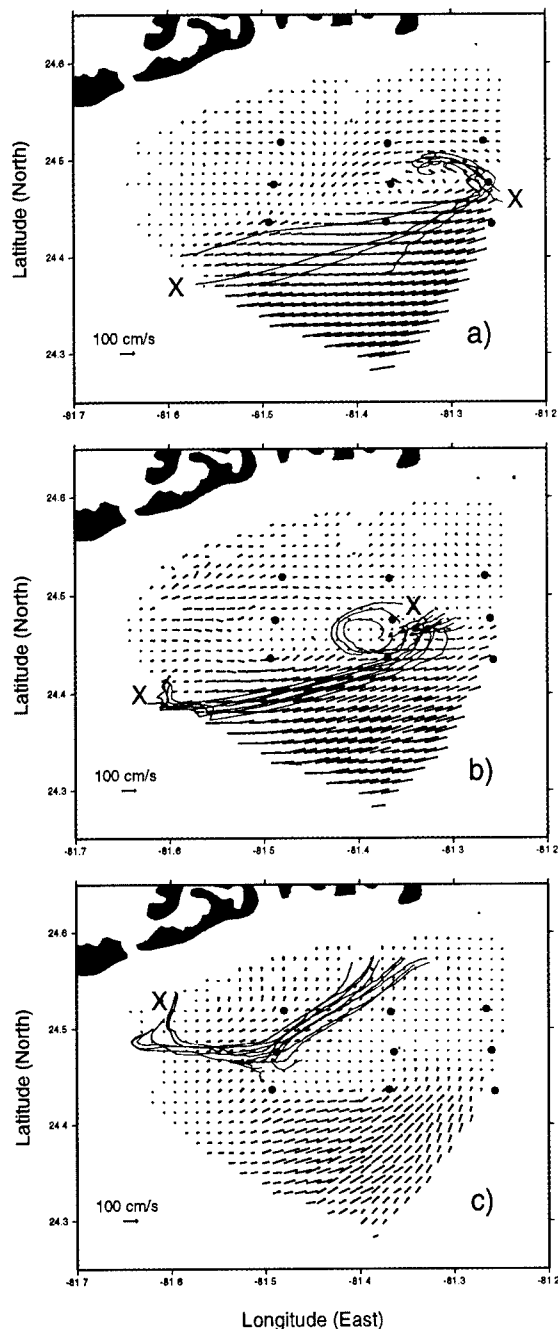


Fig. 3: The trajectories represent the simulated transport patterns of fish larvae when treated as passive particles. The surface current maps in each panel corresponds to the flow field at the sampling time,  $T_0$ , of the selected station. A cluster of trajectories from the nine OSCR cells surrounding a station were computed for a period of 12 h before and after the sampling time. X, start of each trajectory bundle (i.e.,  $T_0-12$ ).

3a). Similar conditions existed at the offshore station (106) of the central transect. Here FC water was mixed with entrained coastal water as a result of a current reversal induced by the eddy (Fig. 3b). This clearly shows that the central stations (105 and 106) were both exposed to water of oceanic origin, which crossed the boundary current into the coastal domain by means of eddy entrainment. During the western

transect at station 108 (Fig. 3c), the trajectories showed purely coastal origin, with possible tidal influence, moving slower but in the same direction (alongshore) as the main eastward flowing FC.

### Translocation

Results from the upper 40-m samples strongly suggest species specific distributions were largely influenced by the dynamics of eddies. As a response to the eddy effect, representative species of each ecological grouping (i.e., reef, coastal, and oceanic) showed anomalies in regard to their distribution across the strong FC frontal boundary. The displacement of oceanic tuna larvae (*Thunnus* sp.) toward shore in the middle transect in the convergence zone suggests that eddy dynamics allowed cross-frontal exchanges, translocating larvae shoreward (Fig. 4a). Most coral reef species spawn pelagic eggs; these eggs and newly hatched larvae move passively through the water column. They could be entrained from upstream locations in the FC front, having distributions more like larvae of oceanic fishes than reef fishes (Leis, 1993). Larvae from squirrelfishes (*Holocentrus* sp.) behaved in the same way as tuna larvae and were translocated shoreward by the spin-off eddy (not shown).

The spawning behavior of nonreef shorefishes (i.e., coastal group) in tropical areas is less understood. They apparently migrate to the shelf edge to spawn (Leis and Reader, 1991). Tonguefish (*Symphurus* sp.) larvae representative of the coastal group were distributed further from shore than the tuna larvae, with highest abundance in the convergence zone of the main eddy (Fig. 4b).

The spin-off eddies could also contribute to alongshore dispersal of shore fishes which spawn on the reef zone. Lower swirl speeds on the inshore edge of the eddy compared to its offshore edge could possibly trap early larvae. The simulated trajectories agree well with these biological interpretations; Figure 4 depicts the influence of eddies on the spatial distribution of members of oceanic, shore, and reef fish groups depending on their origin.

### Conclusions

This study has demonstrated the importance of eddy dynamics in assessing the distribution and abundance of reef fish larvae. The employment of radar remote sensing has provided not only a new perspective on larval ecology but also a viable approach to direct biological sampling and made it possible to interpret the biological response to observations of the dynamics of small-scale flow features. Our results revealed that the evolution of spin-off eddies along the edge of the FC front serve as recruitment mechanism for reef fishes by enhancing the following: 1) longshore dispersal of larvae from coastal origin and 2) cross-frontal exchange of larvae from the adjacent oceanic FC (i.e., from oceanic origin) into settlement sites. Because of the highly dynamic nature of coastal processes and the complexity of larval behavior, re-

. . . radar remote sensing has provided not only a new perspective on larval ecology but also a viable approach to direct biological sampling . . .

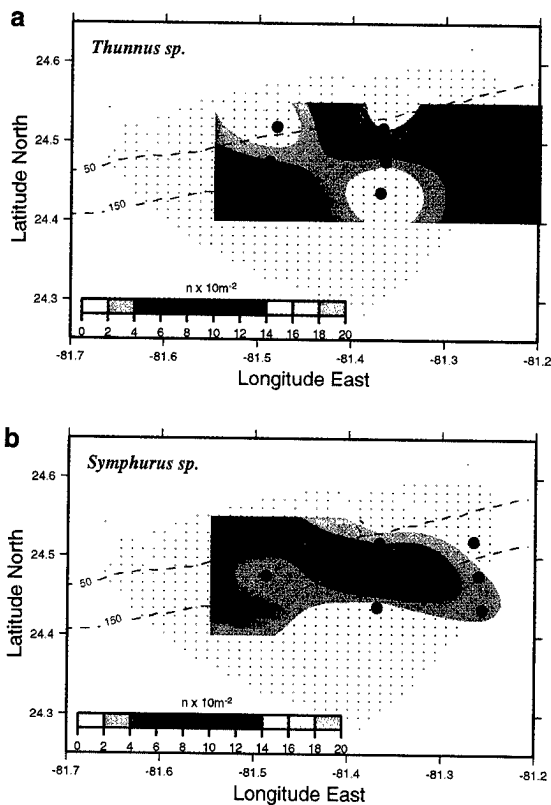


Fig. 4: Spatial distribution of tropical larval fish abundances for representative species of the oceanic group (a) tuna (*Thunnus* sp.) and of the coastal group (b) tonguefish (*Symphyrus* sp.).

remote sensing of surface processes provide crucial observations to advance our understanding in variations of larval supply and recruitment rates. By linking remote sensing with other *in situ* and biological measurements, we will not only identify the influence of nearshore physical forcing (tides, winds, and waves) on reef fish larvae transport, but we will also be able to determine the predictability of small-scale eddies in the Florida Straits and their impact in the coral reef ecosystems.

#### Acknowledgments

Numerous personnel, especially Brian Haus, Nick Shay, Dave Jones, and Bill Richards, made this unique study possible by helping with OSCR, ichthyoplankton sampling on the R/V *Oregon II*, and biological analysis. Special thanks goes to Slavica Nikolic, who produced the graphics. This study was sponsored by the U.S. Coast Guard through South Florida Ocean Pollution Research Center (SFOPRC) and the National Oceanic and Atmospheric Administration under the Southeast Florida Caribbean Recruitment Project (SEFCAR).

#### References

- Cowen, R.K., J.A. Hare, M.P. Fahay, H.G. Moser, P.E. Smith and L.A. Fuiman, 1993: Beyond hydrography: can physical processes explain larval fish assemblages within the Middle Atlantic Bight? Advances in the early life history of fishes. *Bull. Mar. Sci.*, 53, 567–587.
- and S. Sponaugle, 1997: Relationships between early life history traits and recruitment among coral reef fishes. In: *Early Life History in Fish Populations*. R.C. Chambers and E.A. Trippel, eds. Chapman & Hall, London, 423–449.
- Criales, M.M. and T.N. Lee, 1995: Larval distribution and transport of penaeoid shrimps during the presence of the Tortugas Gyre in May–June 1991. *Fish. Bull. US*, 93, 471–482.
- Graber, H.C., T.N. Lee, B.K. Haus, C.G.H. Rooth, E.J. Williams and L.K. Shay, 1995: Observations of ocean surface currents off the south Florida Keys using an HF Doppler radar. SFOSRC/SEFCAR Pilot Field Study PFS-2: 14 May–13 June 1994. SFOSRC Technical Report, University of Miami, Miami, FL, 175 pp.
- Haus, B.K., H.C. Graber and L.K. Shay, 1997: Synoptic measurement of dynamic oceanic features. *Oceanography*, 10, 45–48.
- Lee, T.N., 1975: Florida Current spin-off eddies. *Deep-Sea Res.*, 22, 753–765.
- , M.E. Clarke, E.J. Williams, A.F. Szmant and T. Berger, 1994: Evolution of the Tortugas gyre and its influence on recruitment in the Florida Keys. *Bull. Mar. Sci.*, 54, 621–646.
- , C.G.H. Rooth, E.J. Williams, M.F. McGowan, M.E. Clarke and A.F. Szmant, 1992: Influence of Florida Current, gyres and wind-driven circulation on transport of larvae and recruitment in the Florida Keys coral reefs. *Cont. Shelf Res.*, 12, 971–1002.
- Leis, J.M., 1993: Larval fish assemblages near Indo-Pacific coral reefs. *Bull. Mar. Sci.* 53, 362–392.
- Leis, J.M. and S.E. Reader, 1991: Distributional ecology of larval milkfish *Chanos chanos* (*Pisces: Chanidae*) in the Lizard Island region. *Environ. Biol. Fish.*, 30, 315–405.
- Limouzy-Paris, C.B., M.F. McGowan, W.J. Richards, J.P. Uman and S.S. Cha, 1994: Diversity of fish larvae in the Florida Keys: results from SEFCAR. *Bull. Mar. Sci.*, 54, 857–870.
- , H.C. Graber, D.L. Jones, A. Röpke and W.J. Richards, 1997: Translocation of larval coral reef fishes via sub-mesoscale spin-off eddies from the Florida Current. *Bull. Mar. Sci.*, 60, 966–983.
- Milicich, M.J., 1994: Dynamic coupling of reef fish replenishment and oceanographic processes. *Mar. Ecol. Prog. Ser.*, 110, 135–144.
- Porch, C.E., 1993: A numerical study of larval retention in the southern Straits of Florida. Ph.D. dissertation, University of Miami, 245 pp.
- Richards, S.A., H.P. Possingham and B.J. Noye, 1995: Larval dispersion along a straight coast with tidal currents: complex distribution patterns from a simple model. *Mar. Ecol. Prog. Ser.* 122, 59–71.
- Shay, L.K., T.N. Lee, E. Williams, H.C. Graber and C. Rooth, 1997: Vertical structure variations in ocean currents detected by HF radar and an acoustic Doppler current profiler. *J. Geophys. Res.* In press.
- Yeung, C., 1991: The vertical, horizontal, and seasonal distribution and abundance of palinurid and scyllarid lobster phyllosomat larvae in the Florida Keys in relation to the circulation, May 1989–February 1990. M.S. thesis, University of Miami, Miami, FL, 141 pp. □

. . . to determine the predictability of small-scale eddies in the Florida Straits and their impact in the coral reef ecosystems.

# EVOLUTION OF BEARING DETERMINATION IN HF CURRENT MAPPING RADARS

By Donald E. Barrick and Belinda J. Lipa

**N**EARLY ALL TARGET detection "radars" in existence operate at microwave frequencies because their wavelengths are small enough that compact antennas provide both good angular resolution and high sensitivity. By contrast, at high frequency (HF) very large antenna arrays are needed to achieve similar results using traditional signal processing techniques. (To form and scan a beam equal in width to that from a 2-m microwave dish demands an HF receive antenna that is 2–3 km in length.) Despite this physical drawback, only at HF is the first and second-order sea echo directly relatable to surface waves and winds and, through the Doppler relation, to surface currents (Crombie, 1955; Barrick, 1972). For example, at microwave frequencies Doppler shifts depend on many scattering properties of the surface in addition to the wave and current speeds.

At HF as well as at microwave, range to a radar cell can be obtained accurately from the echo's time delay; Doppler is likewise obtained from spectral analysis of the echo time series. The problem lies in the accurate determination of bearing. Much of the effort in HF radar hardware and software research over the past 20 years has been in the development of smaller, affordable antenna systems that maintain the bearing accuracy of the larger antenna arrays. Our paper summarizes the latest advance in this quest, describing a powerful new direction finding (DF) algorithm called Multiple Signal Classification (MUSIC), which is particularly well suited for application to HF radar sea echo. Its performance is demonstrated using simulation analyses.

## Direction Finding Bearing Estimation

As old as radio itself, the simplest DF system is a loop antenna rotated until the incoming signal vanishes. Knowledge of this null direction and the angular response function of the antenna provides

information about the direction from which the radio signal is originating.

Use of DF for current mapping began in 1975. The most compact realizations of DF techniques for this purpose have been the CODAR-type HF radars, which employ two crossed loops mounted around a whip (vertical monopole). An example of this antenna configuration is shown in Figure 1, along with stylized plots of the ideal angular amplitude patterns for each of the three elements. In addition to the theoretical (and achieved) shape of the antenna patterns, the accuracy of all DF algorithms also depend on the signal-to-noise (S/N) ratio of the measured backscatter.

Historically, current-mapping DF antennas and algorithms have taken several forms. Barrick *et al.* (1977) and Gurgel (1997) used antenna elements separated by short distances and relied on phase-path differences to extract bearing. We focus here on the most compact systems where the antenna elements are colocated. Their inherent amplitude and phase pattern differences have led to use of the following DF techniques:

1. The simplest algorithm, which takes the ratio of signals from the two loops (with sine and cosine patterns) and the whip (with omni-directional reception), and extracts bearing using the arctangent function. This closed-form algorithm is applied to each spectral bin constituting the Bragg peak. Although conceptually simple, this method is not robust in the presence of spatially complex current fields or when antenna patterns are distorted.

2. A least-squares algorithm that best-fits a model for each received Doppler frequency to measured cross spectra among the three antenna signals as demonstrated by Lipa and Barrick (1983). This method can handle both single- and dual-angle solutions (1 or 2 signals at the same frequency from different bearings) and provides limited statistical means for testing which solution fits the data better. Unlike closed-form solutions, the method can incorporate measured antenna patterns that may be distorted from the ideal patterns by nearby environmental obstacles (Barrick and

Donald E. Barrick and Belinda J. Lipa, CODAR Ocean Sensors, LTD., 1000 Fremont Ave., Los Altos, CA 94024, USA.

Much of the effort in HF radar hardware and software research . . . has been in the development of smaller, affordable antenna systems . . .

Lipa, 1986). Used for 15 years, this method suffers from the following two defects: 1) it is numerically inefficient because it uses a two-dimensional grid search to find best solutions to the nonlinear problem; hence, it is not easily extended to more complex antennas and 2) the covariance matrix among antenna signals for sea echo is singular because they are correlated. This inefficiency restricts the use of objective hypothesis testing to select between single and dual-angle solutions.

3. The MUSIC algorithm as presented by Schmidt (1986). Using an eigenfunction analysis of signals received on  $N$  antennas, MUSIC can find up to  $N-1$  signal bearings at the same frequency. It takes advantage of the covariance matrix singularity in extracting bearing.

### MUSIC Applied to HF Current Mapping

We provide here a stepwise procedural outline for the application of MUSIC to the HF direction finding problem:

- Form a sample covariance matrix of the complex spectrally analyzed signals from the  $N$  antenna elements. (For the SeaSonde with  $N = 3$ , this is  $3 \times 3$ .) Each spectral bin corresponds to a known current radial velocity, which is the independent variable of the problem. In practice, several consecutive cross spectra are averaged to get the sample covariance matrix.
- Perform an eigenfunction analysis of the covariance matrix and order the eigenvectors from largest to smallest by eigenvalue. The biggest of these represents sea echo from one or more bearings at the given radial velocity, whereas the smaller eigenvectors are noise. By definition, all of the eigenvectors are mutually orthogonal.
- Create the signal-model vector from the known antenna patterns. For our idealized case, these are sine, cosine, and constant functions of angle. If the patterns are distorted, their measured responses are used instead. This becomes an  $N$ -element vector.
- Determine candidate bearings using the fundamental principle behind MUSIC; i.e., the signal model vector at a correct incoming echo bearing from the sea is orthogonal to all of the noise eigenvectors. The algorithm finds the angle(s) at which this condition occurs. For example, with the SeaSonde, one does this first for a single-angle possibility where  $N - 1 = 2$  eigenvectors are assumed to be noise, followed by the dual-angle possibility where only  $N - 2 = 1$  eigenvector remains as noise.
- Test to find which candidate bearings best-fit the data; Schmidt (1986) suggests the statistical chi-squared and F-tests. For the  $N = 3$  SeaSonde system, which allows up to two angles for each radial speed from each Bragg peak, there can be from one to four angles found (each Bragg peak has independent information).

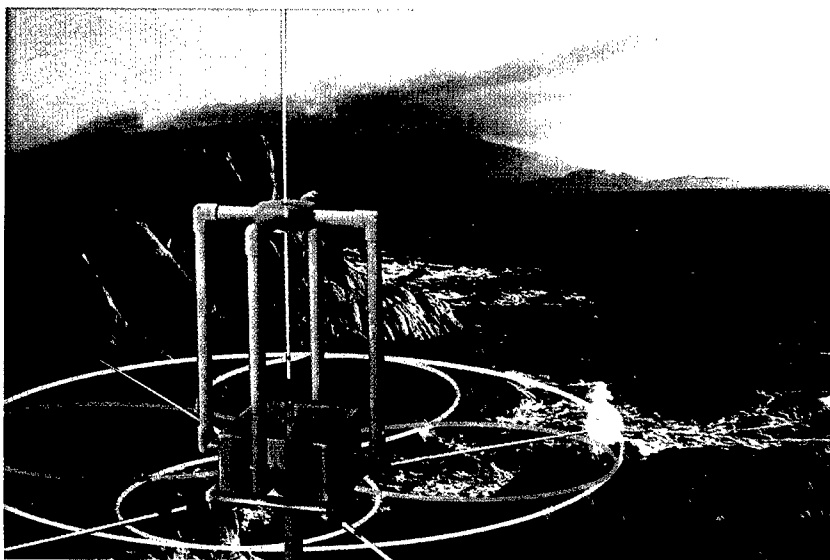


Fig. 1: Stylized view of a coastal SeaSonde crossed-loop/monopole receive antenna. Indicated at the antenna base are idealized patterns of the two loops (yellow and pink) and the vertical whip/monopole (white).

More antenna elements admit more bearing solutions, as well as better angular accuracy and resolving capability, as demonstrated below.

### Simulations Using the MUSIC Algorithm

The most obvious scenarios for developing and optimizing bearing-estimation algorithms involve the collection of "ground-truthing" current measurements. However, such endeavors are expensive and generally woefully inadequate in terms of the amount of data collected. Sometimes overlooked is the capability of simulations to offer cost-effective ways to optimize candidate algorithms. In this case, one controls the input current pattern against which extracted estimates are compared on a point-by-point basis, giving statistical estimates of error. The essence of our simulations with the MUSIC algorithm are given in the following paragraph; details, such as the spectral models used to represent sea echo, can be found in Barrick and Lipa (1996).

We evaluated the performance of the MUSIC algorithm under different ocean wave and current conditions. In these cases, the following three deterministic patterns as a function of bearing angle were used as input to the simulations: 1) antenna element responses, 2) mean wind-wave (Bragg-signal) distribution, and 3) mean radial current speeds. In addition, the following two input variables were randomized: 1) the HF signal voltage at each bearing step, which was a zero-mean Gaussian sample whose variance followed the Bragg-signal distribution, and 2) radial current fluctuations about the mean current at each bearing step.

### Scenarios Studied

In this paper we examine two ocean scenarios that are both commonly encountered and reason-

Sometimes overlooked is the capability of simulations to offer cost-effective ways to optimize candidate algorithms.

The first scenario represents summertime upwelling . . .

ably complex. The first scenario represents summertime upwelling off the U.S. west coast. In this case, persistent winds from the northwest drive an offshore surface current to the southwest that brings deeper water to the surface along the coast. We consider the HF radar (SeaSonde) to be deployed on a straight coastline, as shown in the inset of Figure 2a. We assume that the wind-wave pattern has a typical  $\cos^4[(\varphi - \varphi_w)/2]$  distribution over bearing  $\varphi$ , where  $\varphi_w$  is the onshore wind direction (Fernandez *et al.*, 1997). The mean radial current pattern for an annular range cell is modeled by the solid curve shown on Figure 2a. This scenario is a good test for any algorithm because it has both single- and dual-valued speed ranges versus angle. The open circles on Figure 2a are estimates retrieved using MUSIC with no randomization of the input current, whereas the x's are the estimates for which a  $\pm 10$  cm/s [root mean square (rms)] fluctuation was added to the mean pattern. These results are based on the optimized processing and algorithm parameters described in the next section.

The second scenario tested includes an oceanographic front.

The second scenario tested includes an oceanographic front. During this rare but interesting event, the current changes abruptly, as much as 50 cm/s, over a very short distance. We model this by shifting a portion of the upwelling current pattern (Fig. 2a) upward by 45 cm/s. The result (Fig. 2b) is quite stressing for any bearing estimation method, both because of the difficulty of resolving the discontinuity as well as the fact that the problem is now triple- or quadruple-valued. For example, a beam-scanning phased array with a 100-m antenna and resulting  $14^\circ$  beamwidth would smear (i.e., low-pass-filter) through this front. To test the direction-finding MUSIC algorithm on this scenario, we added a  $\pm 5$  cm/s (rms) random current component to the mean pattern. Results are presented in Figure 2b for the standard, three-element antenna configuration used in the SeaSonde and for an expanded, five-element array with two additional monopole elements positioned as shown in the inset. The results are encouraging, even for this extreme frontal situation.

### Optimization of the MUSIC Algorithm

Although continued experience always leads to improvements, a considerable amount of testing and comparisons with input have led to what we consider at this point to be the best mix of processing and algorithm parameters. These have been used to obtain the extracted points displayed in the above figures. They are based on two fairly stressing current scenarios with up to quadruple-angle solutions, as well as an abrupt jump. The optimum processing flow that we now recommend involves the following steps:

- Perform fast Fourier transforms on the N antenna signals every 256 s. At 13 MHz this results in a velocity resolution of 4.5 cm/s.

- Form three-sample covariance-matrix averages of these N signals versus Doppler shift (radial speed) with  $\sim 30\%$  overlap. This provides radial current estimates every 10 min.
- Accumulate MUSIC-derived bearings versus radial velocity every 10 minutes over one hour.
- Apply a running average filter over  $10^\circ$  in bearing angle stepped along every  $2^\circ$ .

To resolve the multiple-angle hypotheses within the MUSIC algorithm, the dual-angle solution is selected for our N = 3 SeaSonde if the following three conditions are all met: 1) The ratio of the largest two eigenvalues is  $\geq 20$ , 2) the ratio of the two signal powers is  $\geq 10$ , and 3) the ratio of

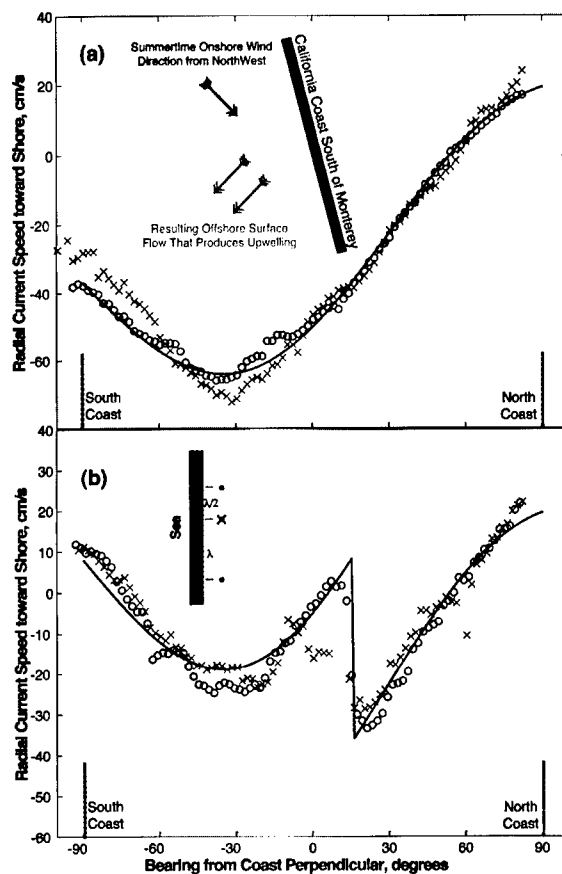


Fig. 2: Input mean radial current pattern versus bearing (solid curves) for California coastal upwelling scenario (a) showing retrieved MUSIC bearings for a three-element SeaSonde antenna with no random current component (green circles; rms error = 2.1 cm/s) and with a 10 cm/s rms random fluctuation (red crosses; rms = 4.9 cm/s) and for a frontal jump of 45 cm/s at  $15^\circ$  bearing (b) showing retrieved bearings for a three-element SeaSonde antenna (red crosses; rms error = 5.7 cm/s) and for a five-element antenna with two elements added off to the side (green circles; rms error = 3.8 cm/s). For case (b) a random 5 cm/s rms fluctuation was added to mean currents for both antenna configurations.

the minor diagonal element product to the principal diagonal product of the  $2 \times 2$  signal matrix is  $1/3$ , which is a measure of the matrix' positive definiteness.

The present SeaSonde operates with  $N = 3$  antenna elements, all mounted on a single post. We examined various configurations where extra elements were added off to the side. The  $N = 5$  configuration found to be best is that shown on Figure 2b where whips (monopoles) are placed  $\frac{1}{2}$  and 1 wavelength to either side of the crossed-loop/monopole unit.

### Summary and Conclusions

Analysis of different ocean wind, wave, and current scenarios in simulations of radial current retrieval algorithms using HF radar backscatter should continue. This endeavor helps us both to develop new algorithms and to quantify the accuracy of these algorithms. The present study is a snapshot of some recent progress in this area applied to small-footprint, direction-finding systems. The same techniques can be applied to algorithms used with beam-forming systems (e.g., Barrick and Lipa, 1996). A summary of what we have found using the MUSIC algorithm reveals:

- Errors with the 3-antenna SeaSonde system using 1-h averaging are  $\sim 2$  cm/s for dual-angle scenarios, like the upwelling example, when no random current fluctuations are added to the mean current pattern. These errors increase to  $\sim 5$  cm/s when  $\pm 10$  cm/s rms fluctuations are added to the mean currents.
- Adding additional antenna elements to the basic three-element SeaSonde configuration improves its ability to map complicated current scenarios, such as the quadruple-angle front scenario. The

five-element configuration tested here was able to retrieve the abrupt current jump across the front in the presence of  $\pm 5$  cm/s rms current noise. In the case of the smoother current patterns, such as the upwelling scenario, there is no appreciable accuracy difference between the three- and five-element antenna configurations.

### Acknowledgments

We are grateful for the technical and editorial improvements made by Dr. Jeff Paduan of the Naval Postgraduate School.

### References

- Barrick, D.E., 1972: First-order theory and analysis of MF/HF/VHF scatter from the sea. *IEEE Trans. Antennas Propag.*, AP-20, 2-10.
- , M.W. Evans and B.L. Weber, 1977: Ocean surface currents mapped by radar. *Science*, 198, 138-144.
- and B.J. Lipa, 1986: Correcting for distorted antenna patterns in CODAR ocean surface measurements. *IEEE J. Ocean. Engr.*, OE-11, 304-309.
- and B.J. Lipa, 1996: Comparison of direction-finding and beam-forming in HF radar ocean surface current mapping, Phase 1 SBIR Final Report. Contact No. 50-DKNA-5-00092. National Oceanic and Atmospheric Administration, Rockville, MD.
- Crombie, D.D., 1955: Doppler spectrum of sea echo at 13.56 Mc/s, *Nature*, 175, 681-682.
- Fernandez, D.M., H.C. Graber, J.D. Paduan and D.E. Barrick, 1997: Mapping wind direction with HF radar. *Oceanography*, 10, 93-95.
- Gurgel, K.-W., 1997: Experience with shipborne measurements of surface current fields by radar. *Oceanography*, 10, 82-84.
- Lipa, B.J. and D.E. Barrick, 1983: Least-squares methods for the extraction of surface currents from CODAR crossed-loop data: application at ARSLOE. *IEEE J. Ocean. Engr.*, OE-8, 226-253.
- Schmidt, R.O., 1986: Multiple emitter location and signal parameter estimation. *IEEE Trans. Antennas Propag.*, AP-34, 276-280. □

. . . a snapshot of some recent progress in this area applied to small-footprint, direction-finding systems.

# VALIDATION OF HF RADAR MEASUREMENTS

By Rick D. Chapman and Hans C. Graber

**H**F RADARS ARE A UNIQUE and powerful tool for measuring surface currents. They provide an unparalleled window into the spatial variations of near-surface currents. But oceanographers who are more accustomed to measuring currents with instruments that actually get wet may reasonably ask how accurate can such remote measurements be made? And while this is an easy and obvious question to ask, it is an interestingly difficult question to answer.

We have been studying the accuracy of the OSCAR HF radar system through analysis of data from the Office of Naval Research (ONR)-sponsored High-Resolution Remote-Sensing Experiment that was conducted off Cape Hatteras, North Carolina during the summer of 1993. This experiment provided a unique opportunity to examine the complex questions of HF radar accuracy. Along with several weeks of HF radar data, we had access to multiple *in situ* measurements of current from both moored and ship-based devices. In a series of analyses, we have attempted to validate the HF current measurements through comparison with the *in situ* data. The key has been to examine the temporal and spatial variations within these data in order to distinguish the sources of the underlying differences between the systems we compare.

## Comparisons with *In Situ* Instruments

When evaluating the accuracy of a new instrument, the typical procedure is to compare side-by-side measurements made with both the new instrument and an older instrument of known accuracy. It is important in such a comparison that the two instruments are measuring the same physical quantities, but this is a problem in evaluating the accuracy of an HF radar. The canonical HF radar measures near surface currents integrated over the upper 50 cm, averaged over a 1-km square and averaged over a 10-min period. Typical *in situ* current meters measure currents at fixed depths that are typically greater than the HF radar's effective depth, at essentially a single point in space and

offer fast response. The differences observed when these systems are compared are a result of differences in the measured quantity combined with the sampling techniques and inaccuracies of the instruments themselves. This makes it difficult to isolate the accuracy of the HF radar from other sources of observed difference.

The first pioneers in this field compared HF radar measurements with drifters (Stewart and Joy, 1974; Barrick *et al.*, 1977; Frisch and Weber, 1980). These comparisons were limited by the paucity of data and limits on the spatial and temporal coverage of the drifters, but they served to provide an upper bound on the errors of the HF system of 15–27 cm/s. Some later investigations compared the HF radar data with bottom-mounted Acoustic Doppler Current Profilers (ADCPs) or moored instruments (Holbrook and Frisch, 1981; Leise, 1984; Porter *et al.*, 1986; Matthews *et al.*, 1988; Shay *et al.*, 1995), finding differences ranging from 9 to 17 cm/s. Prandle (1991) performed a similar study but limited the comparisons to tidal and lower frequencies. The argument was made that these low temporal frequencies imply low spatial frequencies, making the *in situ* measurements made at a point more comparable to the area- and time-averaged HF radar measurements.

In our initial study (Chapman *et al.*, 1997) we compared *in situ* measurements from ship-mounted and towed ADCPs with HF radar measurements. We began by averaging the *in situ* data into 20-min samples, corresponding to the OSCAR sampling period. A pseudo time series was then constructed from the time series of OSCAR current maps, by tracking the movement of the ship through the OSCAR measurement domain. Thus we constructed a subset of the OSCAR data that was directly comparable with the *in situ* data set.

The direct comparisons of HF and *in situ* current measurements made in this way, an example of which is shown in Figure 1, indicate differences of 8–15 cm/s. But from this limited form of comparison, it is impossible to determine how these differences are apportioned between errors in the HF radar, errors in the *in situ* sensors, or differences in the measured quantities.

We have improved on these analyses by creating a model of the errors in the HF radar, and ex-

But oceanographers . . . may reasonably ask how accurate can such remote measurements be made?

Rick D. Chapman, Applied Physics Laboratory, Johns Hopkins University, Johns Hopkins Road, Laurel, MD 20723, USA. Hans C. Graber, Rosenstiel School of Marine and Atmospheric Science, University of Miami, Miami, FL 33149, USA.

amining how these errors differ from those of the *in situ* sensors. This simple model allows us to separate out the various sources of difference. We began by considering the geometric dependence of errors in the HF radar.

### Geometric Model of HF Radar Errors

As described elsewhere in this issue, the HF radar estimates vector currents by measuring the radial currents from two separate stations. These two radial estimates are then combined to form estimates of the vector current at each point in the measurement domain. It is reasonable to assume that each of the stations measures the radial velocity to the same levels of accuracy. We will further assume that, with proper installation of the HF radar systems (in particular the proper physical and electrical alignment of the phased array antennas), these radial velocity errors are relatively position independent, at least for those ranges where the signal-to-noise ratio is sufficiently high. It then turns out that combining these two radial velocity measurements into a vector current measurement imposes a position-dependent error on the vector components.

This is most easily seen by considering Figure 2, which indicates the station locations and coverage area of the OSCAR system for the High-Res experiment. Assume that each radial velocity measurement has an associated root-mean-square (rms) error of  $\sigma_r$ . Consider the errors in the North and East current components determined at a point at the far extreme of the map, due East of the stations. As the range increases, the East component of the velocity takes the form of the average of the two radial components, and thus the rms error in the east component approaches  $\sigma_r/\sqrt{2}$ . In contrast, the North component of the current is related to the difference of the radial components, a difference of large numbers, and so we would expect the errors to be significantly larger than  $\sigma_r$ .

We in fact have worked out a model for the positional dependency of the rms errors in the current components, the results of which are shown by the contours in Figure 2. We write that the errors in a current component are given by

$$\sigma_n = GDOP_n \cdot \sigma_r, \sigma_e = GDOP_e \cdot \sigma_r$$

where  $\sigma_n$  and  $\sigma_e$  are the rms errors in the north or east directions,  $\sigma_r$  is the radial velocity error from a single station, and  $GDOP_n$  and  $GDOP_e$  are the Geometric Dilution of Precisions, factors determined by our model. (The GDOP terminology was borrowed from the Global Positioning System (GPS) community, e.g., see Wells *et al.*, 1986).

The contours of constant GDOP in Figure 2 indicate that the errors in the north component of the HF radar current measurements will be larger than in the eastern component. Furthermore, the errors in the HF radar determination of the north component of the current vary sig-

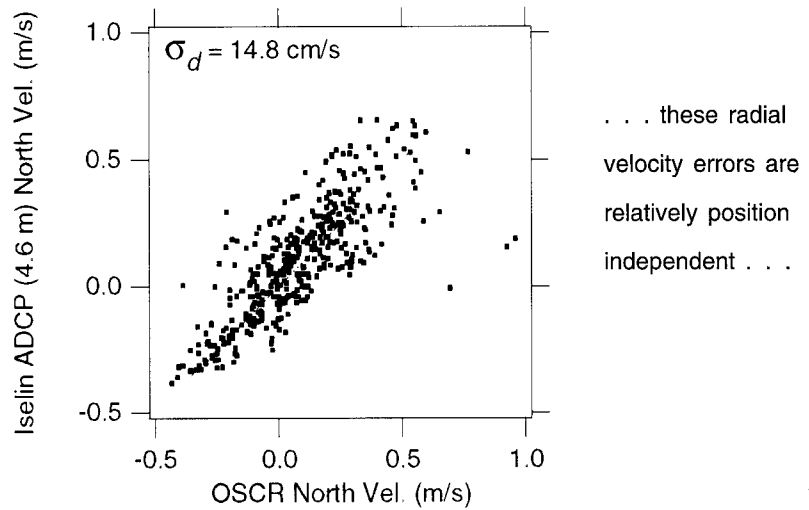


Fig. 1: Comparison of north component of near-surface current as determined by a ship-mounted ADCP at 4.6 m depth and OSCAR. The rms difference between the estimates is 14.8 cm/s. The dotted line is a line of equal velocity.

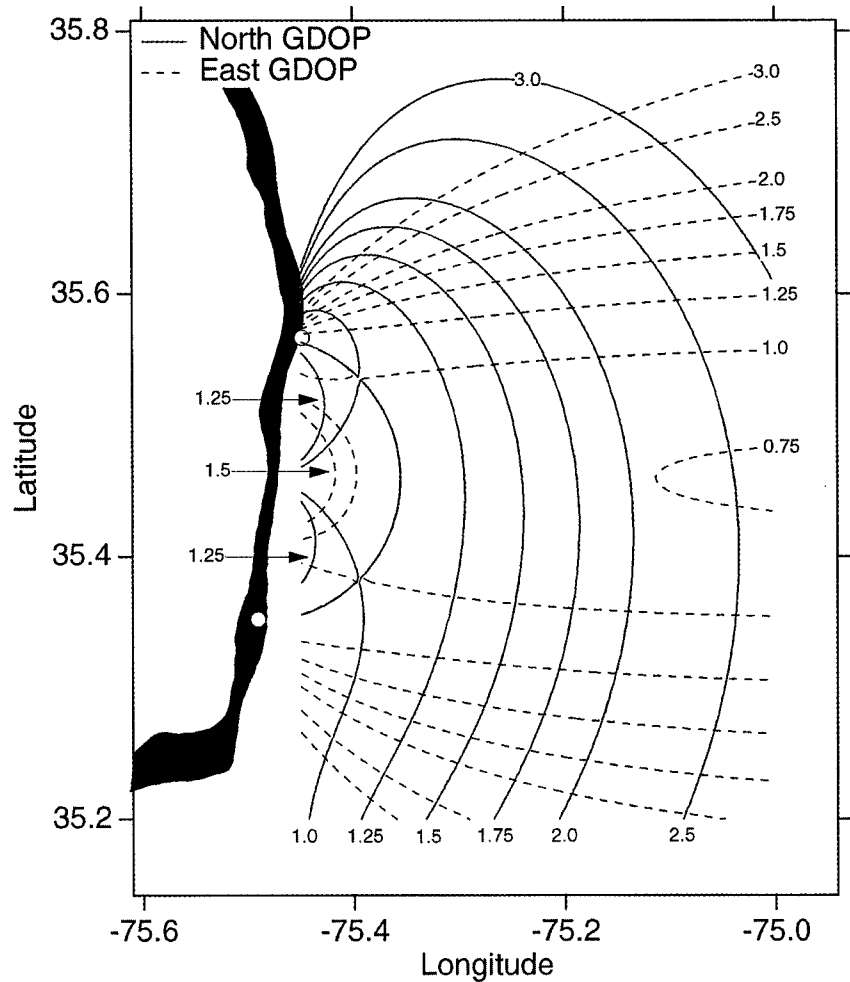


Fig. 2: Map of the North (solid red lines) and East (dashed blue lines) Geometric Dilution of Precision (GDOP) for the OSCAR measurement domain. The circles along the coast designate the OSCAR sites, and the gray dots indicate the OSCAR measurement locations.

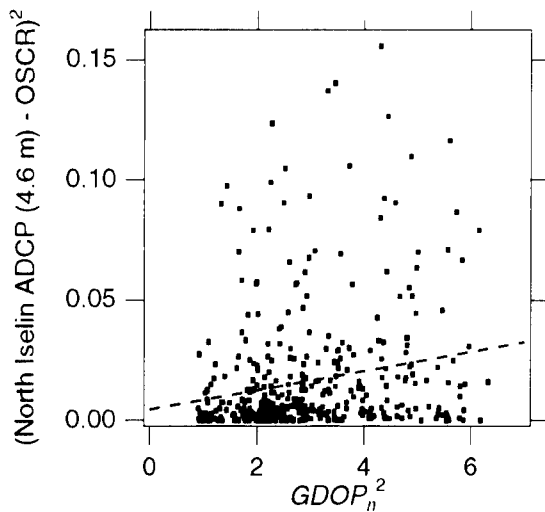


Fig. 3: Variations of the square of observed current component differences with  $GDOP_n^2$ . The dashed line represents a least-squares linear fit to these data, the slope of which indicates  $\sigma_r$ , the noise in the radial component of OSCR currents.

The alignment of the mean differences with the Gulf Stream is evident . . .

nificantly with location within the measurement footprint.

As mentioned above, the differences between the HF radar and *in situ* data can be attributed to three terms:

$$\sigma_{diff}^2 = \sigma_{HF}^2 + \sigma_{in\ situ}^2 + \sigma_{physics}^2$$

where  $\sigma_{diff}$  is the rms difference between the measurements,  $\sigma_{HF}$  is the rms error in the HF radar measurement,  $\sigma_{in\ situ}$  is the rms error in the *in situ* measurement, and  $\sigma_{physics}$  is the rms difference in the physical parameters measured by the HF radar and *in situ* instruments. We have assumed here that the errors in the *in situ* measurements and the rms differences in the physical parameters are uncorrelated with the rms errors in the HF radar measurements, an assumption that we have verified by statistical analysis of our data sets.

Our problem is thus reduced to finding  $\sigma_{HF}^2$  given the observed  $\sigma_{diff}^2$ . Our model suggests that the observed errors should be expressible as

$$\sigma_{diff}^2 = \sigma_r^2 \cdot GDOP^2 + \sigma_{other}^2$$

Figure 3 is a plot of the squares of the observed differences in the north current component versus the square of  $GDOP_n$  as determined by the model and the *in situ* measurement location. Although these data are obviously noisy, a least-squares linear fit does suggest that  $\sigma_r$  is of the order of 7–8 cm/s, a value comparable with the rms noise in the *in situ* sensors. Although all of this might seem a bit round about, we know of no other way of separating the accuracy of the HF radar from the other sources of differences.

### Error Budget

As a further check, the error budget above can be further expanded, with the individual terms  $\sigma_{physics}^2$  each accounted for separately. This can be done either from the data or from geophysical models.

The data-centric approach examines the structure functions of the current, or the expected rms value associated from currents measured at two different locations, depths or times, as a function of distance, depth, or lag. Figure 4 contains the spatial structure function of the expected differences as estimated from the OSCR data sets and several moored current meters.

While Figure 4 provides an estimate of the magnitude of the differences attributable to spatial inhomogeneities in the currents, these differences do in fact vary in a complex manner. This is shown in Figure 5, which plots contours of the rms differences (black), along with the magnitude of the complex correlation coefficient (red), for the OSCR currents referenced to a single OSCR cell near the middle of the measurement domain. The alignment of the mean differences with the Gulf Stream is evident, along with associated cross-stream decorrelation of the current fluctuations.

Alternatively, geophysical models can provide estimates of the expected differences, by modeling such physical processes as horizontal current variability, the Stokes drift, Ekman drift, and current-induced baroclinicity.

Graber *et al.* (1997) combined these approaches to examine how much of the total observed variance can be accounted for. They con-

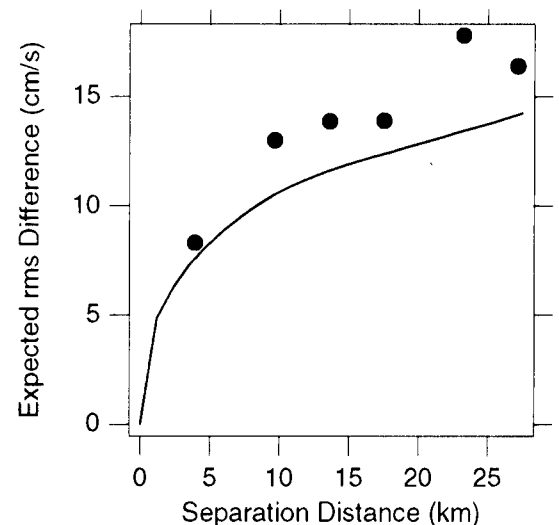


Fig. 4: Expected rms differences between near-surface observations as a function of cross-shelf separation. The solid line shows estimates of the rms differences for OSCR versus cross-shelf lag, and the solid dots show values for pairs of moored current meters.

cluded that 40–60% of the observed rms differences between the radar-derived surface current and the near-surface current measurements can be explained. Their study indicated that differences due to spatial separation and baroclinicity appear to be comparable with the errors in the radar measurements themselves. However, in strongly wind-forced ocean conditions, the Stokes and Ekman drift terms can easily dominate these differences.

### Conclusion

Direct comparisons of HF radars with *in situ* instruments place an upper bound on the accuracy of the radar-derived current measurements of 10–15 cm/s. These estimates can be improved by examining the spatial dependence of the variability of observed current differences. This procedure suggests that the radar-derived radial velocity errors are more likely on the order of 7–8 cm/s. Further analysis of the underlying causes of differences suggests that most of the differences can be accounted for in terms of surface current variability in space, depth, and time, as well as errors in the *in situ* and radar-derived currents. We conclude that when properly deployed, HF radars can accurately measure ocean surface currents, providing a unique tool for near-shore monitoring.

### Acknowledgments

The authors gratefully acknowledge the contributions of their other collaborators in this research: L.K. Shay, J.B. Edson, A. Karachintsev, C.L. Trump, D.B. Ross, and B.K. Haus. This research was supported, in part, by grants N00039-91-C-0001 (R.D. Chapman) and N00014-91-J-1775 (H.C. Graber) from the Office of Naval Research.

### References

- Barrick, D.E., M.W. Evans and B.L. Weber, 1977: Ocean surface currents mapped by radar. *Science*, 198, 138–144.
- Chapman, R.D., L.K. Shay, H.C. Graber, J.B. Edson, A. Karachintsev, C.L. Trump and D.B. Ross, 1997: On the accuracy of HF radar surface current measurements: intercomparisons with ship-based sensors. *J. Geophys. Res.*, 102, 18,737–18,748.
- Frisch, A.S. and B.L. Weber, 1980: A new technique for measuring tidal currents by using a two-site HF doppler radar system. *J. Geophys. Res.*, 85, 485–493.
- Graber, H.C., B.K. Haus, L.K. Shay and R.D. Chapman, 1997: HF radar comparisons with moored estimates of current speed and direction: expected differences and implications. *J. Geophys. Res.*, 102, 18,749–18,766.
- Holbrook, J.R. and A.S. Frisch, 1981: A comparison of near-surface CODAR and VACM measurements in the Strait of Juan De Fuca, August 1978. *J. Geophys. Res.*, 86, 10908–10912.

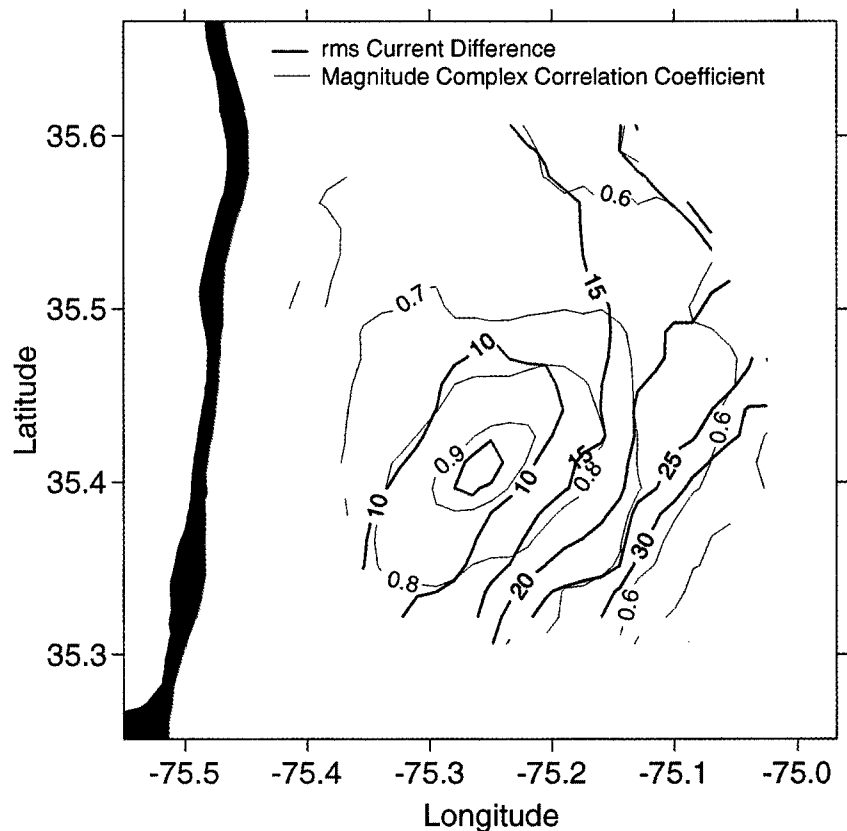


Fig. 5: Spatial variability of OSCAR surface currents calculated with respect to a single OSCAR cell. The black contours are the rms difference for speed, and the red contours are the magnitude of the complex correlation coefficient at zero temporal lag.

- Leise, J.A., 1984: The analysis and digital signal processing of NOAA's surface current mapping system. *IEEE J. Oceanic Eng.*, OE-9, 106–113.
- Matthews, J.P., J.H. Simpson and J. Brown, 1988: Remote sensing of shelf sea currents using a high-frequency ocean surface current radar system. *J. Geophys. Res.*, 93, 2303–2310.
- Porter, D.L., R.G. Williams and C.R. Swassing II, 1986: CODAR intercomparison: Delaware Bay 1984. *Proceedings of IEEE Third Working Conference on Current Measurement*, 36–44, Pergamon Press, UK.
- Prandle, D., 1991: A new view of near-shore dynamics based on observations from HF radar. *Prog. Oceanogr.*, 27, 403–438.
- Shay, L.K., H.C. Graber, D.B. Ross and R.D. Chapman, 1995: Mesoscale ocean surface current structure detected by HF radar. *J. Atmos. Ocean. Tech.*, 12, 881–900.
- Stewart, R.H. and J.W. Joy, 1974: HF radio measurements of surface currents. *Deep Sea Res.*, 21, 1039–1049.
- Wells, D.E., N. Beck, D. Delikaraoglou, A. Kleusberg, E.J. Krakiwsky, G. Lachapelle, R.B. Langley, M. Naki-boglu, K.P. Schwarz, J.M. Tranquilla and P. Vanicek, 1986: *Guide to GPS Positioning*. Canadian GPS Associates, Fredericton, N.B., Canada. □

Direct comparisons of HF radars with *in situ* instruments place an upper bound on the accuracy of the radar-derived current measurements . . .

# SHIPBOARD DEPLOYMENT OF A VHF OSCR SYSTEM FOR MEASURING OFFSHORE CURRENTS

By Richard A. Skop and Nicholas J. Peters

**I**N JULY 1994, an OSCR unit was deployed aboard the R/V *Columbus Iselin* to explore the feasibility of obtaining offshore, vector surface currents from a single platform. The concept is straightforward. With the vessel stationary at some location, the OSCR transmit-receive cycle is initiated, and the measured radial currents over the OSCR grid are recorded. The ship then transits to a new location, the transmit-receive cycle is reinitiated, and the measured radial currents are again recorded. With the existing OSCR system, the OSCR grid moves along with the ship. Hence, to construct vector surface currents from the measured radial currents at the two ship locations, pairs of cells within reasonable proximity to each other are identified (in our case, post-experiment), the average position of the pair is calculated, and both radial currents are assumed to have their origins at this average position.

In practice, a ship cannot remain stationary at a fixed location. To maintain the constant heading necessary for beamforming, the *Columbus Iselin* was operated at a forward speed of  $\sim 1 \text{ m s}^{-1}$  during the 5-min OSCR transmit-receive cycle. The forward speed was determined from two or three successive, 2-min interval, Global Positioning System (GPS) readings during the transmit-receive cycle. The forward speed biases a measured radial current by adding to it the component of the forward speed in the direction of the radial. To correct for this bias and obtain the radial current that would be measured from a stationary site, the appropriate component of the forward speed must be subtracted from the measured radial current (Peters and Skop, 1997).

Additionally, wave-induced, periodic ship motions can degrade the spectral returns to the point where the Bragg peaks cannot be identified, as dis-

cussed by Skop *et al.* (1994) and Peters and Skop (1997). The periodic motions were monitored continuously during a transmit-receive cycle using a six-channel accelerometer system (Skop *et al.*, 1994). The motions were found to be negligible, and the spectral returns were unaffected, because of the light seas encountered during the experiment.

Finally, the transmit antenna and the receive antenna elements must be mounted aboard the vessel in a manner that minimizes ship hull and superstructure interference with the transmitted and backscattered signals. The mounting arrangement for the July 1994 deployment was identical to one used in an earlier deployment where the *Columbus Iselin* was four-point anchored and shared an OSCR grid with a land-based unit. The analysis of the ship and shore-based spectra from this earlier deployment demonstrated that the mounting arrangement used successfully averted ship hull and superstructure interference (Skop *et al.*, 1994).

The July 1994 experiment was conducted with the ship-referenced OSCR grids overlapping in the high-speed, northerly flowing Florida Current. The vector surface currents extracted from the OSCR measurements agreed well with the expected values of the speed and direction of the Florida Current (Peters and Skop, 1997). These results establish the feasibility of measuring ocean surface

... the mounting arrangement used successfully averted ship hull and superstructure interference.

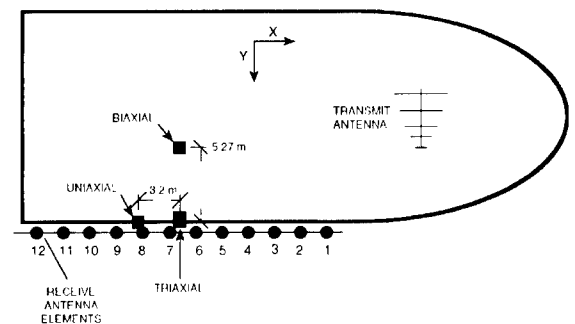


Fig. 1: The OSCR and accelerometer system arrangements aboard the *Columbus Iselin*. Not to scale.

Richard A. Skop, Rosenstiel School of Marine and Atmospheric Science, University of Miami, Miami, FL 33149, USA.  
Nicholas J. Peters, Prince William Sound Science Center, Cordova, AK 99574, USA.

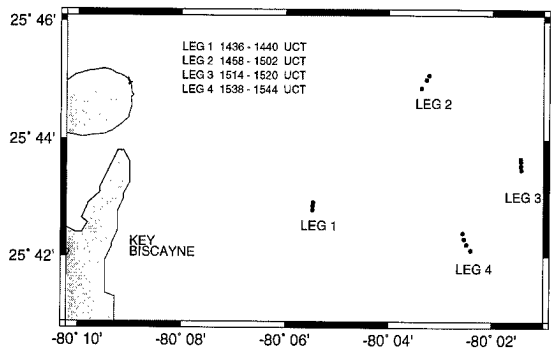


Fig. 2: Ship trajectories for the first diamond transect during the July 1994 offshore experiment.

currents from a single platform using an OSCRTYPE system.

### Conduct of the Experiment

The OSCRTYPE installation aboard the *Columbus Iselin* is depicted in Figure 1. The unit was used in its very high frequency (VHF; 50 MHz) mode. The Yagi transmit antenna was located as far toward the bow as possible and positioned so that its main lobe did not intersect the ship superstructure. The antenna was also raised on pylons to prevent any intersection between its main lobe and the bulwarks. The receive antenna elements were mounted, whip ends vertically upward, slightly

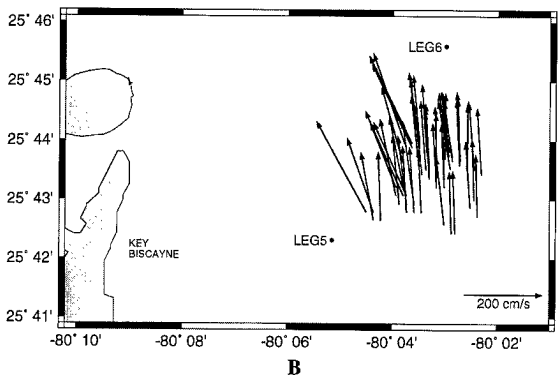
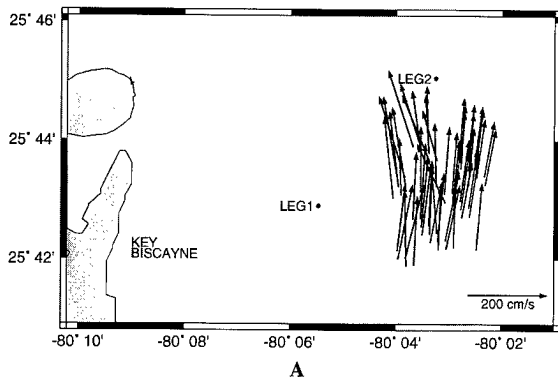


Fig. 3: Vector current maps of the Florida Current on July 22, 1994. (A) From legs 1 and 2 at 1500 UTC; (B) from the corresponding legs of the second offshore transect at 1700 UTC.

outboard of the hull and slightly above the bulwarks. Twelve receive antenna elements were used with a horizontal spacing of 3 m between elements. The transmit antenna and the receive elements were electrically insulated from direct contact with the ship and were commonly grounded to the ship electrical ground.

The ship made transects, twice, in a diamond pattern offshore of Key Biscayne and within the Florida Current. The transmit-receive cycles coincided with the ship at the corners of the diamond. The ship path and UTC times from immediately preceding to immediately following each data collection cycle are shown in Figure 2 for the first diamond transect. Each diamond transect was initiated with a south to north pass (leg 1), followed by a west to east pass (leg 2) and a north to south pass (leg 3), and concluded by an east to west pass (leg 4). The influence of the northerly flow of the Florida Current can be seen in Figure 2 through the northerly drift of the ship during the west to east and east to west passes.

### Vector Surface Currents

The vector surface current maps constructed from legs 1 and 2 of the first offshore transect and from the corresponding legs of the second offshore transect are shown, respectively, in Figure 3, A and B. A northerly surface current on the order of 170 cm/s was found from the data. For the vector current map constructed from legs 1 and 2 (Fig. 3A), the mean value of the current over the OSCRTYPE grid is 163 cm/s with a standard deviation of 20 cm s<sup>-1</sup>. The mean direction (bearing from north) of the flow is 1° with a standard deviation of 10°. For the vector current map constructed from the corresponding legs of the second offshore transect (Fig. 3B), the mean value of the current over the OSCRTYPE grid is 177 cm s<sup>-1</sup> with a standard deviation of 24 cm s<sup>-1</sup>. The mean direction of the flow is 352° with a standard deviation of 8°. The mean values of the current magnitude and direction are consistent with the values measured in the Florida Current by Leaman *et al.* (1987).

### Acknowledgments

This work was supported by the U.S. Naval Research Laboratory (SSC) and the U.S. Office of Naval Research under grant N00014-93-1-G900 and by the U.S. Naval Research Laboratory (SSC) under grant N00014-95-1-G905.

### References

- Leaman, K.D., R.L. Molinari and P.S. Vertes, 1987: Structure and variability of the Florida Current at 27°N: April 1982–July 1984. *J. Phys. Oceanogr.*, 17, 565–583.
- Peters, N.J. and R.A. Skop, 1997: Measurements of ocean surface currents from a moving ship using VHF radar. *J. Atmos. Oceanic Technol.*, 14(3), 676–694.
- Skop, R.A., D.B. Ross, N.J. Peters and L. Chamberlain, 1994: Measurements of coastal currents using a ship-based VHF radar system. *RSMAS Tech. Rep. 94-001*, Rosenstiel School of Marine and Atmospheric Science, University of Miami, 25 pp. □

The mean values of the current magnitude and direction are consistent with the values measured in the Florida Current . . .

# EXPERIENCE WITH SHIPBORNE MEASUREMENTS OF SURFACE CURRENT FIELDS BY HF RADAR

By Klaus-Werner Gurgel

There are several difficulties to be solved for successful measurements of surface current fields from a slowly sailing ship . . .

OCEANOGRAPHIC RESEARCH using HF radar techniques started in Germany in 1980 by adopting NOAA's CODAR (Coastal Ocean Dynamics Applications Radar), which has originally been introduced by Barrick *et al.* in 1977. In Germany, the CODAR has been modified and used during several experiments since 1981. From 1985 to 1992, the University of Hamburg CODAR has been extended for shipborne operation. The first experiment has been carried out on board the German icebreaker *Polarstern*, which most of the time has been sailing within the ice, far away from open water. The main result of this experiment was that the attenuation of ice-covered sea reduces the performance and working range extremely. Good measurements have only been possible with the ship sailing at the ice edge or in open water. However, this application did not need an icebreaker, so the following experiments have been carried out using the University of Hamburg *R/V Valdivia*.

The intention for operating the CODAR onboard a ship was to enable the measurement of surface current fields in front of the rough Norwegian coast, where the combination of a land-based and a shipborne CODAR has been used during the NORCSEX'88 experiment (Essen *et al.*, 1989), and on the open sea at the ice edge and at the Arctic Front. There are several difficulties to be solved for successful measurements of surface current fields from a slowly sailing ship, which will be discussed in the following sections. Finally, some results of a measurement campaign at the Arctic Front are shown. A more complete discussion of the shipborne CODAR can be found in Gurgel (1993) and Gurgel (1994).

## Difficulties in Operating a Shipborne HF Radar

During several experiments using three different ships, some main difficulties have been identified:

- to measure speed and direction of the ship and keep it as constant as possible;
- to compensate the influence of the ship on the antenna array; and
- to filter out the additional phase modulation of the sea echoes due to the pitch and roll motion of the ship.

The Global Positioning System (GPS) has been used for navigation. In near shore areas, other systems show acceptable accuracy and can also be used. The other difficulties are described in the following sections.

### *Antenna Arrangement to Minimize the Distortion of the Antenna Pattern*

The first problem when setting up a HF radar onboard a ship is to find an appropriate location for the antenna systems. In contrast to the land-based radar, there is a severe interaction between the ship's body and the receiving antenna array, which still must be usable to find the direction of the sea echoes. Similar to the land-based system, the receiving antenna is a four-element array of vertical polarized  $\lambda/4$  ground planes arranged in a square as described in Weber and Leise (1982). The arrangement of antennas finally selected can be seen in Figure 1.

The amplitude characteristics and phase differences of the four antennas are calibrated in the ship's environment before starting a measurement campaign. This is done by transmitting a constant signal from the coast and receiving it at the ship about 5 nautical miles away. To find the incident angle of a sea echo, a least-squares-fit of the measured phase differences to the calibration values is used.

Although the calibration values are used in finding the incident angle, in the presence of superposed gaussian noise on the sea echo's phase differences, a non-gaussian distribution of resolved incident angles can be observed. The average angle, therefore, can be distorted by an offset, which increases with growing noise due to pitch and roll motions or decreasing strength of the sea echoes.

Klaus-Werner Gurgel, Universität Hamburg, Institut für Meereskunde, Tropelwitzstrasse 7, D-22529 Hamburg, Germany. Email: gurgel@ifm.uni-hamburg.de

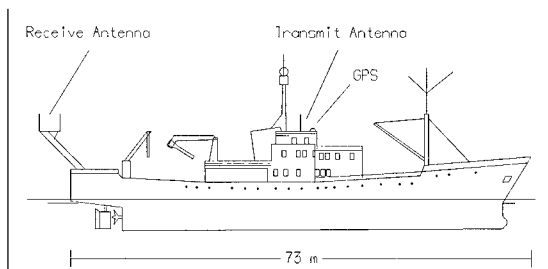


Fig. 1: The arrangement of antennas on R/V Valdivia.

### Ship's Pitch and Roll Movement

Another difficulty in analyzing the backscattered sea echoes is the ship's pitch and roll movement causing the sea echoes to be superposed by amplitude and phase modulation. Amplitude modulation is due to rotating the antenna out of the vertical polarization and changing the antenna's coupling to the sea surface; phase modulation is caused by changing the distance from the scattering area to the antenna. It turned out that phase modulation is the major effect.

A filter algorithm has been developed to separate this modulation from the sea echoes, which works well to  $-10$  dB modulation strength. A high roll frequency of the ship will be an advantage in this context. As the ship's movement is a function of the sea state and the sea state a function of wind speed,  $-10$  dB modulation strength will be exceeded at wind speeds above  $19 \text{ m s}^{-1}$  for R/V Valdivia.

### Hints on Operation of a HF Radar Onboard a Ship

- A big and heavy ship has the advantage of weak pitch and roll movements, reducing modulation effects.
- If only a smaller ship is available, it should roll at a frequency higher than  $0.12 \text{ Hz}$  to get the modulation products as far away from the sea echoes as possible.
- The ship should run at the lowest speed possible to sail a constant course. Because of errors in the direction finding algorithm for the sea echoes, the ship's speed may be compensated by a wrong value.
- The ship's speed must be  $< 3 \text{ kt}$  to resolve current velocities up to  $1 \text{ m s}^{-1}$ .
- Installing the receiving antenna low above the sea reduces phase modulation due to pitch and roll movements, but the distortion of the antenna pattern may increase because of a nearer distance to the ship's body.

### System Accuracy

If the above requirements are met, an accuracy of  $2\text{--}5 \text{ cm s}^{-1}$  for the radial component of the current velocity and an azimuthal resolution of  $3^\circ$  can be achieved. These values can be calculated from the statistics of the data. A practical working range

at a radar frequency of  $29.85 \text{ MHz}$  is  $45\text{--}50 \text{ km}$ , when integrating the sea echoes over an 18-min time interval. These characteristics are valid up to sea states at  $19 \text{ m s}^{-1}$  windspeed for R/V Valdivia and using GPS without Selective Availability (SA) activated for correction of the ship's speed. SA has been introduced to degrade the accuracy of GPS available to nonmilitary users.

### Surface Currents at the Arctic Front

The shipborne CODAR has been used during several cruises to the Arctic Front above Mohn's Ridge near Svalboard. The Arctic Front is originated by the West Svalboard Current carrying warm and salty North Atlantic water to the north and recirculation of cold and less salty Arctic water carried by the East Greenland Current to the south. Eddies at  $10\text{--}20 \text{ km}$  diameter and current speeds up to  $50 \text{ cm s}^{-1}$  can be observed.

### HF Radar Measurements

Because there was only one ship available during the campaign in August 1989, the ship had to be moved to different positions to obtain the measurements of radial components of the surface current field from different angles. Additionally, the GPS navigation had been available for some hours a day only, so scanning the complete area took one and a half day. Fortunately, SA had not been activated at that time, so GPS accuracy was sufficient without additional equipment.

Under these conditions, it must be assumed that the surface current field is stable over one and a half day. Because the windspeed kept changing during this time, the wind-driven part of the surface current was estimated to be

$$\vec{V}_0 = 0.018 \cdot \begin{vmatrix} \cos(-15^\circ) & -\sin(-15^\circ) \\ \sin(-15^\circ) & \cos(-15^\circ) \end{vmatrix} \cdot \vec{W}$$

and subtracted from each measurement of radial components before calculating the two-dimensional current field. The ratio  $|\vec{V}_0|/|\vec{W}| \approx 0.018$  and angle  $\approx 15^\circ$  have been published by Essen (1992). The result can be seen in Figure 2a.

### Current Field Calculated From CTD and XBT Data

Standard oceanographic equipment has been used on R/V Valdivia parallel to the HF radar, which includes a temperature/salinity sensor mounted at the ship,  $4 \text{ m}$  below the sea surface, CTD (Conductivity Temperature Depth) and XBT (eXpendable Bathy Thermograph) sondes.

To get a fast overview, the area has been scanned by the temperature/salinity sensor and XBTs. Only a few CTD measurements were taken at that time. After knowing the location of the Arctic Front from the temperature signal, the CTD measurements were intensified and the density field at the front has been measured.

A big and heavy ship has the advantage of weak pitch and roll movements . . .

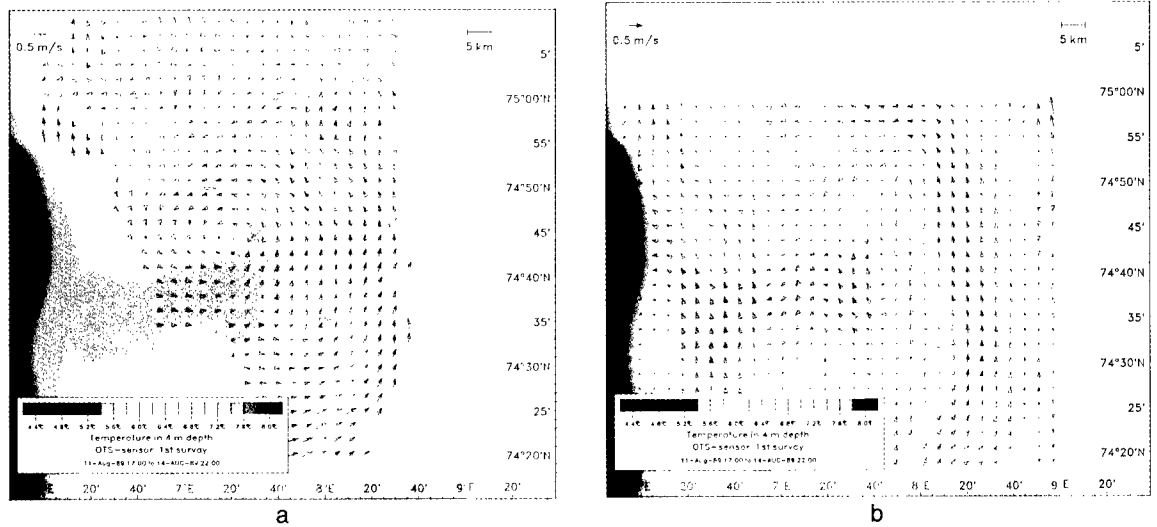


Fig. 2: (a) Surface current field calculated from 10 measurements of radial components taken by the shipborne HF radar at different positions and courses between 15 AUG 1989 17:08 UT and 17 AUG 1989 09:41 UT. The varying wind-driven part of the surface current has been removed. (b) Surface Current field calculated from the three-dimensional density field, derived from CTD and XBT measurements between 11 AUG 1989 17:00 UT and 14 AUG 1989 22:00 UT.

... good agreement with the geostrophical current field can be found within the calculated accuracy of the HF radar measurements.

Because the fast survey gives a more synoptic approach, which can better be compared with the HF radar measurements, a typical temperature-salinity correlation has been derived from all CTD data and was then used for the XBT data to add a typical salinity profile. By this way, all XBT and CTD measurements during the fast survey could be used to calculate geostrophical currents at the sea surface. The result can be seen in Figure 2b.

When subtracting the varying wind-driven part from the radial components of the current fields as measured by HF radar, a good agreement with the geostrophical current field can be found within the calculated accuracy of the HF radar measurements. The main current structure of the Arctic Front can be seen in both figures. Additionally, one has to keep in mind that there is a time lag of some days between the two current fields, that the density field has been modeled using a typical temperature-salinity correlation, and that none of the current fields shows a real synoptic approach.

### Conclusion

HF radars can successfully be operated on-board a ship as long as the weather conditions do not cause the ship to roll and pitch too heavily. *R/V Valdivia* can be used up to sea states generated by  $19 \text{ m s}^{-1}$  wind speed. To compensate the ship's movement during operation of the HF radar, GPS can be used, as long as SA can be removed from the satellite data, which can be done by *Differential GPS* or by using state-of-the-art receivers. Because one radar measures only the radial component of the surface current field, ei-

ther a second radar must be used, or, if the currents are stable over some hours, the ship can be moved to get measurements from different directions. Measured surface current fields at the Arctic Front have shown good agreement with conventional methods using CTD and XBT data.

### Acknowledgments

This work was supported by the German Research Foundation (DFG) in the Sonderforschungsbereich 318, Klimarelevante Prozesse im System Ozean-Atmosphäre-Kryosphäre. The author thanks the members of the German CODAR group, H.H. Essen, T. Schlick, F. Schirmer, and our technician M. Hamann for supporting the experiments; the scientific crew of *R/V Valdivia* for taking the CTD and XBT measurements; and the ship's crew for sailing the difficult CODAR courses.

### References

- Barrick, D.E., M.W. Evans and B.L. Weber, 1977: Ocean surface current mapped by radar. *Science*, 198, 138-144.
- Essen, H.H., K.W. Gurgel, F. Schirmer and T. Schlick, 1989: Surface currents during *NORCSEX '88*, as measured by a land- and a ship-based HF-radar. *Proc. IGARSS'89*, Vol. 2, 730-733.
- Gurgel, K.-W., 1993: Flächenhafte Messung der Oberflächenströmung vom fahrenden Schiff aus. Ph.D. thesis, Universität Hamburg.
- , 1994: Shipborne Measurement of Surface Current Fields by HF Radar. *L'onde Electrique*, 74, No. 5, 54-59.
- Weber, B.L. and J.A. Leise, 1982: A four-element direction finding antenna. *NOAA Tech. Memo., ERL WPL-99*, U.S. Dept. Commerce, NOAA/ERL, Boulder, CO. □

# THE OCEAN WAVE DIRECTIONAL SPECTRUM

By Lucy R. Wyatt

**T**HE DIRECTIONAL SPECTRUM  $S(k)$  [or  $S(f,\theta)$ ] measures the distribution of wave energy in wave number,  $k$ , (or frequency,  $f$ ) and direction. Different contributions to local wave energy, e.g., swell from distant storms and locally wind-generated waves, can be identified in a measurement of the directional spectrum (see Fig. 1). The direction of propagation of wave energy and the period ( $1/f$ ) of the most energetic waves are important for many practical applications, e.g., the design and operation of coastal and offshore structures and storm surge forecasts.

The use of HF radar to make measurements of the spectrum is based on equations developed by Barrick (1972a,b) that relate the power spectrum of the backscattered signal to the ocean wave spectrum through a nonlinear integral equation. The backscattered signal is dominated by Bragg scattering, i.e., the ocean waves responsible for the scatter have a wavelength of one-half the radio wavelength. The measurement of the directional spectrum is only possible because ocean waves are not simple sinusoidal forms satisfying the linear dispersion relationship. If they were linear there would be only the two first-order peaks in the backscattered power (Doppler) spectrum. The nonlinear properties of ocean waves give rise to waves with the correct wavelength for Bragg scatter but with different frequencies and hence different Doppler shifts. This is the second-order part of the spectrum described by Barrick's integral equation.

To make the measurement, the integral equation must be solved. This is not straightforward and a number of methods have been proposed (Lipa, 1978; Wyatt, 1990; Howell and Walsh, 1993; Hisaki, 1996). No method as yet has gained widespread acceptance and there are no operational HF radars making routine wave measurements. Here we concentrate on the Wyatt method and show some measurements from the Ocean Surface Current Radar (OSCR) HF radar system

that is marketed by Marconi Radar Co. as a surface current measurement radar and has a maximum range of ~20 km for wave measurement. The method has also been used with two different radar systems: Pisces, a system developed by Neptune Radar Ltd. from a University of Birmingham, U.K., prototype that has a maximum range of ~150 km for wave measurement (Wyatt, 1991), and WERA (Wellen RADar), a system under development at the Institut für Meereskunde, University of Hamburg, Germany, with a maximum range similar to OSCR.

## The Method

The concept of the method is simple. Significant waveheight and wind direction are estimated from the radar data using methods referred to elsewhere in this issue (Fernandez *et al.*, 1997; Graber and Heron, 1997; see also Wyatt 1988; Wyatt *et al.*, 1997). These are used to derive a model directional spectrum using both the waveheight to determine a Pierson-Moskowitz wave number spectrum and also the wind direction in a directional distribution. This model spectrum is fed into the integral equation that is integrated directly to determine the corresponding Doppler spectrum. Differences between this Doppler spectrum and the measured spectrum are used to modify the directional spectrum at each wave number (within a limited range) and direction. This process is repeated until the differences become sufficiently small. The way in which the modification is carried out is the key to the success of the method. The details are too complicated to be included here, but it is important to realize that although the method starts with a simple directional spectrum with a single wind-wave mode, the solution (when the procedure has converged) can be very different; for example, it has no problem detecting the presence of swell propagating in a very different direction.

The method does not provide a measurement of the directional spectrum at all wave frequencies. High-frequency waves are not adjusted in the procedure and retain the memory of the initializing spectrum. The cutoff, at OSCR frequencies, is

**T**he measurement of the directional spectrum is only possible because ocean waves are not simple sinusoidal forms . . .

Lucy R. Wyatt, Sheffield Centre for Earth Observation Science School of Mathematics and Statistics (AM), University of Sheffield, Hounsfield Road, Sheffield S3 7RH, UK.

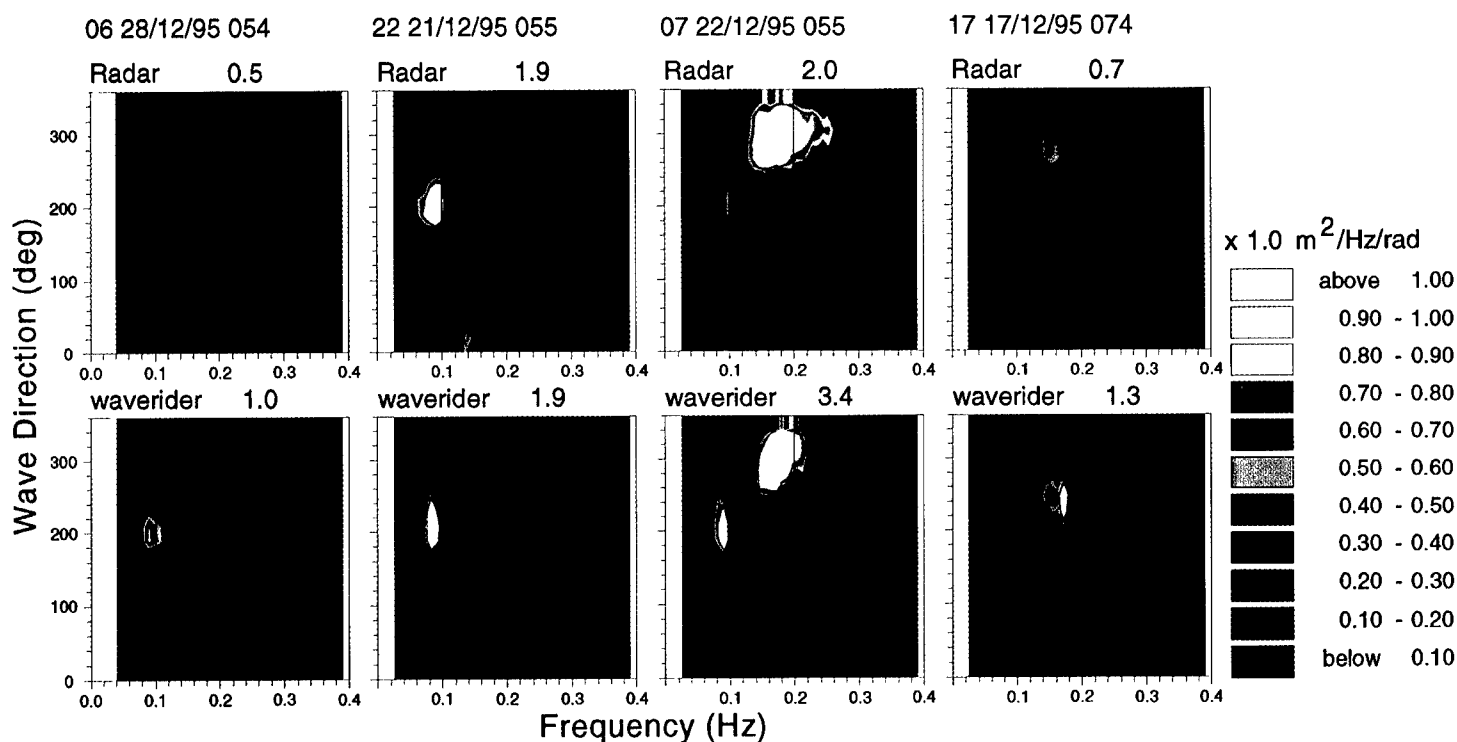


Fig. 1: Directional spectra measured by the radar (top row) and estimated from the directional waverider measurement (bottom row) with frequency in Hz on the horizontal axis and direction toward which the waves are propagating on the vertical. Four different types of wavefield are shown: (left) swell-dominated sea with a peak frequency of 0.09 Hz; (mid-left) swell (0.09 Hz) with some wind sea with a peak frequency  $\sim 0.18$  Hz; (mid-right) wind-sea (0.16 Hz) with some swell (0.09 Hz); (right) wind-sea peaking at 0.14 Hz. The hour and date of each measurement is shown together with the cell location of the radar measurement (all close to the wavebuoy site). The number above each plot is the peak in the directional spectrum for that plot. Arrow heads, short wave direction. The color coding is indicated on the right: dark blue,  $< 0.1$ ; yellow,  $> 1.0$ .

One advantage of this method is that wave components in the spectrum that are similar in frequency but different in direction emerge naturally during the inversion.

$\sim 0.38$  Hz, the exact value depending on the look directions of the two radars at the measurement point. The Lipa, Howell, and Walsh methods have similar limitations, the exact cutoff in each case depends on the model assumed for high frequencies and on the range of Doppler frequencies included in their analyses. Hisaki's method is a non-linear optimization method and in principle extends the range of frequencies, although the method has not been exhaustively verified. For most applications it is the longer, lower-frequency, energy-containing waves that are of interest. Wind speeds would have to be very low or fetch very short for the peak in the spectrum to be at frequencies close to the cutoff.

An important difference between the Wyatt method and those of Lipa, Howell and Walsh, and Hisaki is the form of the solution. In the other three methods the directional spectrum is discretized in scalar wave number or frequency and is expressed as a truncated Fourier series in direction, which allows the problem to be expressed as a matrix equation for the Fourier coefficients. The Fourier coefficients used are the same five used in the analysis of directional wavebuoys; methods employed in the interpretation of buoy data can be applied directly. One limitation is difficulty in identifying wave

components in the spectrum that are similar in frequency but different in direction. This, of course, applies both to the wavebuoy and the radar analysis. In the Wyatt method the directional spectrum is discretized in vector wave number and the solution is determined at each discrete vector wave number. One advantage of this method is that wave components in the spectrum that are similar in frequency but different in direction emerge naturally during the inversion (Wyatt and Holden, 1994). Validating the detailed structure in the radar-measured spectrum is not straightforward because wavebuoys only measure limited detail. One approach is to partition the wave spectra into swell and wind-wave modes and compare integrated parameters for these. Such an approach is under development (Isaac and Wyatt, 1997).

### Holderness Measurements

The data set used here to demonstrate the success of the method was collected using the OSCAR HF radar during a deployment on the U.K. coast at Holderness. Directional waveriders were deployed at two offshore locations about midway between the radar sites, one in  $\sim 10$  and the other in  $\sim 20$  m water depth. Depth contours are roughly parallel to the coast deepening to 10 m  $\sim 1$  km offshore. The

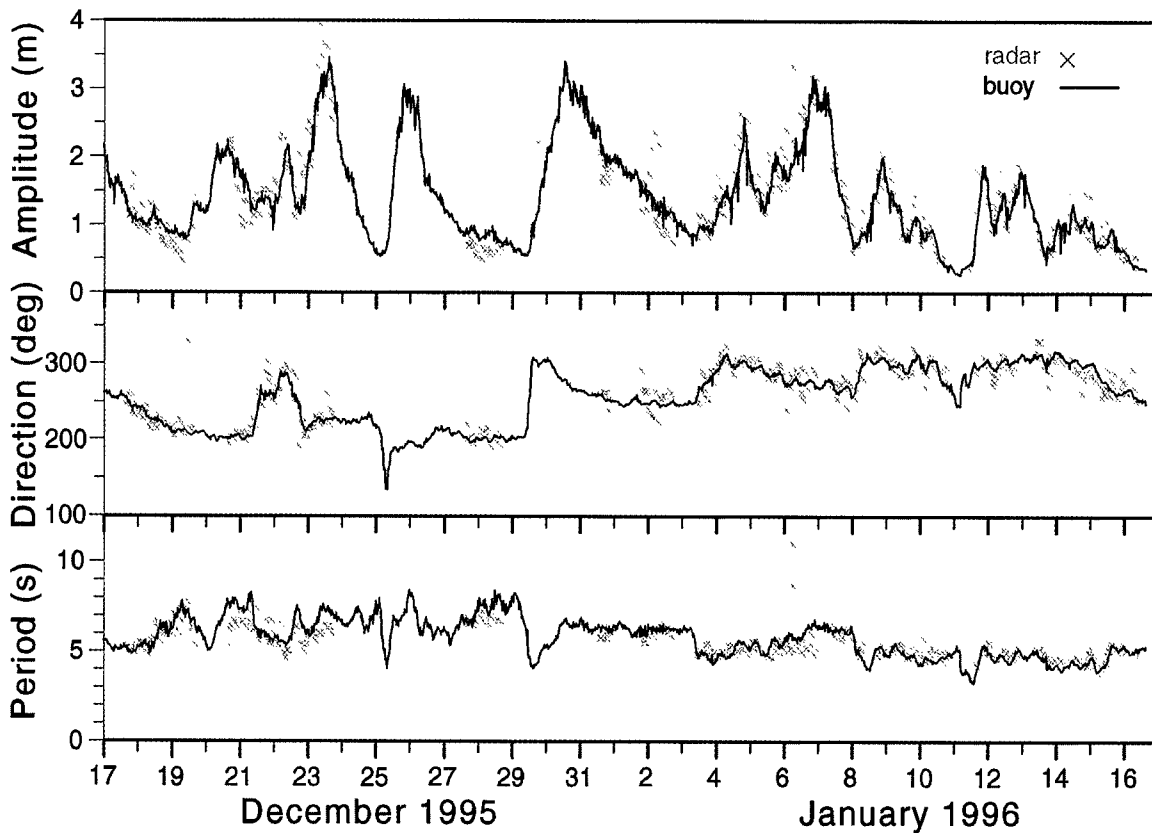


Fig. 2: Time series of amplitude (significant waveheight), mean direction, and mean period obtained from the directional spectra measured by the radar (x) and from the directional parameters measured by the waverider (—) in both cases integrated over the frequency band of 0.05–0.4 Hz.

OSCR system used was provided by Wimpey Environmental (now GEOS Ltd.). Data were collected over a period of 1 mo from 17 December 1995 to 16 January 1996 with short breaks over the Christmas-New Year period (the data requirements for wave measurement require an operator to be on site). The radar measurement period included two high sea-state events, high for this region at least, with significant waveheights reaching >3 m at the buoy positions (Fig. 1). Surprisingly for this region, there were very few examples of fetch-limited development. Figure 2 shows time series comparisons of significant waveheight, mean direction, and mean period obtained from the directional spectrum measured by the radar and a co-located wavebuoy; very good agreement can be seen. Similar comparisons can be made for these parameters measured over limited frequency bands; for example, waves with frequencies <0.1 Hz, which, during this experiment at least, are swell waves. Again good agreement is found. Quantitative measures of the accuracy of a range of parameters describing the directional spectrum are being determined.

One big advantage HF radar has over conventional wave measurement systems is the ability to monitor wave development in space as well as over time. This advantage is demonstrated very clearly with data collected on 21 December 1995

in the early afternoon, a relatively calm period with high pressure over eastern Europe, low pressure over Scandinavia and to the west of the British Isles, driving a weak south-easterly wind

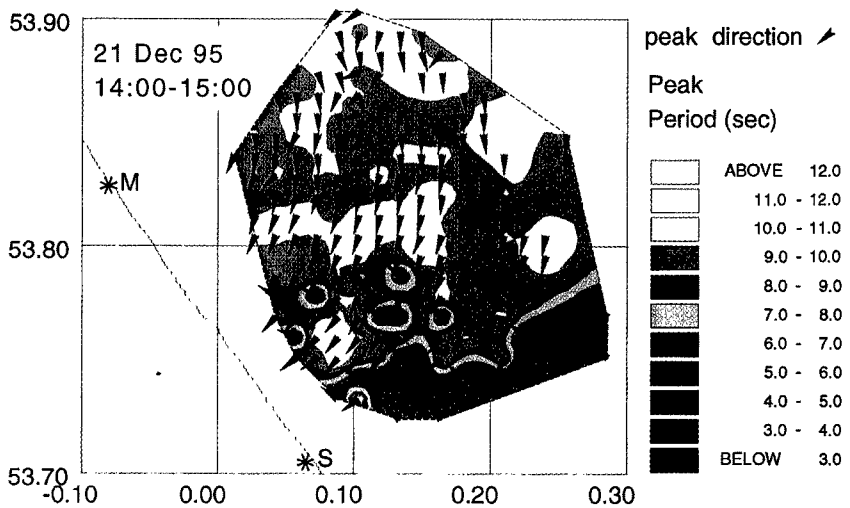


Fig. 3: The Holderness coastline is shown to the south-west of the map with the two radar sites indicated as M and S. Directions shown with arrowheads are those toward which the peak of the radar measured spectrum is propagating. The period of the peak is color coded as shown. This figure shows swell dominating over most of the region propagating from the north and refracting toward the coast. To the south, south-easterly wind waves dominate.

One big advantage HF radar has . . . is the ability to monitor wave development in space as well as over time.

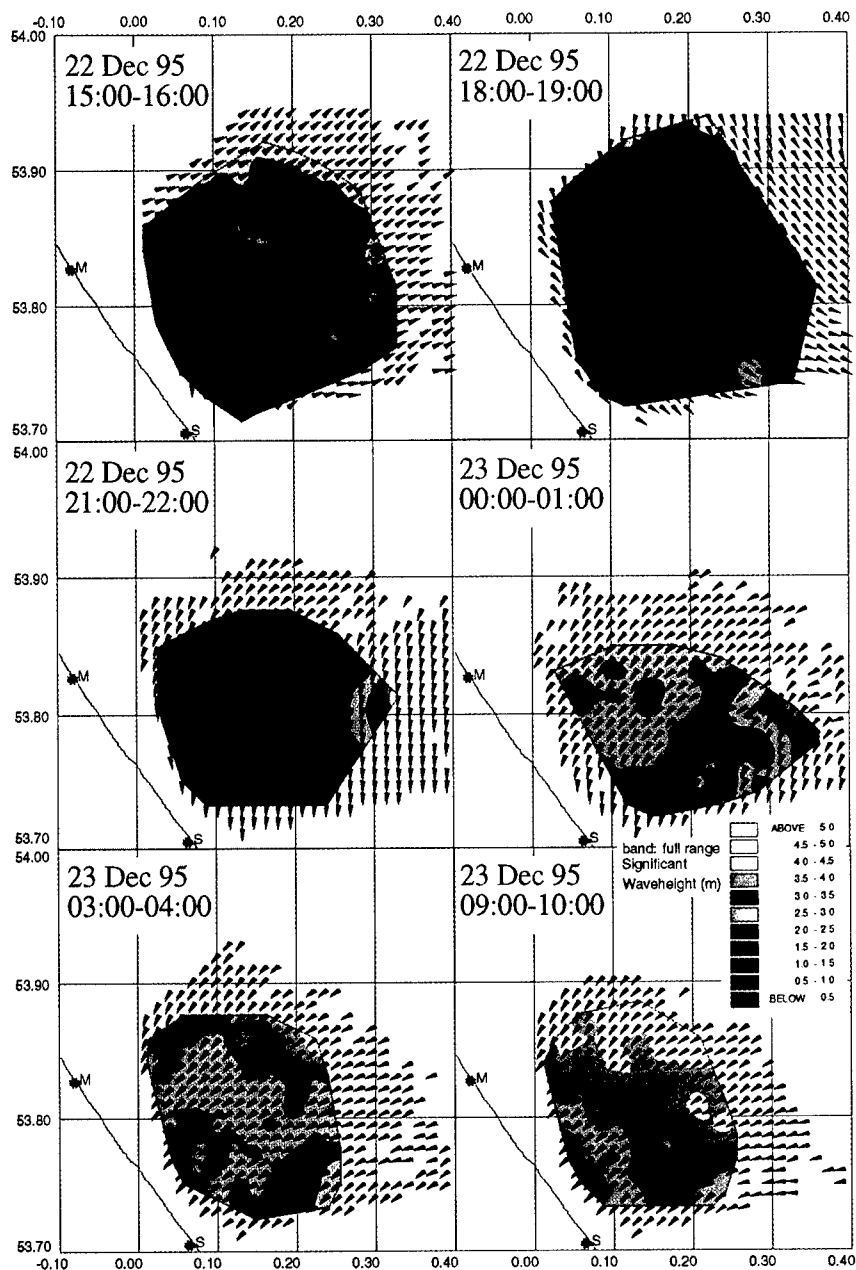


Fig. 4: Short-wave (wind) directions are shown with arrowheads. Significant waveheight is color-coded as shown and varies from <1.0 m near to the shore on 22 December 1995 at 1500 to >5 m offshore at 0900 on 23 December 1995. The figure shows changes because of the passage of a low-pressure system through the region.

The data presented here have demonstrated that OSCAR can measure the ocean wave directional spectrum.

over the region. Fronts were building up in the west to come through the region over the next 24 h, but in the meantime the synoptic pattern suggested that the wave field would be dominated by swell propagating southward down the North Sea. This pattern is exactly the same as seen over most of the radar coverage region. Figure 3 shows the direction of the peak of the spectrum superimposed on the contoured peak period. Of interest is the spatial variation in these parameters. Swell, with a period of ~10 s (yellow shades), can be seen propagating from the north and being refracted toward the coast as bottom depth de-

creases. Swell energy is dissipated (not shown here), probably by bottom friction or by wave-current interaction. Tidal current speeds were large at the time of the measurement ( $\geq 0.5$  m/s), and although uniform in direction themselves (in roughly a southward direction), the direction relative to the swell varies as the swell is refracted by the bottom topography. Wave breaking is unlikely to be a problem at these amplitudes in these depths. As a result of the dissipation of swell energy, the spectral maximum in the south of the region shifts to the wind-wave field with a peak period of  $\leq 5$  s (blue shades on the figure). Comparisons of amplitude, direction, and spread as functions of frequency measured by the radar and wave buoy confirm the swell and wind-sea directions and also show good agreement in relative amplitudes at the buoy location.

A second example showing both temporal and spatial variability is presented in Figure 4 and shows significant waveheight determined from the directional spectra and short-wave directions (Wyatt *et al.*, 1997) at each measurement position. Short-wave directions can be made over a wider area because they use only the first order part of the Doppler spectrum. The figure shows the response of the wave field to a passing low-pressure system. Waveheights are initially low in response to offshore winds but increase after the low has passed through, leaving a strong north-easterly wind pattern and hence longer fetch.

### Concluding Remarks

The data presented here have demonstrated that OSCAR can measure the ocean wave directional spectrum. These OSCAR measurements are much better than those previously published (Wyatt and Ledgard, 1996) because this Holderness deployment configuration was optimized for wave measurement. Good agreement with wave buoy parameters was shown and the comparison is now the subject of rigorous evaluation to provide quantitative measures of parameter accuracy. Oceanographic consistency of the data over the region of the measurements is also being demonstrated.

There remain some problems that need to be overcome before OSCAR can become an operational tool for wave monitoring. Some of these are purely technical; for example, the use of modern computer systems and, in particular, reliable and high-capacity data storage devices would significantly increase the temporal coverage because there would no longer be an onsite operator requirement. Others require further research, some of which is currently underway at Sheffield. One of the problems we have identified is a reduction in data availability during periods of varying surface current. This is because the first order peaks move about in frequency during the measurement period (responding to different current components) and prevent a clear distinction between first

and second order in the power spectrum. At present OSCR data from three separate surface current measurement periods (10 min in every 20) are averaged before extracting wave information (a statistical requirement). Any current variability on time scales of <1 h causes a problem. This could be overcome by longer coherent data collections, thus obtaining sufficient averaging for wave measurement from a shorter time period, but at the expense of reduced surface current sampling. Other approaches to this problem are under development. Another important problem, identified many years ago by Lipa and Barrick (1986), is a possible upper waveheight limit beyond which the theory used in the inversion no longer applies. So far we have seen no evidence of the particular problem they describe, although there are certainly differences between the second-order theory and the radar measurements in higher sea-states that may be affecting the accuracy of our measurements (Wyatt, 1995). Measurements are required in sea-states higher than are seen in the Holderness region to investigate these issues further. Recent measurements with the WERA system off the north Netherlands' coast at Petten during a very stormy period in November 1996 may provide some answers.

#### Acknowledgments

The observations off Holderness described here were funded in part by the Ministry of Agriculture Fisheries and Food (U.K.) under its Flood Protection Commission with NERC's Proudman Oceanographic Laboratory. The data were collected and analyzed by Louise Ledgard. The Natural Environment Research Council also supported these observations through its Land Ocean Interaction Studies project. Other support has come from the EC MAST SCAWVEX project (MAS2CT940103) and EPSRC (grants GR/J07341, GR/J50934).

#### References

- Barrick, D.E., 1972a: First-order theory and analysis of MF/HF/VHF scatter from the sea. *IEEE Trans. Antennas Propag.*, AP-20, 2-10.
- , 1972b: Remote sensing of sea state by radar. In: *Remote Sensing of the Troposphere*. V.E. Derr, ed. NOAA/Environmental Research Laboratories, Boulder, CO, 12.1-12.6.
- Fernandez, D.M., H.C. Graber, J.D. Paduan and D.E. Barrick, 1997: Mapping wind direction with HF radar. *Oceanography*, 10, 93-95.
- Graber, H.C. and M.L. Heron, 1997: Waveheight measurements from HF radar. *Oceanography*, 10, 90-92.
- Hisaki, Y., 1996: Nonlinear inversion of the integral equation to estimate ocean wave spectra from HF radar. *Radio Sci.*, 31, 25-39.
- Howell, R. and J. Walsh, 1993: Measurement of ocean wave spectra using narrow beam HF radar. *IEEE J. Ocean. Eng.*, 18, 296-305.
- Isaac, F.E. and L.R. Wyatt, 1997: Segmentation of HF radar measured directional wave spectra using the Voronoi Diagram. *J. Atmos. Ocean. Tech.*, 14, 950-959.
- Lipa, B.J., 1978: Inversion of second-order radar echoes from the sea. *J. Geophys. Res.*, 83, 959-962.
- and D.E. Barrick, 1986: Extraction of sea state from HF radar sea echo: mathematical theory and modelling. *Radio Sci.*, 21, 81-100.
- Wyatt, L.R., 1988: Significant waveheight measurement with HF radar. *Int. J. Remote Sens.*, 9, 1087-1095.
- , 1990: A relaxation method for integral inversion applied to HF radar measurement of the ocean wave directional spectrum. *Int. J. Remote Sens.*, 11, 1481-1494.
- , 1991: HF radar measurements of the ocean wave directional spectrum. *IEEE J. Ocean. Eng.*, 16, 163-169.
- , 1995: High order nonlinearities in HF radar backscatter from the ocean surface. In: *IEE Proceedings on Radar, Sonar and Navigation*, 142, IEE, London, 293-300.
- and G.J. Holden, 1994: HF radar measurement of multi-modal directional wave spectra. *Global Atmos. Ocean Sys.*, 2, 265-290.
- and L.J. Ledgard, 1996: OSCR wave measurement—some preliminary results. *IEEE J. Ocean. Eng.*, 21, 64-76.
- , L.J. Ledgard and C.W. Anderson, 1997: Maximum likelihood estimation of the directional distribution of 0.53 Hz ocean waves. *J. Atmos. Ocean. Tech.*, 14, 591-603. □

# WAVE HEIGHT MEASUREMENTS FROM HF RADAR

By Hans C. Graber and Malcolm L. Heron

Remote sensing offers the only opportunity to obtain high-resolution spatial information about the shoaling wave field.

NEARSHORE AND INNER SHELF dynamics are forced principally by radiation stress gradients induced by shoaling and breaking waves. Waves in shallow water refract due to varying bottom topography. Thus the wave climate can vary significantly alongshore. Remote sensing offers the only opportunity to obtain high-resolution spatial information about the shoaling wave field.

The concept of using high-frequency (HF) radio pulses to probe the ocean surface to deduce near-surface currents has received considerable attention in coastal oceanographic experiments. HF radar systems have been extensively used to measure or predict a range of oceanic processes from tidal currents (e.g., Prandle, 1991; Shay *et al.*, 1995) to wind-induced surface flows (Ng, 1993). More recently, several studies (e.g., Heron *et al.*, 1985; Wyatt, 1988) have focused on extracting additional information about the ocean surface from the Doppler spectrum measured by HF radar. Of particular interest is the height of ocean waves that plays a crucial role in engineering projects, ship navigation and design, and vessel traffic control in harbors as well as shoreline protection, beach erosion, and mitigation of oil spills and ocean pollution.

## Sea Echo Spectrum

The sea echo spectrum measured by HF radars includes the effects of the full ocean wave spectrum. Barrick (1977a,b) has shown that the radar backscatter spectrum is nonlinearly related to the ocean wave spectrum. Extraction of the directional wave spectrum is possible with inverse techniques (e.g., see Wyatt, 1997, this issue). However, these methods are often computationally intensive. An alternative approach is to estimate the wave height from the first-order and second-order radar echoes by using characteristic properties of the spectrum. The square-root of the integral over the directional wave spectrum is di-

rectly related to the rms wave height and is an important parameter used in many studies involving wave dynamics. Barrick (1977b) suggested a simple, yet accurate, method to obtain the rms wave height,  $H_{rms}$ , from the total power in the first-order peak,  $P_1$  and the total power in the second-order weighted spectrum,  $P_2$ . Specifically, this relationship can be expressed,

$$H_{rms} = \left[ \frac{\lambda}{\sqrt{2\pi}} \frac{\int_{-\infty}^{\infty} \sigma_2(f) W^{-1}(f/f_b) df}{\int_{-\infty}^{\infty} \sigma_1(f) df} \right]^{1/2} \quad (1)$$

where  $f_b$  is the Bragg frequency,  $\lambda$  is the radar wavelength,  $W(f/f_b)$  is a weighting function, and  $\sigma_1$ ,  $\sigma_2$  are the first-order and second-order radar cross-sections.

Figure 1 shows a typical Doppler spectrum from ocean surface current radar (OSCR) obtained in DUCK94. On the plot are also indicated the limits of the first-order and inner and outer second-order Doppler regions.

S.F. Heron and M.L. Heron (unpublished data) evaluated several algorithms (e.g., Barrick, 1977; Maresca and Georges, 1980; Heron *et al.*, 1985) based on this simple power law relationship with OSCR data obtained from the DUCK94 experiment. They found that the half-power law,  $H_{rms} = \alpha \lambda R^{1/2}$ , derived from Equation (1) is robust for rms wave heights as low as 20 cm. Here  $\alpha = \frac{1}{3}$  is an empirical constant, and  $R$  is a weighted ratio of the integrals in Equation (1).

## DUCK94 Data

Heron (1996) has examined in detail the application of these three different power law relations for estimating wave heights with HF radar backscatter data acquired during DUCK94. He found that a modified version of Barrick's (1977b) algorithm (Eq. 1) provided the most accurate wave height estimates with a rms error of only 14 cm for wave heights ranging from 50 cm to 4 m. The modified Barrick algorithm was applied to the entire DUCK94 data set that included significant wave

Hans C. Graber, Rosenstiel School of Marine and Atmospheric Science, University of Miami, Miami, FL 33149, USA. Malcolm L. Heron, School of Computer Science, Mathematics and Physics, James Cook University, Townsville, Queensland, 4811, Australia.

heights,  $H_{1/3} = 4 H_{rms}$ , in excess of 6 m during a Nor'easter. Figure 2 shows a comparison of the significant wave height observed by a 3-m National Data Buoy Center (NDBC) discus buoy with those estimated from HF radar. The wave buoy was located ~25 km offshore from the U.S. Army Corps of Engineers Field Research Facility at Duck, North Carolina in 30-m water depth. The agreement is remarkable especially during the growth and decay stages of several frontal passages and the midmonth extra-tropical storm system.

There are several times when the radar overshoots the buoy observations, especially during the storm peak. Some of this discrepancy is caused by broader signal return because of enhanced wave breaking. Interference and poor signal-to-noise ratio are also possible causes for the overestimation. Nevertheless, a statistical analysis with two other wave-measuring systems in the nearshore regime off Duck, North Carolina revealed a small overall positive bias of only 7 cm (i.e., radar wave heights are greater than the buoy measurements) and a rms error not exceeding 38 cm for a range of significant wave heights from 0.5 to 6 m.

Figure 3 shows a sequence of four hourly averaged wave height maps derived from three 20-min OSCR Doppler spectra centered at 12:00, 15:00, 18:00, and 21:00 UT on 15 October 1994 during the peak of the Nor'easter. The maps delineate the spatial evolution of the storm-generated waves as they approach the shore. As the storm strengthened (12:00 and 15:00 UT) the wave heights appear to be uniform in the alongshore direction. Whereas, at the peak of the storm (18:00 and 21:00 UT), the influence of the bottom through shoaling and depth refraction is quite apparent displaying spatially variable wave heights over the inner shelf (water depth  $\leq 25$  m).

### Conclusions

Many advantages of HF radar wave observations exist over standard methods. In particular, the ability to sample a wide region in near real time substantially enhances many marine-related operations including search and rescue mission, oil spill clean up, and dredging operations. While inverse techniques (see Wyatt, 1997, this issue) provide more detail information about the directional distribution of ocean waves, the technique described here emphasizes efficiency and robustness. The need for sea state information around harbors and offshore facilities is crucial for safe and economical operations. In particular, harbor entrances and river mouths can pose treacherous conditions for small craft and medium size vessels when opposing currents (e.g., tides and river flow) interact with ocean waves (wave-current interaction). Furthermore, radar observations can also be made in adverse weather conditions, and the calculation of wave heights is independent of materials in the water. Consequently, such a technique could be used in re-

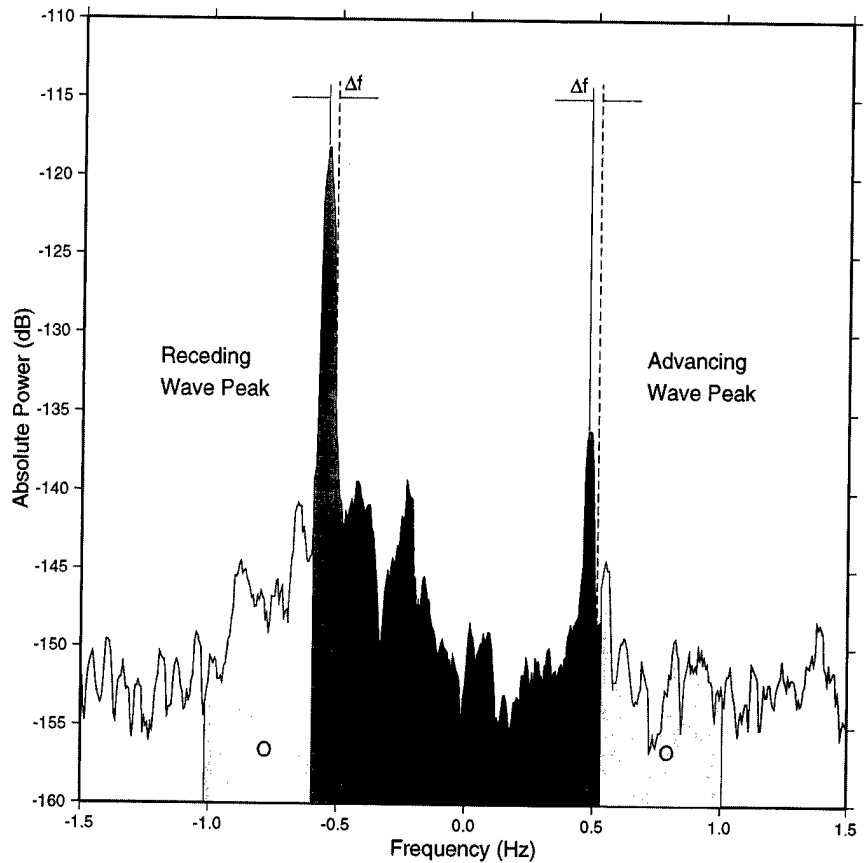


Fig. 1: A typical sea echo spectrum for 25.4 MHz obtained by OSCR during the DUCK94 experiment off the North Carolina coast in October 1994. The shaded regions indicate the first-order (F), inner (I), and outer (O) second-order spectral bands.

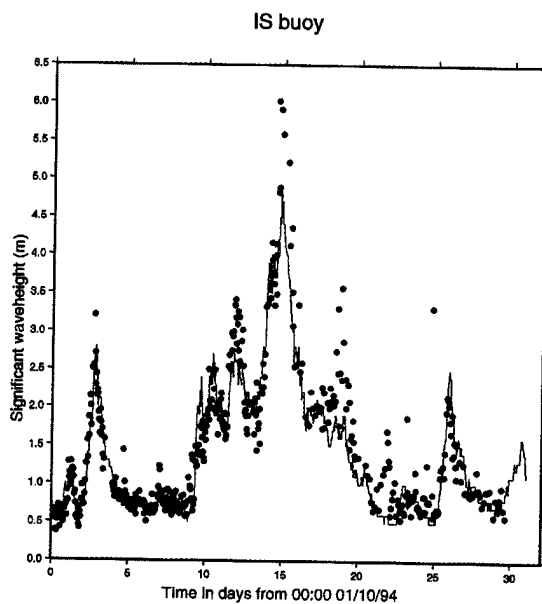


Fig. 2: Comparison of measured wave heights from the inner shelf wave buoy (solid line) with estimates from the OSCR system (red dots) for October 1994. Each dot represents a 10-min average value.

... radar observations can also be made in adverse weather conditions, and the calculation of wave heights is independent of materials in the water.

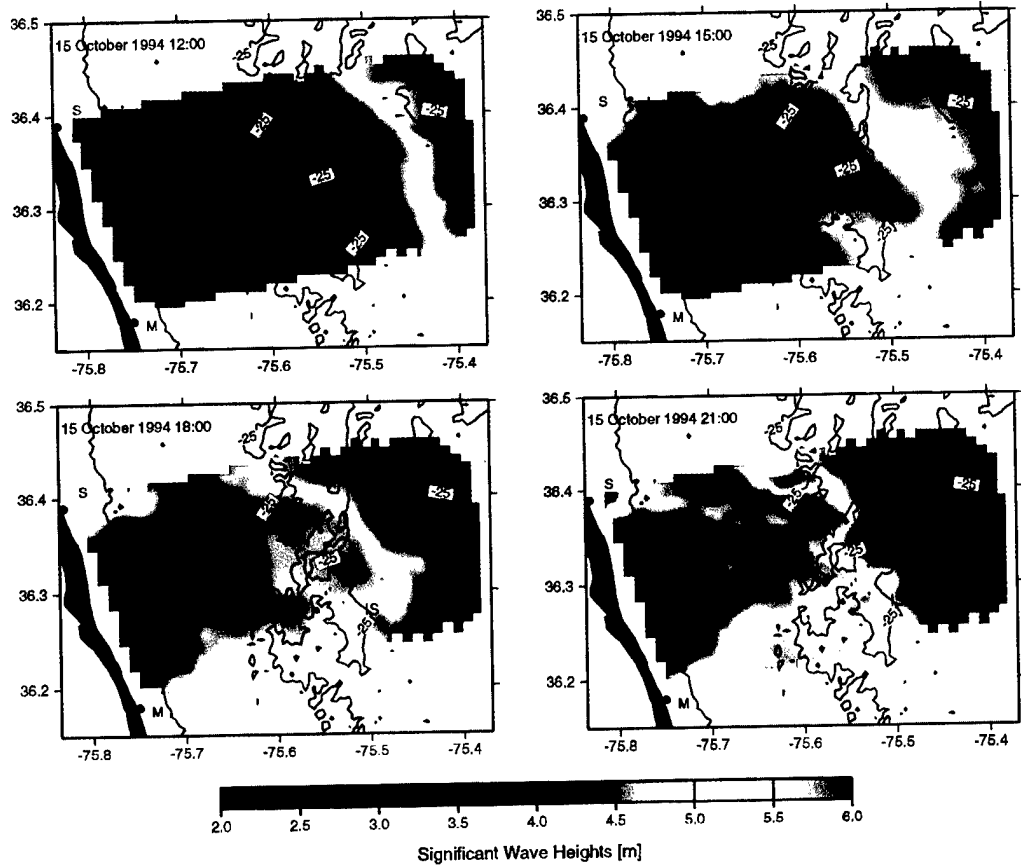


Fig. 3: The figure reveals the evolution and spatial variability of the wave field over the inner shelf with 6.0-m significant wave heights in the outer ranges and 2.5-m significant wave heights close to shore. The four snapshots are hourly-averaged wave height map from three 20-min OSCR observations during a Nor'easter off Duck, NC on 15 October 1994.

gions (e.g., river mouths, estuaries, nearshore, and inner shelf) where the presence of sediment or biological material in the water column could affect other sensors. During and after the passage of storms when biological activity and sediment resuspension is high, observations of the surface wave patterns are important to assess the impact on sediment transport and shoreline erosion.

#### Acknowledgment

The results discussed here were funded in part by the Office of Naval Research through grant N00014-94-1-1016 (DUCK94). The authors thank Brian Haus, Nick Shay, Jorge Martinez, and Nick Peters for the dedicated field work with OSCR. Scott Heron analyzed the extensive set of radar spectra, and Slavica Nikolic generated the graphics.

#### References

- Barrick, D.E., 1977a: The ocean wave height non-directional spectrum from inversion of the HF sea-echo Doppler spectrum. *Rem. Sens. Environ.*, 6, 201-227.
- , 1977b: Extraction of wave parameters from measured HF sea echo Doppler spectra. *Radio Sci.*, 12, 415-424.

- Haus, B.K., H.C. Graber, L.K. Shay and J. Martinez, 1995: Ocean Surface Current Observations with HF Doppler Radar during the DUCK94 Experiment. *Technical Report RSMAS 95-010*, University of Miami, Miami, FL, 104 pp.
- Heron, M.L., P.E. Dexter and B.T. McGann, 1985: Parameters of the air-sea interface by high-frequency ground-wave Doppler radar. *Aust. J. Mar. Freshw. Res.*, 36, 655-670.
- Heron, S.F., 1996: Waveheight analysis using HF radar. Honors Thesis, Department of Physics, James Cook University of North Queensland, 91 pp.
- Maresca, J.W., Jr. and T.M. Georges, 1980: Measuring rms wave height and the scalar ocean wave spectrum with HF skywave radar. *J. Geophys. Res.*, 85, 2759-2771.
- Ng, B., 1993: The prediction of nearshore wind-induced surface currents from wind velocities measured at nearby land stations. *J. Phys. Oceanogr.*, 23, 1609-1617.
- Prandle, D. 1991. A new view of near-shore dynamics based on observations from HF radar. *Prog. Oceanogr.*, 27, 403-438.
- Shay, L.K., H.C. Graber, D.B. Ross and R.D. Chapman, 1995: Mesoscale ocean surface current structure detected by HF radar. *J. Atmos. Ocean. Tech.*, 12, 881-900.
- Wyatt, L.R., 1988: Significant waveheight measurement with h.f. radar. *Int. J. Rem. Sens.*, 9, 1087-1095.
- Wyatt, L.R., 1997: The ocean wave directional spectrum. *Oceanography*, 10, 85-89. □

# MAPPING WIND DIRECTION WITH HF RADAR

By Daniel M. Fernandez, Hans C. Graber,  
Jeffrey D. Paduan and Donald E. Barrick

**B**ESIDES THE MEASUREMENT of ocean surface currents, high-frequency (HF) radar has also been demonstrated to be effective at measuring the wind direction at scales on the order of one to several kilometers and over areas of millions of square kilometers in the case of sky-wave HF radars (Georges *et al.*, 1993) and many hundreds of square kilometers in the case of groundwave HF radars. The capability to estimate the wind direction at high resolution over large areas makes HF radar unique in that it is ground based, yet is capable of collecting remotely sensed measurements of the oceanic wind field that could prove beneficial to mariners, weather forecasters, ocean and atmospheric modelers, offshore operators, and recreational users. Not only are such measurements useful to a variety of people, but they would be expensive and difficult, if not impossible, to obtain through other means, such as through the use of buoys at this resolution.

## Background

Some of the first work that involves measurements of wind parameters using HF backscatter dates back to Long and Trizna (1973), where a sky-wave HF radar at the U.S. Naval Research Laboratory in Maryland was used to obtain measurements of wind direction over large areas of the Atlantic. Sky-wave radars offer wind direction coverage of huge areas of the ocean; however, their spatial resolution (~10 km) does not approach that of ground-wave systems (~1 km).

---

Daniel M. Fernandez, Institute of Earth Systems Science and Policy, California State University, Monterey Bay, 100 Campus Center, Seaside, CA 93955-8001, USA. Hans C. Graber, Rosenstiel School of Marine and Atmospheric Science, University of Miami, Miami, FL 33149-1049, USA. Jeffrey D. Paduan, Code OC/Pd, Naval Postgraduate School, Monterey, CA 93943, USA. Donald E. Barrick, CODAR Ocean Sensors, 1000 Fremontt Avenue, Los Altos, CA 94024, USA.

Since the early sky-wave work, many studies have been conducted by a number of different groups for the purpose of measuring wind direction over both large areas of the ocean using sky-wave radars and in coastal regions using ground-wave radars. A few examples of ground-wave measurements include Heron *et al.* (1985) and Heron and Rose (1986), who used HF radar measurements to obtain estimates of both wind direction and the variability in the winds near the coast.

## How Wind Measurements Are Made

HF radar measurements are unique in the sense that radar backscatter is received from Bragg-resonant waves propagating both away from the radar location and toward the radar location. Furthermore, ocean gravity waves in the Bragg-resonant regime have wavelengths such that they may reasonably be assumed to be locally generated by the wind. If the wind has been blowing for a long enough time and over sufficiently long fetch, the two-dimensional distribution of surface wave energy in equilibrium with the wind can be modeled as a cardioid distribution as a function of angle with respect to the wind direction. The form of this distribution was suggested by Longuet-Higgins *et al.* (1963) to be:

$$G(\theta) = A \cos^s(\theta/2) \quad (1)$$

where  $G(\theta)$  represents the angular distribution of wave energy,  $A$  is a constant,  $\theta$  is the angle from the direction of maximum wave energy (i.e., the angle to the wind), and  $s$  is a spreading parameter. Plots of this cardioid function are shown in Figure 1 along with backscatter spectra corresponding to different radar look directions relative to the wind direction. Positive Bragg peaks in these spectra are associated with waves approaching the radar site, whereas negative Bragg peaks are associated with waves receding from the radar site. The "height" of these peaks is

directly related to the energy within the approaching and receding wave components. It is the relative height (i.e., ratio) of the two Bragg peaks that contains information on the wind direction.

The relationship between the Bragg peaks and wind direction may best be understood through examples with reference to Figure 1, and to the Bragg ratio (in dB), which is defined as:

$$\zeta = 10 \log(B^+/B^-) \quad (2)$$

where  $B^+$  and  $B^-$  are the positive and negative Bragg peak levels, respectively. If, for example, waves propagating toward the radar are much stronger than waves propagating away from the radar, then the Bragg ratio is large and positive, and the wind is assumed to be directed toward the radar (e.g., left panel of Fig. 1). The opposite condition occurs when the wind is directed away from the radar. If the wind is blowing at right angles to the radar direction, then  $B^+ \approx B^-$  and the Bragg ratio is near zero (e.g., center panel of Fig. 1).

If one defines both approaching and receding radar look directions relative to the wind (e.g., Fig. 1), then the Bragg ratio, using (1) and (2), is related to the wind direction by:

$$\zeta = 10 \log \left[ \frac{\cos^s\left(\frac{\theta^- - 180^\circ}{2}\right)}{\cos^s\left(\frac{\theta^-}{2}\right)} \right] \\ = \log \left[ \tan^s\left(\frac{\theta^-}{2}\right) \right] \quad (3)$$

where  $\theta^-$  is the angle between the wind direction and the receding Bragg waves. Equation (3) can be inverted for  $\theta^-$  and, hence, the wind direction if a value for the spreading parameter,  $s$ , is assumed. (Commonly a value of  $s = 4$  is used.) There is, however, a left-right ( $\pm\theta$ ) am-

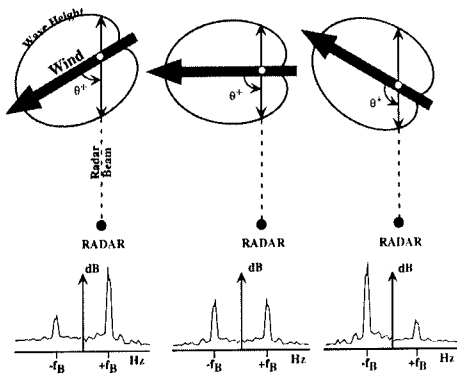


Fig. 1: Sample distributions of surface wave energy as a function of angle relative to the wind direction for cases with wind blowing toward (left), at right angles to (middle), and away from (right) the radar look direction. Sample backscatter spectra below show relative heights of the approaching (+) and receding (-) Bragg peaks for each case and  $\theta$  denotes the angle between the wind and the approaching wave directions.

biguity in the solution that must be resolved using independent observations, assumptions about time continuity, or (preferably) estimates from a second radar site viewing the ocean from a different angle.

### Results from a Phased-Array System

In Wyatt's paper (Wyatt 1997) on directional wave mapping using the Ocean Surface Current Radar (OSCR) system, wind direction maps are also included (see Wyatt 1997, Fig. 4, this issue) that show the effect of a low pressure system moving past the radar sites. Here we present a similar result from an OSCR deployment off Duck, North Carolina in October 1994. Surface current data from this experiment are described by Haus et al. (1995) and Shay et al. (1997). Importantly, the experiment included offshore moored wind measurements within range of the OSCR sites. In addition, the Army Corps of Engineer's research pier at Duck collected wind measurements at the nearshore boundary of the radar field.

Wind direction estimates from the OSCR cell closest to the offshore mooring are shown in Figure 2, together with observed wind directions, for a 2-day period that included the passage of a sharp front on 9 October. The remotely sensed direction estimates agree very well with those measured at the mooring. In this case, data from only one of the two OSCR sites (the master site)

were used, and the directional ambiguity in the Bragg ratio was resolved by minimizing the differences with the mooring data. Hence the OSCR estimates are not independent of the mooring data in this example, but the results are still very encouraging. (During this experiment, the noise level of the OSCR slave site was such that useable Bragg ratios were unavailable most of the time.)

The important potential of HF radar data with regard to the wind field is in their ability to map wind direction and detect frontal boundaries (sudden changes in direction) and small-scale storms (e.g., waterspouts, thunderstorms). High resolution wind direction maps from before and after the frontal passage of 9 October are shown in Figure 3, together with observed directions at the mooring and on the research pier. Again, these estimates were made without the benefit of the second radar site. They are, nonetheless, remarkable in terms of the two-dimensional views they provide. Primarily onshore winds throughout the region shifted to alongshore with the passage of the front. In addition, the radar maps show variations in wind direction over horizontal scales of just a few kilometers. Wind stress divergences and curls over these scales, and their impact on coastal mixing and circulation, can only be investigated using HF radar systems.

### Results from a Direction-Finding System

The wind direction mapping described above was accomplished using

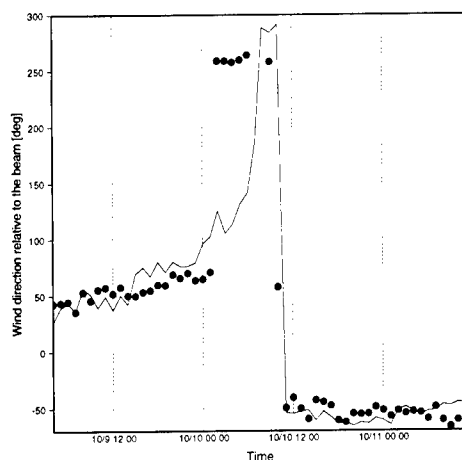


Fig. 2: Wind direction relative to the master radar site measured at a wave buoy off Duck, North Carolina in October 1994 (solid) together with estimates from the HF radar (symbols).

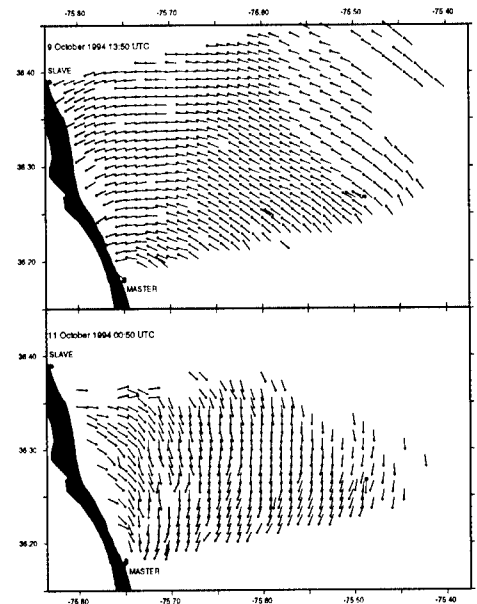


Fig. 3: Wind direction maps from 9 and 11 October 1994 off Duck, North Carolina from OSCR measurements at the master HF radar site. The measured directions at an offshore mooring and from a research pier are also shown in red.

phased-array systems where the beam is electronically "steered" to a particular direction and the entire Bragg peak energy ratio is measured. It is likewise possible to use backscatter data from direction-finding systems, such as the CODAR SeaSonde, to map wind direction using compact colocated antennas. This can be done by extending the surface current algorithms (e.g., Lipa and Barrick, 1983; Barrick and Lipa, 1997) to provide the Bragg power ratio for the extracted bearing angles corresponding to the particular Doppler frequency bin (or radial velocity). The estimation of wind direction is, therefore, more restrictive than surface current estimates, because both Bragg peaks must produce a similar bearing estimate for each radial velocity bin. Like the phased array, wind direction estimates for a particular grid location must be available from both radar sites if two-site data are to be used to resolve the direction ambiguity.

An initial attempt at wind direction mapping using two SeaSonde systems off the Oregon coast is shown in Figure 4. A reversal of alongshore wind direction from downwelling-favorable to upwelling-favorable between 20 May and 21 May 1996 is clear in the figure, along with the suggestion of small-scale structure similar to that observed off North Carolina by the OSCR system.

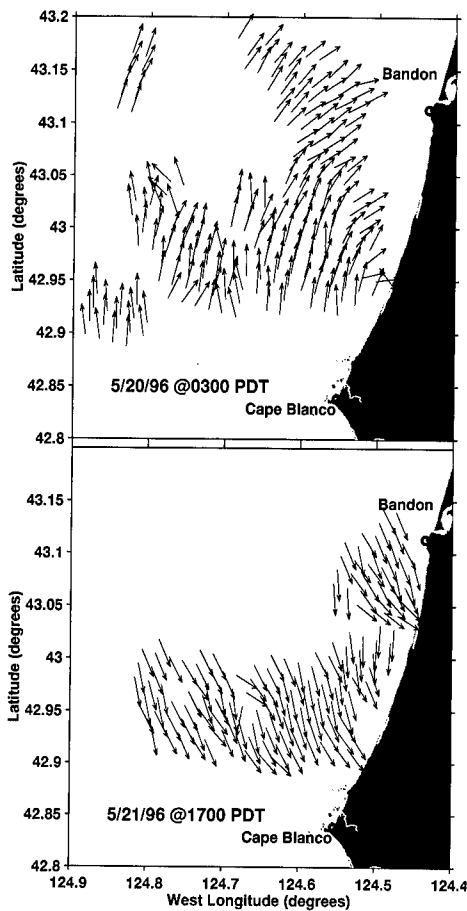


Fig. 4: Wind direction maps from 20 and 21 May 1996 off Bandon, Oregon from two-site SeaSonde measurements at Bandon and Cape Blanco.

## Conclusions

Mapping marine surface wind direction is another unique capability of HF radar systems. Although still in the preliminary stages, this technique may yield synoptic measurements of coastal wind variations with resolutions of only a few kilometers. New systems under development, such as the multifrequency, phased-array system mentioned in Teague *et al.* (1997) should have better sensitivity for both wind and wave calculations because their computer-controlled design will allow rapid changes

in the transmit and receive parameters. The multifrequency aspect of these systems will also allow for comparisons of wind direction estimates from a range of frequencies and, hence, a range of Bragg wavelengths that may help to assess the fundamental assumptions made about equilibrium conditions. Since ocean waves at different wavelengths respond differently (directional relaxation) to changes in wind speed and direction, the methodology described here could also be applied to infer the directional distribution of ocean waves.

Mapping of wind direction is possible from both phased-array and direction-finding HF radar systems. Results from the latter presently can have less spatial resolution due to the need to obtain simultaneous direction solutions from both positive and negative Bragg peaks.

It should be pointed out that the measurements described here yield maps of wind direction only. They do not provide estimates of wind speed. Thus it is not possible to obtain a true vector wind field in this way. Nonetheless, the ability to map an important wind parameter such as wind direction, and to document its hour-to-hour evolution, is unique. For example, real-time observations of approaching atmospheric fronts and thunderstorms are helpful in the safe passage of commercial and recreational vessel traffic inside and outside of ports and harbors. These measurements could be combined with other wind measurements from moorings and the shoreline, and with simultaneous maps of surface current velocities and surface wave heights, to begin to study interaction of the coastal atmosphere and ocean on short time and space scales.

## Acknowledgments

H.C. Graber acknowledges the support by the Office of Naval Research through grant N00014-94-1-1016 (DUCK94). We thank Michael Kosro

(OSU) for providing the SeaSonde data used to produce Figure 4 and Bob Jensen (USAE) for the buoy data in DUCK94. Brian Haus and Nick Shay (RSMAS) collected the OSCR data and Slavica Nikolic generated the OSCR graphics.

## References

- Barrick, D.E. and B.J. Lipa, 1997: Evolution of bearing determination in HF current mapping radars. *Oceanography*, 10, 72-75.
- Georges, T.M., J.A. Harlan, L.R. Meyer and R.G. Peer, 1993: Tracking hurricane claudette with the U.S. Air Force over-the-horizon radar. *J. Atmos. Ocean. Tech.*, 10, 441-451.
- Haus, B.K., H.C. Graber, L.K. Shay and J. Martinez, 1995: Ocean surface current observations with HF Doppler radar during the DUCK94 experiment. Technical Report RSMAS 95-010, University of Miami, Miami, FL, 104 pp.
- Heron, M.L., P.E. Dexter and B.T. McGann, 1985: Parameters of the air-sea interface by high-frequency ground-wave HF Doppler radar. *Aust. J. Mar. Freshw. Res.*, 36, 655-670.
- and R.J. Rose, 1986: On the application of HF ocean radar to the observation of temporal and spatial changes in wind direction. *IEEE J. Oceanic Eng.*, OE-11, 210-218.
- Lipa, B.J. and D.E. Barrick, 1983: Least-squares method for the extraction of surface currents from CODAR Crossed-loop data: Application at ARSLOE. *IEEE J. Oceanic Eng.*, 8, 226-253.
- Long, A.E. and D.B. Trizna, 1973: Mapping of North Atlantic winds by HF radar sea backscatter interpretation. *IEEE Trans. Antennas Propagat.*, AP-21, 680-685.
- Longuet-Higgins, M.S., D.E. Cartwright and N.D. Smith, 1963: Observations of the directional spectrum of sea waves using the motions of a floating buoy. In: *Ocean Wave Spectra*. Proceedings of a Conference, Prentice-Hall, Englewood Cliffs, NJ, 111-136.
- Shay, L.K., S.J. Lentz, H.C. Graber and B.K. Haus, 1997: Current structure variations detected by HF radar and vector measuring current meters during DUCK94. *J. Atmos. Ocean. Tech.* In press.
- Teague, C.C., J.F. Vesecky and D.M. Fernandez, 1997: HF radar instruments, past to present. *Oceanography*, 10, 40-44.
- Wyatt, L., 1997: The ocean wave directional spectrum. *Oceanography*, 10, 85-89. □

# MEETING ANNOUNCEMENT AND PRELIMINARY CALL FOR ABSTRACTS TOS AND IOC 1998 SCIENTIFIC MEETING "Coastal and Marginal Seas"

Paris, France  
UNESCO Headquarters  
June 1-4, 1998

Program Chairs: **Kenneth Brink**, Woods Hole Oceanographic Institution, USA  
and **Katherine Richardson**, Danmarks Fiskeriundersøggelser, Denmark

## PRELIMINARY PROGRAM

Monday, June 1: "Small scale processes: turbulence, particles, and transformations"

Chair: **Thomas Kioerbe**, Danish Institute for Fisheries Research

Tuesday, June 2: "Medium scale processes: transports, physical structures and plankton distributions"

Chair: **John Simpson**, School of Ocean Sciences, Bangor plus Special evening GOOS session

Chair: **Colin Summerhayes**, IOC

Wednesday, June 3: "Regional scales: circulation, budgets and population dynamics"

Chair: **Sharon Smith**, University of Miami, USA

Thursday, June 4: "Policy, Perspectives, New Directions and Late Breaking News"

THE OCEANOGRAPHY SOCIETY (TOS) and the INTERGOVERNMENTAL OCEANOGRAPHIC COMMISSION (IOC), in observance of the Year of the Ocean and the TOS 10th Anniversary, announce their first jointly sponsored meeting to be held in Paris, June 1-4, 1998 at UNESCO headquarters. The meeting format will include morning plenary sessions of invited talks on the daily session themes and contributed poster abstracts in the afternoons focusing on, **but not limited to**, the day's session theme (no poster session on the last day). Commercial exhibits will be co-located with the contributed posters.

Students are invited to attend and participate. Fifty students will be permitted to register at one-half the regular registration fee. The half-price registrations will be allocated on a first-come basis, but preference will be given to students submitting abstracts and presenting posters.

Some financial support will be available from SCOR for oceanographers from developing countries; applications for this support must be received at TOS headquarters by **February 1, 1998**.

## CALL FOR POSTER ABSTRACTS

### ABSTRACT & POSTER INFORMATION

Poster abstracts will be accepted for review **November 1, 1997-March 15, 1998**. Abstract titles and content need not be specific to one of the broad session themes as outlined in the Preliminary Program included here.

Abstracts relating to the session theme of a given day will be presented on that day. Abstracts not specific to the session themes will be presented on the day assigned them by the Abstract Manager. Every attempt will be made to assign posters for presentation on the day preferred by the author but, to balance the number of posters over the course of the meeting, TOS reserves the right to make the final assignments.

All submitted abstracts will be reviewed by the Program Chairs and/or the appropriated Session Chair. Abstract acceptance notices will be issued no later than April 16. Every effort will be made to issue early notifications of poster acceptance to those who submit abstracts in advance of the deadline.

### ABSTRACT FORMAT

*Abstracts are limited to 250 words, including title and author(s) information (name[s], affiliation[s], and address[es]).* An Internet ad-

dress for the first author is requested. Long abstracts will be returned to the author for editing.

### Abstract Submissions

**Electronic mail is the preferred method for submitting abstracts** and will ensure the quickest acceptance notification. Abstracts may also be submitted to TOS via FAX, mail, or other delivery service for an additional fee (see below).

**E-mail and FAX:** Submit abstracts via e-mail as text files (no "attachments"). Abstracts submitted in this manner must include credit card information as below.

**Mail or Delivery Service:** Submit in duplicate to TOS headquarters with a check, money order or credit card information as below.

With all submissions, please indicate the following information:

- If paying by credit card (Master Card or Visa only) indicate account number, expiration date, and name that appears on the card;
- Name, address, E-mail address, phone number, and fax number of the person to receive notification;

- Session to which the abstract relates or preferred day of presentation if the abstract is unrelated to one of the daily session themes.  
Submit to: The Oceanography Society,  
4052 Timber Ridge Drive,  
Virginia Beach, VA 23455, USA  
E-mail: rhodesj@exis.net or jrhodes@ccpo.odu.edu  
FAX: (757) 464-1759; Phone: (757) 464-0131

#### ABSTRACT FEES

The abstract fee is US\$60 (US\$30 for students) for abstracts submitted via e-mail and US\$75 (US\$36 for students) for those submitted

by any other means. Payment of the abstract fee must be made at the time the abstract is submitted and can be made with check or money order, payable to "The Oceanography Society" (*in U.S. funds payable on a U.S. bank*) or with a credit card (Master Card or Visa only). Abstracts submitted via e-mail or FAX must be paid with a credit card for which the account number and expiration date are provided when the abstract is sent. We regret that we are unable to process training or purchase orders and cannot issue invoices for payment. Fees for abstracts that are not accepted will be refunded. Revisions to abstracts are discouraged; revised abstracts will be treated as new submissions and will be charged as an additional abstract.

## GENERAL INFORMATION

#### REGISTRATION

All participants, including poster presenters, must register for the meeting. A brochure containing registration information, forms, and updated program will be available in October 1997.

#### HOTEL ACCOMMODATIONS

No headquarters hotel has been designated for the meeting since all of the activities will be at UNESCO and because there are so many hotels of varying price and degree of luxury in the vicinity of UNESCO (7, Place de Fontenoy, 7th arrondissement bordering with the 15th arrondissement; metro: Segur or Cambronne). The Paris web site ([www.paris.org](http://www.paris.org)) has an extensive list of hotels by arrondissement with notations on price and level of comfort. Your travel agent will also be able to assist with reservations.

June is a busy tourist month in Paris so we urge you to make hotel and flight reservations early. If your attendance at the meeting is predicated on acceptance of your abstract, please submit your abstract as early as possible and make tentative reservations if at all possible.

#### INFORMATION UPDATES

TOS members and those requesting placement on the meeting mailing list will be sent an updated printed brochure as they become available. If you wish to be placed on the mailing list or if you are on the list but have not received the brochure by December 15, 1997, please contact TOS headquarters (E-mail: rhodesj@exis.net or jrhodes@ccpo.odu.edu; phone: (757)464-0131; fax: (757)464-1759). Meeting updates will also appear at the TOS website (<http://www.tos.org>) and various other electronic sites.

## TOS Standing Committees

### *Meetings Committee*

The Meetings Committee is charged with advising the TOS Council on the planning and organization of the TOS meetings within the framework of the Council priorities for the growth and health of the Society. The Meetings Committee advises on themes, chairs, format, location, and policies for all regular TOS meetings. Under the auspices of the Meetings Committee, a Meetings Manual has been developed to provide history and continuity for this important committee. The manual is a dynamic document which is updated as additional policy evolves and new circumstances are encountered. The committee is currently developing and discussing possible meeting themes for 1999, 2000, and onward.

Current committee members and terms of appointment:

|  |  |           |
|--|--|-----------|
| <b>Eric Hartwig</b> , Chair<br>(hartwig@utopia.nrl.navy.mil) | Naval Research Laboratory              | 1994–1998 |
| <b>Otis Brown</b>  | University of Miami                    | 1997–2000 |
| <b>Tom Dickey</b>  | University of California/Santa Barbara | 1997–2000 |
| <b>David Farmer</b>  | Institute of Ocean Sciences (Canada)   | 1995–1998 |
| <b>John Kindle</b>   | Naval Research Laboratory              | 1997–2000 |
| <b>Annelies Pierrot-Bults</b>                                | University of Amsterdam                | 1996–1999 |
| <b>David Schink</b>  | Texas A&M University                   | 1995–1998 |
| <b>Gerold Wefer</b>  | University of Bremen (Germany)         | 1996–1999 |

Ex officio members:

|                             |                                     |
|-----------------------------|-------------------------------------|
| <b>Margaret Leinen</b>      | TOS past President                  |
| <b>Ken Brink</b>            | 1998 Paris meeting program co-chair |
| <b>Katherine Richardson</b> | 1998 Paris meeting program co-chair |
| <b>Judi Rhodes</b>          | TOS Executive Director              |

### *Membership Committee*

The Membership Committee is charged with advising the TOS Council on:

- (1) Strategies for retaining members and for recruiting new members;
- (2) Strategies for recapturing members who have left the Society;
- (3) The design of membership drives for new members from targeted groups; and
- (4) The implications of any proposed changes for dues structure, meetings, publications or other Society services for the membership.

The Membership Committee has reviewed the membership records and from its analysis is preparing a number of recommendations for the Council's consideration.

*Note:* While the Membership Committee is officially charged with overseeing membership matters, the Council hopes that every TOS member considers himself/herself an ex officio member of the committee. Personal endorsements of the Society's activities and suggestions to colleagues to join your society will greatly assist the Membership Committee in its charge.

Current committee members:

|  |  |
|--|--|
| <b>Jonathan Sharp</b> , Chair<br>(jsharp@udel.edu) | University of Delaware                     |
| <b>Neil Andersen</b>                               | University of Maryland                     |
| <b>Winfried Gieskes</b>                            | University of Gronigen (The Netherlands)   |
| <b>David Karl</b>                                  | University of Hawaii                       |
| <b>Tony Knap</b>                                   | Bermuda Biological Station for Research    |
| <b>Gerold Siedler</b>                              | Kiel University (Germany)                  |
| <b>Colin Summerhayes</b>                           | IOC (Paris)                                |
| <b>Echiro Tanoue</b>                               | Meteorological Research Institute of Japan |

\*\*\*\*\*

The TOS Council thanks these committees for their invaluable work and guidance in these two areas of major importance to the Society. Special thanks also for a job well done to those who rotated off the Meetings Committee this year (David Halpern, Jet Propulsion Laboratory; Marlon Lewis, Dalhousie University; and Thomas Stanford, University of Washington).

If you are interested in serving on these committees or should you have comments, questions, or suggestions regarding their work, please contact either the Chair of the committee or TOS headquarters (for forwarding to the appropriate committee).

# ADDENDUM TO "THE OCEANOGRAPHY TEXT PATTERN: A REVIEW AND COMPARISON OF INTRODUCTORY OCEANOGRAPHY TEXTS"

By Richard W. Spinrad\*

SUBSEQUENT TO THE PUBLICATION of the *Review of Oceanography* texts last year (Spinrad, 1996), The Oceanography Society was contacted by two authors. In one case we were asked to include a previously overlooked text, and in the other case, the author was concerned that the text which had been provided by their publisher was not the most recent college-level version. Respectively, these two texts, reviewed here as an addendum to the original assessment (and using the original criteria for review), are

1. David A. Ross  
*Introduction to Oceanography*  
HarperCollins, 1996, ISBN 0-673-46938-7
2. Alyn C. Duxbury and Alison B. Duxbury  
*An Introduction to the World's Oceans, 5th Edition*  
Wm. C. Brown Publishers, 1997, ISBN 0-697-28273-2

Ross' text follows a rather traditional approach to presenting the field of oceanography. It is generally a sound and informative book. Using the same criteria as developed for the previous review of texts, Ross' volume shakes out as follows:

**Tides**—This section is included as part of the treatment of waves. The discussion of forces is very (perhaps too) simplistic, but the use of graphics is very good. There is minimal treatment of dynamic theory, and no real data are included. One unique aspect is the treatment of tidal friction in the context of paleoceanography. The whole discussion on tides covers only about five pages and there is nothing on amphidromic points or cotidal lines. The treatment of tides is slightly disappointing.

**Primary Production**—Ross takes an ecosystem approach which invokes a strong element

of disciplinary integration. Other textbook authors could learn a lot from this approach. There is an excellent treatment of photosynthesis, production, respiration, compensation depth, nutrient supply, and physical controls. There are also good comparisons of photosynthesis and chemosynthesis, and very nice treatments of geographic variability and general measurement techniques. One interesting point is the inclusion of a box on the iron experiments conducted in the Pacific, although this appears in the chapter on climate, and there is no cross reference in the chapter on productivity. Nevertheless, Ross' treatment of primary production is a strong point in the text.

**El Niño**—Ross' treatment of ENSO is very clear and succinct, including a very fair description of the methods of observation and the forecast limitations. He also includes a good discussion of the global implications of El Niño. One change I would recommend is more abundant inclusion of El Niño throughout the rest of the text. I also believe the references specific to El Niño, at the end of the chapter, are not adequately current (the most recent is from 1986).

**Hydrothermal vent biota**—This is an excellent piece of this textbook. Along with some wonderful photographs, Ross has included a nice definition of the wonder of these discoveries, and their implications for understanding life in extreme environments. He also blends this section with a nice discussion on chemosynthesis (see above), and a very good set of references at the end of the chapter. I really enjoyed reading this section.

**Biodiversity**—Except in terms of a general discussion of biological communities, this section is insufficient.

**Acoustic Thermometry**—This text is one of the very few (compared to those reviewed previously) that has a section on this subject. Ross also includes a discussion on the relatively new field of acoustic tomography. The Heard Island experiment is described reasonably well, with, perhaps, a bit too much emphasis on the environmental debates of using sound sources in ocean waters. Overall, Ross treats the subject of acoustics fairly and fully.

**Optics**—Ross has given another fair and accurate treatment of this subject, indepen-

dently, and in the context of biological production. My only objection is that the section is called out as a separate box, thus suggesting that the subject is not central to oceanography.

**References**—The average number of references per chapter is 15, with the oldest being from 1912, the newest from 1993, and the mean age being 1985. The disturbing additional bit of information is that most of the policy-related chapters include virtually no references after 1993. In fact, the chapter dealing with the Law of the Sea has no references since 1989. Otherwise, this text is comparable to most of the others reviewed previously.

**General Comments**—This book includes some unique elements. Ross has included separate sections on the ocean's role in global climate change, as well as chapters on marine archaeology, marine pollution, and Law of The Sea. The text includes over 50 boxes on subjects of a scientific, technological, or general interest. There is good use of color graphics, photographs, and generally a nice mix of schematics and real data. There is a notable bias toward material from scientists at Woods Hole Oceanographic Institution (12 of 20 randomly selected figures had WHOI credits). Each chapter includes a very readable and short introduction and at the end, a good summary. The review questions at the end of each chapter are too regurgitative but might be good for quizzes. Key terms, highlighted in the text, are helpful, albeit a bit numerous. The lists of further reading tend to be non-technical, with a heavy emphasis on *Oceanus*, *Scientific American*, and other texts (each reference includes an informative 1-line description). It would be nice to see more technical journals included. The text's appendices are not particularly helpful. They include a list of conversion tables and description of the metric system, a good (but not great) glossary (e.g., it doesn't include "biogeochemistry" or the Ocean Drilling Program), and a list of references, the relevance of which is unclear.

**Conclusion**—Ross' text is good overall, with some sections that are outstanding. The reader is well advised to carefully review all sections, since some fell short of providing the most current or complete information.

Richard W. Spinrad, Consortium for Oceanographic Research and Education, 1755 Massachusetts Ave. NW, Washington, DC, 20036-2101, USA.

\* The opinions expressed in this article are solely those of the author, not that of TOS or CORE.

The Duxburys' text, hot off the presses, is an extremely impressive and useful book for a college level class. While the version reviewed in the previous assessment was not appropriate for an undergraduate course, this one is outstanding. So much about it reflects the Duxburys' diligence in researching topics, and attention to detail. Let me march through the subjects reviewed:

**Tides**—This subject is covered in a whole chapter of some twenty pages, and specifically geared to students who have little or no understanding of vectors. The chapter starts with a good definition of key tidal characteristics: temporal and spatial patterns and variability (including tidal currents). There is a very nice breakout of equilibrium and dynamic theory; in the former, the authors do a nice job of holding the students' hands through some simplified explanations. The section on dynamic tide analysis is impressive in its ties to previous readings on shallow water waves and the Coriolis effect. I would have liked, however, to see a tabular breakout of tidal components. The coverage of cotidal lines and amphidromic points, done in the context of standing waves (including a method to calculate the natural period of oscillation in a tidal basin) is quite clear. The Duxburys' discussion of the capabilities, benefits and detriments of harnessing tidal energy is, in two words, excellent and fair. I also liked their presentation on tides with respect to estuarine mixing and flushing. In summary, this treatment of tides is the best of any of the eight texts now reviewed.

**Primary Production**—Again, this is a thorough and accurate section. Good, clear definition of gross and net production lead smoothly and logically into a discussion of controls. While there is a disappointing paucity of real data in this section, I was encouraged by the brief, but accurate mention of the recent work on trace metal controls. The discussion continues to include a very nice synopsis of average global distributions of production (including numbers) and a good definition of zonally dependent seasonal variability. Table 14.2, showing relative gross production on land and in the ocean (for different environments), is terrific. The section on measurement methods is short but complete and up-to-date.

**El Niño**—I would put the Duxburys' coverage of El Niño near the top, for all of the texts, mostly by virtue of their comprehensiveness. Physical processes, temporal/spatial scales, current state of forecast capabilities, and the concepts of teleconnections are all included in the text. This is one case where they make nice use of real-world data, and, albeit subtly, they make mention of the relationship between El Niño detection and background global warming signatures. One particularly

noteworthy aspect of their coverage of El Niño is their mention, throughout the book, of the potential impact of the phenomenon on a wide range of such societally important issues as fish stocks, CO<sub>2</sub> exchange, and formation of North Atlantic cold water masses.

**Hydrothermal vent biota**—To their credit the authors include some mention of this subject in their discussion of primary production (in the context of chemosynthesis cf. photosynthesis). They include a few photos, but none as stunning as contained in some of the other texts. Generally, the coverage is good . . . my only complaint is that the excitement of the discovery of hydrothermal vent biota and the potential implications in studies of the origins of life are not appropriately conveyed.

**Biodiversity**—This subject, while mentioned in passing in the preface, is not specifically called out in the body of the text. There are faint allusions by virtue of discussion on genetic manipulation and nonindigenous species, but the coverage overall is lacking.

**Acoustic Thermometry**—The reader is reminded that in the previous review fewer than one-half of the texts discussed this subject, and only one did it well. The Duxburys' excel in this coverage. They include an outstanding definition of the concepts of long-range acoustic transmission and the connection to integrated temperature measurement (as well as a very fair discussion on the marine mammal-related concerns for this research). Their section even has brief mention of the recent Transarctic Acoustic Propagation experiment. A noteworthy related point is their inclusion of a separate section on acoustic tomography (including some discussion on moving source tomography!).

**Optics**—This coverage is a bit disappointing. While generally accurate, the description of the physics behind water color is insufficient. My main complaint, however, is that the definition of the technology for optical measurement is about 20 years out of date (e.g., hand-held photometers with analog voltmeter readouts). This section has not been researched and updated as well as most of the rest of the text.

**References**—The Duxburys make extensive use of references from the general scientific literature (*Scientific American*, *Oceanus*) with a peppering of technical references (*Science*) and an impressive set of references to the classic oceanographic texts (Shepard, Bascom, Parsons/Takahashi/Hargrave, Pickard/Emery, Riley/Chester, Bowditch, etc.). Students should have no problem finding most of the references included in this text. That's a real plus! The numbers are also very good: an average of 23 references per chapter, with a mean date of 1988 (in the random check of five chapters the oldest reference was from 1953 and the newest from 1996). But, perhaps, most impressive about the references is the inclusion of an ex-

tensive set of World Wide Web Home Pages. Regardless of how ephemeral the individual URLs might be, this is an enormously valuable reference tool, and the Duxburys are to be credited for taking a lead among oceanography texts in providing this service.†

**General Comments**—This book is a joy to read! The writing is clear and concise, the use of graphics is quite aesthetically pleasing, and there is an outstanding mix of photos, satellite images, schematics, and plots of data. Each chapter begins with a literary quote and a short intro, both of which are attractive. All of the chapters include good, short summaries, and an adequate list of key terms. Most of the chapters include a section on practical considerations (e.g., Ocean Thermal Energy Conversion, coastal development, fisheries, etc.) which are generally important, relevant, and thought provoking. Boxes for new techniques and new projects (with most of the emphasis on the former) represent an excellent choice of topics, from remote sensing, to the Navy's Sound Surveillance System (SOSUS), to side-scan technology, to viruses, and even the Great Pacific Sneaker Spill. Overall, the Duxburys have done a very nice job of including current interest items throughout the text (including very recent information on cholera). They've also taken a nontraditional view toward inclusion of environmental concerns, by placing that chapter in the middle of the book (following the chapter on coastal processes—good thinking!), rather than at the end of the volume (which for many texts implies that this subject is nothing more than an afterthought). Each chapter ends with study questions that are comprehensive but mostly of a review nature. Some chapters also have study problems, which, while almost exclusively mathematical in form, really do test the understanding of the students; there should be more of these. In summary, had this volume been available during the initial review it would have, undoubtedly ranked in the top group.

The conclusion on these two additional texts is that they are both good. The material which Ross' text covers, is generally dealt with well, but the reader is advised to check carefully on individual subjects (he can be a bit spotty). I am particularly impressed with the Duxburys' volume. This is more than a text book . . . it is also a good reference document. In fact, I will think seriously about using this new volume in my own course next time around. I highly recommend it for its quality, currency, and completeness.

---

† In the undergraduate oceanography course I taught this spring, approximately 90% of my students indicated that they have access to, and use the Web for course-related research.

# MicroCAT sets the **NEW** standard in *accurate* moored C-T instruments

- Higher Accuracy
- Increased Resolution
- Better Stability
- Direct Digital Output
- Proven Fouling Resistance

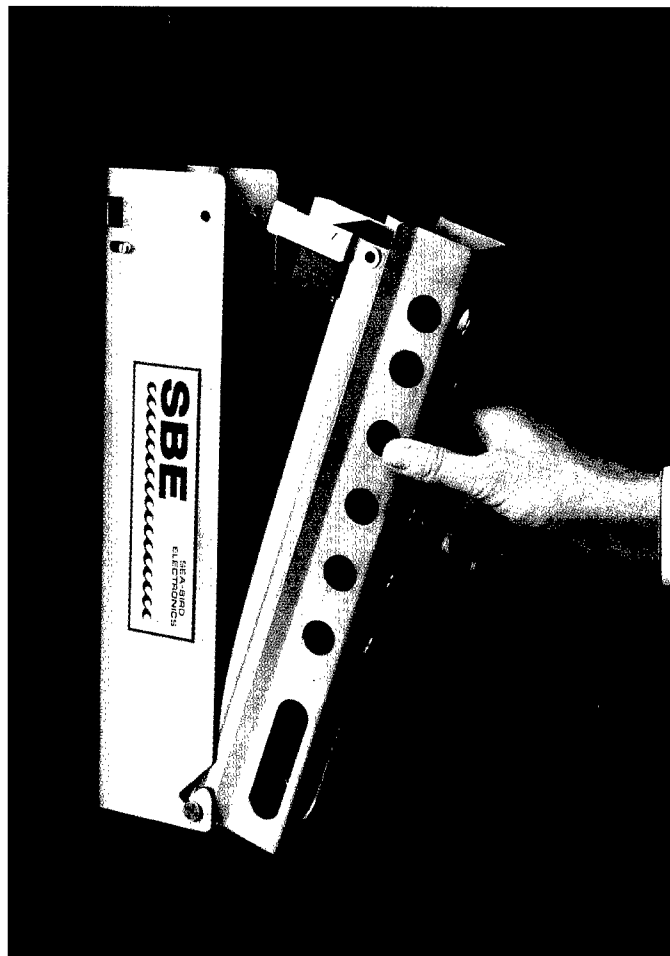
An evolution of the legendary SEACAT, proven by a decade of ocean research; MicroCAT combines our unique internal-field conductivity cell and ultra-stable thermistor with new microelectronics and calibration technology.

## Three New Models with Surprisingly Low Prices!

**SBE 37-SI** with serial interface (no memory or battery) for real-time monitoring or integration with current meters, ROVs, etc.

**SBE 37-SM** with serial interface and large flash memory for conventional moorings or synchronization with ADCP sampling.

**SBE 37-IM** with DPSK inductive modem telemetry (shown at right), outperforms FSK inductive telemetry types. The SBE 37-IM clamp attaches to a jacketed cable, the MicroCAT snaps in place and is then secured in the clamp with two bolts. Up to 100 addressable MicroCATs communicate (half duplex) with an Inductive Modem Controller (sold separately) over cables up to 7000 meters long.



## Other MicroCAT Features

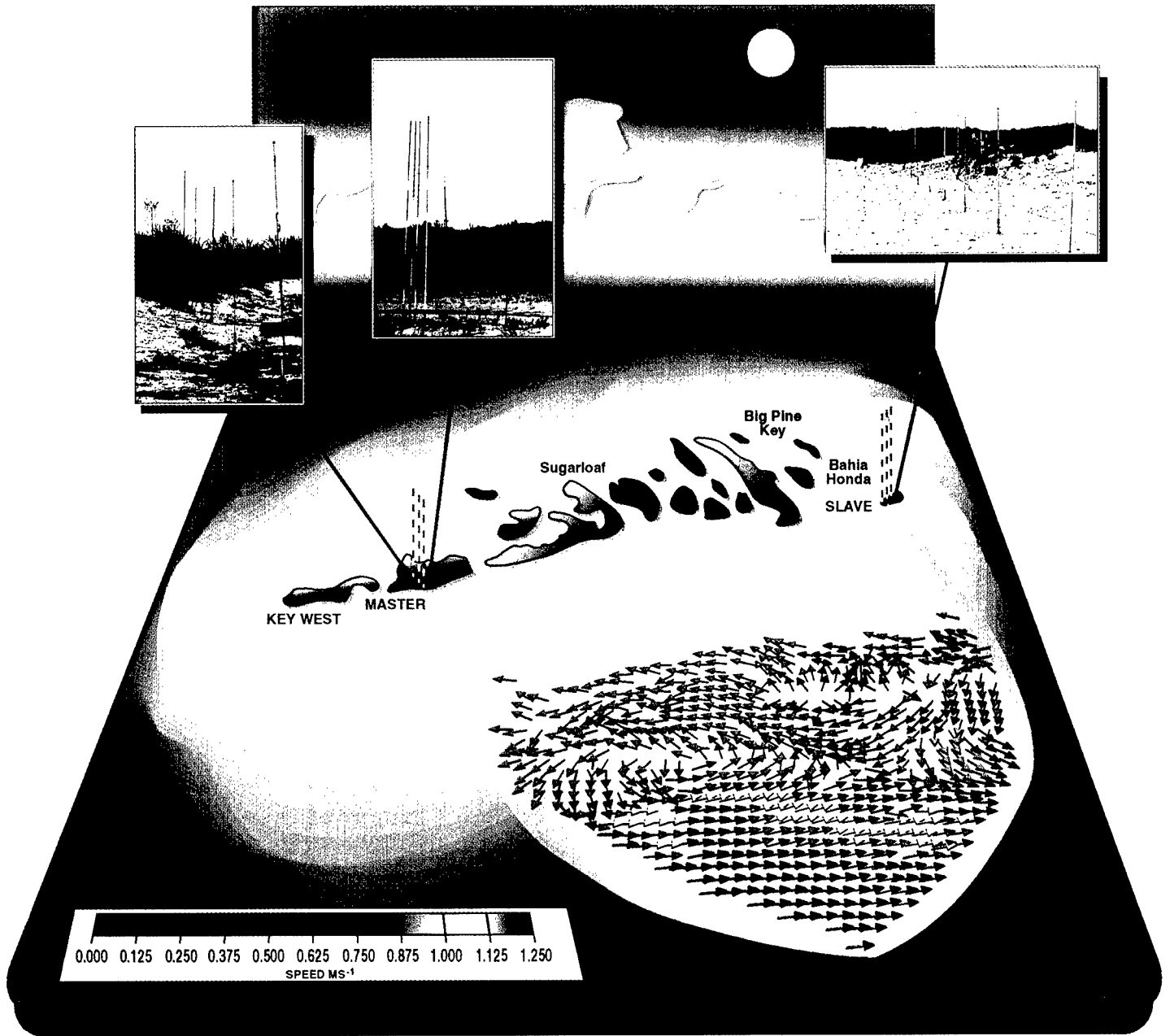
All titanium construction for 7,000 meters depth, RS-232C or RS-485 interface choices, real-time clock, optional strain gauge pressure sensor, non-restricted lithium battery gives endurance for over 100,000 samples, internal references for automatic error correction, calibration coefficients stored in EEPROM allow data output in degrees C, Siemens/meter, decibars and time (month, day, year, hours, minutes, seconds). Data format compatible with SEASOFT® or virtually any spread sheet or data base.

**SBE** SEA-BIRD ELECTRONICS, INC.  
1808 - 136th Place Northeast  
Bellevue, Washington, 98005 USA

web site: [www.seabird.com](http://www.seabird.com)  
Fax (206) 643-9954  
Telephone (206) 643-9866



THE OCEANOGRAPHY SOCIETY  
4052 Timber Ridge Drive  
Virginia Beach, VA 23455 USA  
Phone: (757) 464-0131



**Units:** The International System (SI) should be used throughout. Symbols for a unit of measurement should be used only when preceded by a number (e.g. "10 m" but "several meters"). Unit symbols are not to be punctuated (i.e., they are not treated as abbreviations); the same symbol is used for both singular and plural.

**Abbreviations:** Abbreviations and acronyms must be identified with their first use. The solitary use of acronyms is unnecessary and discouraged. The abbreviation "U.S." is appropriate when it modifies another word (e.g. U.S. Department of Commerce). Names of states and months should be spelled out except in Table and Reference sections.

**Mathematical Formulas:** The use of mathematical symbols and formulas should be held to the absolute minimum necessary, and in those cases all symbols must be clearly defined in the text. For detailed guidelines, see the Author's Guide of the American Meteorological Society.

**Color Photography/Print Material:** The use of color photos or art work is encouraged, if its use enhances the readability, utility, or artistic merit of the article. At present, there are no page charges for publication, but costs for color processing will be charged to the author.

**Covers:** Any author may submit color material to be considered for use on the front or back covers. Cover material must be pertinent and complementary to the author's published article. In some relevant

cases, cover figures with extended captions will be considered for publication without an accompanying article. Cover figures must be oriented vertically.

**Book/Video Reviews:** Reviews are solicited for scientific books and videos, and also for published material with a potentially wider appeal (e.g., novels, biographies, historical anecdotes, etc.). Reviewed material must have relevance to the oceans. Reviewers should keep in mind that a well-written review helps readers decide whether or not it is worth their time to read the book in its entirety. The reader of a review expects basic information about the content and organization of the book, as well as a subjective opinion about the quality, style and relevance of the material.

Reviews should include: complete title of book/video, author or editor, year of publication, number of pages, price, format (hardbound, soft-cover, paperback, etc.), name of publisher, city of publication and the reviewer's name, title and affiliation.

**Reprints:** Offprints of published articles are offered at the time of acceptance and are printed concurrently with the magazine. Contact the editorial office for current estimates of reprint costs.

**"Galley" proofs:** These will be distributed as soon as they are ready, and the author will have one-day turn around time to return them to the editorial office.

**SIGN ME ON!**

Please accept my application for membership in The Oceanography Society. My annual membership dues will support the work of the Society and will entitle me to receive *Oceanography*, to register at discounted rates for meetings sponsored and/or co-sponsored by the Society, to vote in Society elections, and to express my opinion on all matters of interest to the Society. I would like to join in the following category (choose one):

- Regular Member (\$50)
- Student Member (\$25)\*
- Corporate/Institutional Member (\$500)
- Library (\$125)
- Sponsoring Member (\$100)  
((\$50 is tax deductible))

\* Students must provide the following information to certify student status:

Enrolled at \_\_\_\_\_ Major Subject \_\_\_\_\_ Date \_\_\_\_\_  
Certified by \_\_\_\_\_ Certifier's signature & title \_\_\_\_\_

- Enclosed is my check for \$ \_\_\_\_\_  
in U.S. funds payable on a U.S. bank.
- Please charge my credit card:  Mastercard  Visa

Card # \_\_\_\_\_  
Expiration Date \_\_\_\_\_  
Signature \_\_\_\_\_

Name \_\_\_\_\_  
Affiliation \_\_\_\_\_  
Address \_\_\_\_\_  
\_\_\_\_\_  
\_\_\_\_\_  
Phone \_\_\_\_\_  Home  Work  
E-Mail \_\_\_\_\_  
Discipline(s):  Biology  Chemistry  Physics  
 Geology/Geophysics  Applied Technology



THE OCEANOGRAPHY SOCIETY  
4052 Timber Ridge Drive  
Virginia Beach, VA 23455 USA  
Phone: (757) 464-0131

Non-Profit Org.  
U.S. Postage  
**PAID**  
Lancaster  
PA 17603  
Permit 161

---

## *THE OCEANOGRAPHY SOCIETY*

The Oceanography Society was founded in 1988 to disseminate knowledge of oceanography and its application through research and education, to promote communication among oceanographers, and to provide a constituency for consensus-building across all the disciplines of the field. The Oceanography Society is a non-profit, tax-exempt organization incorporated in the District of Columbia.

### **MEMBERSHIP**

**Regular** membership is available to oceanographers, scientists or engineers active in ocean-related fields, or to persons who have advanced oceanography by management or other public service. With proper certification, **Student** membership is available for students enrolled at least half-time in an oceanography or ocean-related program at the baccalaureate or higher level. **Life** members pay a one-time fee for lifelong privileges of membership. **Sponsoring** membership is available to individuals who wish to provide enhanced support annually. In the U.S., \$60 of the annual dues in this category is tax-deductible as a charitable contribution, as are any additional contributions, over and above the annual Regular Member dues. *Note:* no portion of Life Member dues qualifies as a charitable contribution. Organizations and companies may subscribe annually as **Corporate/Institutional** members. Annual **Library** subscriptions are also available. All members are entitled to exercise the rights and responsibilities of active participation in the Society, including the vote. All members receive *Oceanography*. All applications for membership are subject to approval by the Membership Committee of the Society. To join, mail the application with completed information and appropriate payment.